THE UNIVERSITY OF MICHIGAN

COLLEGE OF ENGINEERING
DEPARTMENT OF ELECTRICAL ENGINEERING
Radiation Laboratory

SCATTERING BY HOLLOW FINITE CYLINDERS
AND INFINITE COATED CYLINDERS

Final Report

J. J. Bowman, E. F. Knott and V. H. Weston

January 1966

7456-1-F = RL-2155

THE UNIVERSITY OF MICHIGAN

7456-1-F

SCATTERING BY HOLLOW FINITE CYLINDERS
AND INFINITE COATED CYLINDERS

by

J. J. Bowman, E. F. Knott and V. H. Weston

January 1966

Final Report

Contract A F 33(615)-3166
PO 614 572117

Prepared for

Northrop Corporation
Norair Division
Hawthrone, California

ERRATA TO REPORT 7456-1-F "SCATTERING BY HOLLOW FINITE CYLINDERS AND INFINITE COATED CYLINDERS"

Corrections to: "Scattering by Hollow Finite Cylinders and Infinite Coated Cylinders," J. J. Bowman, E. F. Knott and V. H. Weston, University of Michigan Radiation Laboratory Report No. 7456-1-F.

In Section 2.3 concerning the case of two spaced absorbing layers, and in the following section concerning two resistance foils, an error has been made in calculating the asymptotic approximations for large indices of refraction. In particular, the quantities $C^{(1)}$ and $C^{(3)}$ have been erroneously taken to be zero asymptotically, and since they are not zero, this leads to the following set of corrections.

J. J. Bowman

ERRATA TO REPORT 7456-1-F "SCATTERING BY HOLLOW FINITE CYLINDERS AND INFINITE COATED CYLINDERS"

P. 18, Eq. (43) should read

$$C^{(1)} = \frac{\left[\dfrac{in\cos\beta}{kb\lambda_o^2} + C^{(2)}\right](1 + \cot^2 k_1\delta_1)}{\left[A^{(2)} + \sqrt{\dfrac{\epsilon_1}{\mu_1}}\cot k_1\delta_1\right]\left[B^{(2)} + \sqrt{\dfrac{\mu_1}{\epsilon_1}}\cot k_1\delta_1\right] + \left[\dfrac{in\cos\beta}{kb\lambda_o^2} + C^{(2)}\right]^2}.$$

P. 18, Eq. (44) should read

$$D = -(A^{(0)} - A^{(1)})(A^{(0)} - B^{(1)}) - \left[\frac{in\cos\beta}{ka\lambda_o^2} - C^{(1)}\right]^2.$$

P. 19, in Eq. (45), read

$$\left[\frac{in\cos\beta}{kc\lambda_o^2} - C^{(3)}\right]^2 \quad \text{instead of} \quad \left[\frac{in\cos\beta}{kc\lambda_o^2}\right]^2.$$

P. 19, Eq. (47) should read

$$C^{(2)} = \frac{\dfrac{16}{\pi^2(k_o b)(k_o c)}\left[\dfrac{in\cos\beta}{kc\lambda_o^2} - C^{(3)}\right]\left[Y^{(2)}\right]^{-2}}{\left[A^{(3)} - \dfrac{1}{\lambda_o}\dfrac{\partial \ell n Y^{(2)}}{\partial(k_o c)}\right]\left[B^{(3)} - \dfrac{1}{\lambda_o}\dfrac{\partial \ell n Y^{(2)}}{\partial(k_o c)}\right] + \left[\dfrac{in\cos\beta}{kc\lambda_o^2} - C^{(3)}\right]^2}.$$

P. 20, Eq. (50) should read

$$C^{(3)} = \frac{\left[\dfrac{in\cos\beta}{kd\lambda_o^2}\right](1 + \cot^2 k_3\delta_3)}{\left[A^{(4)} + \sqrt{\dfrac{\epsilon_3}{\mu_3}}\,\cot k_3\delta_3\right]\left[B^{(4)} + \sqrt{\dfrac{\mu_3}{\epsilon_3}}\,\cot k_3\delta_3\right] + \left[\dfrac{in\cos\beta}{kd\lambda_o^2}\right]^2} \ .$$

P. 23, Eq. (59) should read

$$C^{(1)} = -i\,\frac{R_{s_1}}{Z_o}\,\frac{\dfrac{in\cos\beta}{kb\lambda_o^2} + C^{(2)}}{B^{(2)} - i\,\dfrac{R_{s_1}}{Z_o}} \ .$$

P. 23, Eq. (62) should read

$$C^{(3)} = -i\,\frac{R_{s_3}}{Z_o}\,\frac{\dfrac{in\cos\beta}{kd\lambda_o^2}}{B^{(4)} - i\,\dfrac{R_{s_3}}{Z_o}} \ .$$

THE UNIVERSITY OF MICHIGAN

ABSTRACT

To assist in the design of computational programs for scattering cross-sections, investigations of cylindrical objects are considered. In particular, measurements are carried out to determine the surface currents induced in the vicinity of the leading end of finite, hollow conducting cylinders, by an incident plane wave. Theoretical analysis is undertaken to obtain the scattered and surface fields produced by a plane wave incident obliquely to an infinite coated cylinder. The particular case of a perfectly conducting cylinder surrounded by two resistive sheets (separated by an air gap) is given.

TABLE OF CONTENTS

I

INTRODUCTION

In the determination of the radar cross-section or scattered field produced by a plane electromagnetic wave incident upon a given obstacle of complicated shape and material composition, the use of computer techniques has recently come into practice. The computation involved is a two stage process which first involves solving a vector integral equation for the various unknown quantities as a function of position, and then utilizing these results to compute the scattered field. For perfectly conducting obstacles, the unknown quantities that are first determined are the induced surface currents which are a function of position on the surface of the obstacle. As in the usual practice of numerical analysis, the surface is approximated by a finite set of mesh points. The integral equation is then approximated by a set of algebraic equations, with the unknown quantities being the currents at the mesh points. For general coated objects, the set of mesh points must approximate not only the surfaces of the coating, but the interior region.

The accuracy of the numerical procedure depends upon the maximum number of mesh points which can be handled, and the degree that the set of mesh points approximate the surface or volume region, as the case may be.

Thus, for scattering from very large objects, the fundamental limitation to accuracy is the limited number of mesh points that can be used due to storage capacity. The best way to increase accuracy, in such a case, is to reduce the volume or surface region for which the sought for quantities are unknown. This can be achieved by using known theoretical results to determine the unknown quantities over portions of the surface or volume beforehand. The unknown

quantities then only have to be determined by numerical means over the re-
maining region. In regard to this approach, for perfectly conducting objects,
Norair Northrup has developed a computer program "S.D.T.-Physical Optics",
which employs the physical optics approximation for the surface current on the
illuminated portion of the surface. The accuracy of the physical physics ap-
proximation at a given point depends upon the local radii of curvature, the dis-
tance the point is from the shadow boundary, and from regions of surface dis-
continuities, such as edges. With regard to the latter problem, a series of
measurements is carried out in Chapter III to determine the surface currents
in the vicinity of the edges of hollow finite perfectly conducting cylinders, for
plane wave incidence. The results can then be used to determine when, and how
close to the edges, the physical optics approximation is useful. No analysis is
presented in Chapter III.

At present, Norair is extending numerical procedures to determine the
scattered field from coated objects. As a check against such numerical proce-
dures, the exact theoretical expression for the total field produced by a plane
wave incident obliquely upon an infinite coated cylinder is obtained in Chapter II
where the coatings are composed of homogeneous layers of different material.
The results are expressed in terms of modal series, which are useful for cal-
culations for frequencies around and below the resonance region of the cylinder.
Results are also given for the special cases where the coating consists of one or
two resistive sheets concentric with the inner perfectly conducting cylindrical
core.

II

SCATTERING FROM COATED CYLINDERS AT OBLIQUE INCIDENCE

2.1 Introduction

It is desired to derive the solution for the problem of a plane wave incident obliquely on an infinitely long circular cylinder coated with several uniform layers of material. In considering this problem it is convenient to confine attention to a cylindrical core on which an impedance boundary condition is imposed and surrounding which are two layers with arbitrary complex refractive indexes. The solution, whose form is the exact Mie series solution for incident energy of both TE and TM polarizations, may be immediately extended by inspection to include the case of an arbitrary number of layers. Such a generalization will be employed to discuss the four layer case of a perfectly conducting cylinder surrounded by two impedance sheets, the impedance sheets being separated from each other and from the inner core by air spaces. These results are simplified in the case of two resistance foils with air space separation.

The problem of scattering of plane waves obliquely incident on a solid dielectric cylinder has been solved by Wait (1955), who presented the exact Mie series solution and discussed some special cases. This solution is, of course, encompassed by the present investigation and thus serves as a check on the work. The scattering of plane waves incident perpendicularly on composite infinite cylinders has been considered by many authors of which we mention Kerker and Matijević (1961), who solved the boundary value problem for an arbitrary number of concentric cylinders.

3

Simplification of the expressions can be achieved for thin absorbing layers of materials with large complex indexes of refraction. In this case, the asymptotic analysis carried out by Weston and Hemenger (1962) for the absorber coated sphere may be applied to the coated cylinder to simplify the scattering coefficients of the absorbing layer in question. When such a layer, or impedance sheet, is backed by a perfect conductor, the total tangential field components may be shown to satisfy an impedance boundary condition on the outer surface of the layer. As a sufficiently general example, the scattered field produced by a plane wave incident normally on a conducting cylinder coated with two thin absorbing layers has been examined by Bowman and Weston (1965). The present investigation differs from Bowman and Weston not only in the assumption of oblique incidence, but in supposing the two impedance sheets to be separated from each other and from the conducting core. The existence of a transmitted field in the air spaces greatly complicates the expressions for the scattered field. However, simplification results when the thin absorbing layers are non-magnetic and have electric permittivities with predominately large imaginary parts. Such layers are resistive layers. Scattering of normally incident waves by a conducting cylinder surrounded by a single resistance foil has been discussed by Schmitt (1957).

2.2 Scattering by a Doubly-Coated Cylinder with Impedance Boundary Condition at the Core

The inner cylindrical core will have radius c and its axis will be the z-axis of the cylindrical polar coordinate system (r, ϕ, z). Numbering from the outer layer inwards, let ϵ_1 and μ_1 be, respectively, the relative electric permittivity and the relative magnetic permeability of the outer coating, while ϵ_2 and μ_2 refer to the inner coating. The inner coating will be of thickness

$\delta_2 = b-c$, where b is the outer radius of the cylindrical surface formed by this layer. The outer layer will be of thickness $\delta_1 = a-b$, where a is the outer radius of this cylindrical shell.

The source of excitation will be a plane wave incident obliquely on the coated cylinder. The field of the incident plane wave is taken in the form

$$\vec{E}_o = \hat{a}\, e^{i\vec{k}\cdot\vec{r} - i\omega t} \quad , \qquad \vec{H}_o = \sqrt{\frac{\epsilon_o}{\mu_o}}\, \hat{b}\, e^{i\vec{k}\cdot\vec{r} - i\omega t} \qquad (1)$$

where the polarization vectors $\hat{a}, \hat{b}$ and the propagation vector $\vec{k}$ are given by

$$\hat{a} = \hat{x}\cos\alpha\cos\beta + \hat{y}\sin\alpha + \hat{z}\cos\alpha\sin\beta ,$$

$$\hat{b} = \hat{x}\sin\alpha\cos\beta - \hat{y}\cos\alpha + \hat{z}\sin\alpha\sin\beta , \qquad (2)$$

$$\vec{k} = \omega\sqrt{\epsilon_o\mu_o}\,(\hat{x}\sin\beta - \hat{z}\cos\beta).$$

The direction of the incident plane wave makes an angle β with the negative z axis; the special case $\beta = \frac{\pi}{2}$ results in normal incidence. The angle α determines the state of polarization of the wave: $\alpha = 0$ corresponds to an incident TM (transverse magnetic) mode while $\alpha = \frac{\pi}{2}$ corresponds to an incident TE (transverse electric) mode. Due to the presence of the dielectric coatings on the cylinder, the total electromagnetic field must be expressed as a superposition of both TE and TM modes, even though the incident wave may be a pure TE or a pure TM mode. This coupling effect disappears in the case of normal incidence $(\beta = \frac{\pi}{2})$.

5

Since ϵ, μ with appropriate subscripts 1 or 2 denote relative material parameters, Maxwell's equations read

$$\nabla \wedge \vec{E} = i\omega\mu_0\mu\vec{H} \ ,$$

$$\nabla \wedge \vec{H} = -i\omega\epsilon_0\epsilon\vec{E}$$

where ϵ_0, μ_0 refer to the free-space constants. In the region exterior to the cylinder ($r > a$), the z components of the total electromagnetic field may be represented in the form

$$E_z = e^{-ikz\cos\beta} \sum_{n=-\infty}^{\infty} i^n \left[\sin\beta\cos\alpha \, J_n(kr\sin\beta) + a_n H_n^{(1)}(kr\sin\beta) \right] e^{in\phi} \ ,$$

$$H_z = \sqrt{\frac{\epsilon_0}{\mu_0}} \, e^{-ikz\cos\beta} \sum_{n=-\infty}^{\infty} i^n \left[\sin\beta \sin\alpha \, J_n(kr\sin\beta) + \tilde{a}_n H_n^{(1)}(kr\sin\beta) \right] e^{in\phi} \ .$$

$$(3)$$

Within the outer dielectric layer ($a > r > b$) these components are written in the following manner

$$E_z = e^{-ikz\cos\beta} \sum_{n=-\infty}^{\infty} i^n \left[a_n^{(1)} H_n^{(1)}(k_1 r) + b_n^{(1)} H_n^{(2)}(k_1 r) \right] e^{in\phi} \ ,$$

$$H_z = \sqrt{\frac{\epsilon_0}{\mu_0}} e^{-ikz\cos\beta} \sum_{n=-\infty}^{\infty} i^n \left[\tilde{a}_n^{(1)} H_n^{(1)}(k_1 r) + \tilde{b}_n^{(1)} H_n^{(2)}(k_1 r) \right] e^{in\phi} \ ,$$

$$(4)$$

while for the inner layer $(b > r > c)$

$$E_z = e^{-ikz\cos\beta} \sum_{n=-\infty}^{\infty} i^n \left[a_n^{(2)} H_n^{(1)}(k_2 r) + b_n^{(2)} H_n^{(2)}(k_2 r) \right] e^{in\phi} \quad ,$$

$$H_z = \sqrt{\frac{\epsilon_0}{\mu_0}} e^{-ikz\cos\beta} \sum_{n=-\infty}^{\infty} i^n \left[\tilde{a}_n^{(2)} H_n^{(1)}(k_2 r) + \tilde{b}_n^{(2)} H_n^{(2)}(k_2 r) \right] e^{in\phi} \quad . \tag{5}$$

The parameters k_1, k_2 appearing in the arguments of the Hankel functions $H_n^{(1)}$, $H_n^{(2)}$ are defined as follows:

$$k_1 = \lambda_1 k , \qquad \lambda_1 = (\epsilon_1 \mu_1 - \cos^2\beta)^{1/2} \quad ,$$

$$\tag{6}$$

$$k_2 = \lambda_2 k , \qquad \lambda_2 = (\epsilon_2 \mu_2 - \cos^2\beta)^{1/2} \quad .$$

Analogously, it is convenient to define

$$k_o = \lambda_o k , \qquad \lambda_o = (1 - \cos^2\beta)^{1/2} = \sin\beta , \tag{7}$$

where k_o is merely the x component of the free-space propagation vector $\vec{k}$.

The total electromagnetic field is completely determined upon specifying the ten unknown coefficients a_n, $\tilde{a}_n$, etc., which occur in the summations above. These unknown coefficients are obtained, of course, by imposing the boundary conditions on the general solution. In particular, the tangential fields must be matched across the dielectric boundaries $r = a$ and $r = b$. However, in

addition to these usual continuity requirements, we shall impose an impedance boundary condition at $r = c$, namely

$$E_z = \eta_3 \sqrt{\frac{\mu_0}{\epsilon_0}} H_\phi \quad ,$$

$$E_\phi = -\eta_3 \sqrt{\frac{\mu_0}{\epsilon_0}} H_z \qquad (8)$$

where η_3 represents a constant surface impedance. At each of the dielectric interfaces, the continuity conditions give rise to four boundary equations, making a total of eight equations, while the impedance condition on the inner core contributes two more equations. There is, then, a set of ten linear, inhomogeneous equations for the ten unknown coefficients. The equations are complicated by the coupling between TE and TM modes.

In enumerating the ten boundary equations we shall drop the summation index n; no confusion should arise. Beginning with $r = c$ and applying the impedance condition (8), one obtains the two equations

$$a^{(2)}\left[H^{(1)}(k_2 c) - i\eta_3 \frac{\epsilon_2}{\lambda_2} H'^{(1)}(k_2 c)\right] + b^{(2)}\left[H^{(2)}(k_2 c) - i\eta_3 \frac{\epsilon_2}{\lambda_2} H'^{(2)}(k_2 c)\right]$$

$$= \frac{\eta_3 n}{kc} \frac{\cos\beta}{\lambda_2^2} \left[\tilde{a}^{(2)} H^{(1)}(k_2 c) + \tilde{b}^{(2)} H^{(2)}(k_2 c)\right] \quad , \qquad (9)$$

$$\tilde{a}^{(2)}\left[H^{(1)}(k_2 c) - \frac{i}{\eta_3}\frac{\mu_2}{\lambda_2}H'^{(1)}(k_2 c)\right] + \tilde{b}^{(2)}\left[H^{(2)}(k_2 c) - \frac{i}{\eta_3}\frac{\mu_2}{\lambda_2}H'^{(2)}(k_2 c)\right]$$

$$= -\frac{n}{\eta_3 kc}\frac{\cos\beta}{\lambda_2^{2}}\left[a^{(2)}H^{(1)}(k_2 c) + b^{(2)}H^{(2)}(k_2 c)\right] . \tag{10}$$

At r = b the continuity of the z components requires the following two equations

$$a^{(2)}H^{(1)}(k_2 b) + b^{(2)}H^{(2)}(k_2 b) = a^{(1)}H^{(1)}(k_1 b) + b^{(1)}H^{(2)}(k_1 b) , \tag{11}$$

$$\tilde{a}^{(2)}H^{(1)}(k_2 b) + \tilde{b}^{(2)}H^{(2)}(k_2 b) = \tilde{a}^{(1)}H^{(1)}(k_1 b) + \tilde{b}^{(1)}H^{(2)}(k_1 b) , \tag{12}$$

while continuity of the ϕ components gives

$$\frac{\epsilon_1}{\lambda_1}\left[a^{(1)}H'^{(1)}(k_1 b) + b^{(1)}H'^{(2)}(k_1 b)\right] + \frac{in\cos\beta}{kb}\left(\frac{1}{\lambda_2^{2}} - \frac{1}{\lambda_1^{2}}\right)\left[\tilde{a}^{(1)}H^{(1)}(k_1 b) + \tilde{b}^{(1)}H^{(2)}(k_1 b)\right]$$

$$= \frac{\epsilon_2}{\lambda_2}\left[a^{(2)}H'^{(1)}(k_2 b) + b^{(2)}H'^{(2)}(k_2 b)\right] , \tag{13}$$

$$\frac{\mu_1}{\lambda_1}\left[\tilde{a}^{(1)}H'^{(1)}(k_1 b) + \tilde{b}^{(1)}H'^{(2)}(k_1 b)\right] - \frac{in\cos\beta}{kb}\left(\frac{1}{\lambda_2^{2}} - \frac{1}{\lambda_1^{2}}\right)\left[a^{(1)}H^{(1)}(k_1 b) + b^{(1)}H^{(2)}(k_1 b)\right]$$

$$= \frac{\mu_2}{\lambda_2}\left[\tilde{a}^{(2)}H'^{(1)}(k_2 b) + \tilde{b}^{(2)}H'^{(2)}(k_2 b)\right] . \tag{14}$$

9

At r = a one obtains from z component continuity

$$a^{(1)}H^{(1)}(k_1 a) + b^{(1)}H^{(2)}(k_1 a) = a_n H^{(1)}(k_o a) + \sin\beta \cos\alpha J(k_o a) , \quad (15)$$

$$\tilde{a}^{(1)}H^{(1)}(k_1 a) + \tilde{b}^{(1)}H^{(2)}(k_1 a) = \tilde{a}_n H^{(1)}(k_o a) + \sin\beta \sin\alpha J(k_o a) , \quad (16)$$

and from ϕ component continuity

$$\frac{\epsilon_1}{\lambda_1}\left[a^{(1)}H'^{(1)}(k_1 a) + b^{(1)}H'^{(2)}(k_1 a)\right] + \frac{\ln \cos\beta}{ka}\left(\frac{1}{\lambda_o^2} - \frac{1}{\lambda_1^2}\right)\left[\tilde{a}^{(1)}H^{(1)}(k_1 a) + \tilde{b}^{(1)}H^{(2)}(k_1 a)\right]$$

$$= \frac{1}{\lambda_o}\left[a_n H'^{(1)}(k_o a) + \sin\beta \cos\alpha J'(k_o a)\right] , \quad (17)$$

$$\frac{\mu_1}{\lambda_1}\left[\tilde{a}^{(1)}H'^{(1)}(k_1 a) + \tilde{b}^{(1)}H'^{(2)}(k_1 a)\right] - \frac{\ln \cos\beta}{ka}\left(\frac{1}{\lambda_o^2} - \frac{1}{\lambda_1^2}\right)\left[a^{(1)}H^{(1)}(k_1 a) + b^{(1)}H^{(2)}(k_1 a)\right]$$

$$= \frac{1}{\lambda_o}\left[\tilde{a}_n H'^{(1)}(k_o a) + \sin\beta \sin\alpha J'(k_o a)\right] . \quad (18)$$

A perusal of the boundary equations shows that in the case of normal incidence $(\beta = \frac{\pi}{2})$ the ten equations decouple into two sets of five equations, one set for the electric coefficients and one set for the magnetic coefficients.

As might be expected, there are many ways to solve the boundary equations; however, it is wise to look before leaping and to attempt to preserve the natural duality inherent both in Maxwell's equations and in the boundary conditions. The method by which we proceed is the following. From the first four Eqs. (9) to (12) we obtain the coefficients of the second dielectric layer in terms of the first layer coefficients. The resultant expressions are then substituted into (13) and (14) to obtain two homogeneous equations for the four coefficients of the first layer. Two inhomogeneous equations for these coefficients are obtained from the last four boundary Eqs. (15) to (18) upon eliminating a_n and $\tilde{a}_n$. We now have four equations for the four first layer coefficients; these yield expressions which, when substituted into (15) and (16), give a_n and $\tilde{a}_n$ explicitly.

The final solution in the case of TM incidence ($\alpha = 0$) may be written in the form

$$a_n = -\lambda_0 \frac{J(k_0 a)}{H_0^{(1)}(k_0 a)} - \frac{2i}{\pi k_0 a} \frac{1}{\left[H^{(1)}(k_0 a)\right]^2} \frac{1}{D} \left(A^{(0)} - B^{(1)}\right) , \qquad (19)$$

$$\tilde{a}_n = \frac{2i}{\pi k_0 a} \frac{1}{\left[H^{(1)}(k_0 a)\right]^2} \frac{1}{D} \left[\frac{in \cos\beta}{ka} \left(\frac{1}{\lambda_0^2} - \frac{1}{\lambda_1^2}\right) - C^{(1)}\right] ; \qquad (20)$$

in the case of TE incidence ($\alpha = \frac{\pi}{2}$) one obtains

$$a_n = -\frac{2i}{\pi k_0 a} \frac{1}{\left[H^{(1)}(k_0 a)\right]^2} \frac{1}{D} \left[\frac{in \cos\beta}{ka} \left(\frac{1}{\lambda_0^2} - \frac{1}{\lambda_1^2}\right) - C^{(1)}\right] , \qquad (21)$$

$$\tilde{a}_n = -\lambda_0 \frac{J(k_0 a)}{H^{(1)}(k_0 a)} - \frac{2i}{\pi k_0 a} \frac{1}{\left[H^{(1)}(k_0 a)\right]^2} \frac{1}{D} \left(A^{(0)} - A^{(1)}\right) , \qquad (22)$$

where

$$A^{(0)} = \frac{H'^{(1)}(k_0 a)}{\lambda_0 H^{(1)}(k_0 a)} = \frac{H'^{(1)}(ka \sin\beta)}{\sin\beta \, H^{(1)}(ka \sin\beta)} , \qquad (23)$$

$$D = -\left(A^{(0)} - A^{(1)}\right)\left(A^{(0)} - B^{(1)}\right) - \left[\frac{n \cos\beta}{ka}\left(\frac{1}{\lambda_0^2} - \frac{1}{\lambda_1^2}\right) - C^{(1)}\right]^2 . \qquad (24)$$

The remaining quantities $A^{(1)}$, $B^{(1)}$, $C^{(1)}$ are related to the parameters of the coatings by the following set of relationships

$$A^{(1)} A^{(1)} = -\frac{\epsilon_1}{\lambda_1}\left[A^{(2)} \frac{\partial Y^{(1)}}{\partial(k_1 a)} - \frac{\epsilon_1}{\lambda_1} \frac{\partial^2 Y^{(1)}}{\partial(k_1 a)\partial(k_1 b)}\right]\left[B^{(2)} Y^{(1)} - \frac{\mu_1}{\lambda_1} \frac{\partial Y^{(1)}}{\partial(k_1 b)}\right]$$

$$-\frac{\epsilon_1}{\lambda_1}\left[\frac{n \cos\beta}{kb}\left(\frac{1}{\lambda_1^2} - \frac{1}{\lambda_2^2}\right) - C^{(2)}\right]^2 Y^{(1)} \frac{\partial Y^{(1)}}{\partial(k_1 a)} , \qquad (25)$$

$$\Delta^{(1)}B^{(1)} = -\frac{\mu_1}{\lambda_1}\left[B^{(2)}\frac{\partial Y^{(1)}}{\partial(k_1 a)} - \frac{\mu_1}{\lambda_1}\frac{\partial^2 Y^{(1)}}{\partial(k_1 a)\partial(k_1 b)}\right]\left[A^{(2)}Y^{(1)} - \frac{\epsilon_1}{\lambda_1}\frac{\partial Y^{(1)}}{\partial(k_1 b)}\right]$$

$$-\frac{\mu_1}{\lambda_1}\left[\frac{\text{in}\cos\beta}{kb}\left(\frac{1}{\lambda_1^2} - \frac{1}{\lambda_2^2}\right) - C^{(2)}\right]^2 Y^{(1)}\frac{\partial Y^{(1)}}{\partial(k_1 a)}, \qquad (26)$$

$$\Delta^{(1)}C^{(1)} = \frac{\epsilon_1 \mu_1}{\lambda_1^2}\left[\frac{\text{in}\cos\beta}{kb}\left(\frac{1}{\lambda_1^2} - \frac{1}{\lambda_2^2}\right) - C^{(2)}\right]\frac{-16}{\pi^2(k_1 a)(k_1 b)}, \qquad (27)$$

$$\Delta^{(1)} = -\left[A^{(2)}Y^{(1)} - \frac{\epsilon_1}{\lambda_1}\frac{\partial Y^{(1)}}{\partial(k_1 b)}\right]\left[B^{(2)}Y^{(1)} - \frac{\mu_1}{\lambda_1}\frac{\partial Y^{(1)}}{\partial(k_1 b)}\right]$$

$$-\left[\frac{\text{in}\cos\beta}{kb}\left(\frac{1}{\lambda_1^2} - \frac{1}{\lambda_2^2}\right) - C^{(2)}\right]^2\left(Y^{(1)}\right)^2, \qquad (28)$$

where similar expressions are obtained for the second layer, namely

$$\Delta^{(2)}A^{(2)} = \frac{\epsilon_2}{\lambda_2}\left[\frac{\partial Y^{(2)}}{\partial(k_2 b)} - i\eta_3\frac{\epsilon_2}{\lambda_2}\frac{\partial^2 Y^{(2)}}{\partial(k_2 b)\partial(k_2 c)}\right]\left[Y^{(2)} - \frac{i}{\eta_3}\frac{\mu_2}{\lambda_2}\frac{\partial Y^{(2)}}{\partial(k_2 c)}\right]$$

$$+\frac{\epsilon_2}{\lambda_2}\frac{n^2\cos^2\beta}{(kc)^2\lambda_2^4}Y^{(2)}\frac{\partial Y^{(2)}}{\partial(k_2 b)}, \qquad (29)$$

$$\Delta^{(2)}{}_B{}^{(2)} = \frac{\mu_2}{\lambda_2} \left[\frac{\partial Y^{(2)}}{\partial (k_2 b)} - \frac{i}{\eta_3} \frac{\mu_2}{\lambda_2} \frac{\partial^2 Y^{(2)}}{\partial (k_2 b) \partial (k_2 c)} \right] \left[Y^{(2)} - i\eta_3 \frac{\epsilon_2}{\lambda_2} \frac{\partial Y^{(2)}}{\partial (k_2 c)} \right]$$

$$+ \frac{\mu_2}{\lambda_2} \frac{n^2 \cos^2 \beta}{(kc)^2 \lambda_2^4} Y^{(2)} \frac{\partial Y^{(2)}}{\partial (k_2 b)} \quad , \tag{30}$$

$$\Delta^{(2)}{}_C{}^{(2)} = \frac{\epsilon_2 \mu_2}{\lambda_2^4} \frac{\ln \cos \beta}{kc} \frac{-16}{\pi^2 (k_2 b)(k_2 c)} \quad , \tag{31}$$

$$\Delta^{(2)} = \left[Y^{(2)} - i\eta_3 \frac{\epsilon_2}{\lambda_2} \frac{\partial Y^{(2)}}{\partial (k_2 c)} \right] \left[Y^{(2)} - \frac{i}{\eta_3} \frac{\mu_2}{\lambda_2} \frac{\partial Y^{(2)}}{\partial (k_2 c)} \right] + \frac{n^2 \cos^2 \beta}{(kc)^2 \lambda_2^4} \left(Y^{(2)} \right)^2 . \tag{32}$$

In the above, $Y^{(1)}$ and $Y^{(2)}$ represent combinations of Hankel functions given by

$$Y^{(1)} = H^{(2)}(k_1 a) H^{(1)}(k_1 b) - H^{(1)}(k_1 a) H^{(2)}(k_1 b) \quad ,$$

$$\tag{33}$$

$$Y^{(2)} = H^{(2)}(k_2 b) H^{(1)}(k_2 c) - H^{(1)}(k_2 b) H^{(2)}(k_2 c) \quad .$$

This completes the specification of the scattered field. We note the identity

$$Y^{(1)} \frac{\partial^2 Y^{(1)}}{\partial(k_1 a)\partial(k_1 b)} - \frac{\partial Y^{(1)}}{\partial(k_1 a)} \frac{\partial Y^{(1)}}{\partial(k_1 b)} = \frac{-16}{\pi^2 (k_1 a)(k_1 b)} \tag{34}$$

which derives from the Wronskians of the Hankel functions. Of course, an analogous identity holds for $Y^{(2)}$.

The z components of the total field on the outer surface (r=a) of the cylindrical structure have a particularly compact form. In the case of TM incidence ($\alpha = 0$) one finds

$$E_z^{surf.} = -\frac{2i}{\pi k_o a} e^{-ikz\cos\beta} \sum_{n=-\infty}^{\infty} \frac{e^{in\phi}}{H_n^{(1)}(k_o a)} \frac{A_n^{(0)} - B_n^{(1)}}{D_n} , \tag{35}$$

$$H_z^{surf.} = \sqrt{\frac{\epsilon_o}{\mu_o}} \frac{2i}{\pi k_o a} e^{-ikz\cos\beta} \sum_{n=-\infty}^{\infty} \frac{e^{in\phi}}{H_n^{(1)}(k_o a)} \frac{1}{D_n} \left[\frac{in\cos\beta}{ka} \left(\frac{1}{\lambda_o^2} - \frac{1}{\lambda_1^2} \right) - C_n^{(1)} \right], \tag{36}$$

and in the case of TE incidence ($\alpha = \frac{\pi}{2}$)

$$E_z^{surf.} = -\frac{2i}{\pi k_o a} e^{-ikz\cos\beta} \sum_{n=-\infty}^{\infty} \frac{e^{in\phi}}{H_n^{(1)}(k_o a)} \frac{1}{D_n} \left[\frac{in\cos\beta}{ka} \left(\frac{1}{\lambda_o^2} - \frac{1}{\lambda_1^2} \right) - C_n^{(1)} \right], \tag{37}$$

$$H_z^{surf.} = -\sqrt{\frac{\epsilon_o}{\mu_o}} \frac{2i}{\pi k_o a} e^{-ikz\cos\beta} \sum_{n=-\infty}^{\infty} \frac{e^{in\phi}}{H_n^{(1)}(k_o a)} \frac{A_n^{(0)} - A_n^{(1)}}{D_n} . \tag{38}$$

The other components of the field may be obtained by reverting to Maxwell's equations which are, explicitly

$$E_\phi = -\frac{i}{\lambda_0}\left[\frac{\cos\beta}{k_0 r}\frac{\partial E_z}{\partial\phi}+\sqrt{\frac{\mu_0}{\epsilon_0}}\frac{\partial H_z}{\partial(k_0 r)}\right] \quad,$$

$$E_r = -\frac{i}{\lambda_0}\left[\cos\beta\frac{\partial E_z}{\partial(k_0 r)}-\frac{1}{k_0 r}\sqrt{\frac{\mu_0}{\epsilon_0}}\frac{\partial H_z}{\partial\phi}\right] \quad,$$

$$H_\phi = -\frac{i}{\lambda_0}\left[\frac{\cos\beta}{k_0 r}\frac{\partial H_z}{\partial\phi}-\sqrt{\frac{\epsilon_0}{\mu_0}}\frac{\partial E_z}{\partial(k_0 r)}\right] \quad,$$

$$H_z = -\frac{i}{\lambda_0}\left[\cos\beta\frac{\partial H_z}{\partial(k_0 r)}+\frac{1}{k_0 r}\sqrt{\frac{\epsilon_0}{\mu_0}}\frac{\partial E_z}{\partial\phi}\right] \quad.$$

(39)

It is well to point out that the basic symmetry of the boundary equations has indeed been retained in our solution. Thus, with the transformations

$$\epsilon \longrightarrow \mu \,, \qquad \mu \longrightarrow \epsilon \,, \qquad \eta \longrightarrow \frac{1}{\eta}$$

one easily verifies that

$$a_n^{TM} \longrightarrow \tilde{a}_n^{TE} \,, \qquad \tilde{a}_n^{TM} \longrightarrow -a_n^{TE} \,,$$

and this is a result of the natural duality of Maxwell's equations and the boundary conditions. The form of the solution is also quite amenable to generalization. In particular, it is clear that the solution for a larger number of layers is obtained by generalizing the quantities $A^{(2)}$, $B^{(2)}$, $C^{(2)}$, $\Delta^{(2)}$ of the second layer to the form of the first layer quantities $A^{(1)}$, $B^{(1)}$, $C^{(1)}$, $\Delta^{(1)}$ and introducing further such quantities to correspond to the added layers. Finally, we remark that the solution has been checked in several special cases by comparing it to solutions derived independently in these cases.

2.3 Scattering by Conducting Cylinder Surrounded by Two Spaced Absorbing Layers.

A special scattering structure of interest consists of a perfectly conducting cylindrical core surrounded by two absorbing layers, the core and the layers each being separated by an air gap. The problem of scattering from this structure is, in essence, a four layer problem: two thin absorbing layers and two air spaces comprise the four layers. The scattered field may be obtained as a straightforward generalization of the solution we have presented above. We shall further suppose, however, that the indices of refraction of the two absorbing layers are very large. The asymptotic analysis of Weston and Hemenger (1962) may then be employed to simplify the expressions. A particular instance of the general absorbing layer would be that of a thin resistance foil discussed by Schmitt (1957). This case is easily derived from the ensuing equations.

Consider first the outer absorbing layer of thickness $\delta_1 = a-b$ and index of refraction $N_1 = (\epsilon_1 \mu_1)^{1/2}$. The procedure of Weston and Hemenger is centered around the leading terms in the asymptotic approximations to the

coefficients corresponding to $A^{(1)}$, $B^{(1)}$ and $C^{(1)}$ in (25) to (27). For a thin layer with very large index of refraction, the function $Y^{(1)}$ has the following asymptotic form

$$Y^{(1)} \sim \frac{4}{\pi i} \frac{\sin k_1 \delta_1}{\sqrt{(k_1 a)(k_1 b)}} \tag{40}$$

where $k_1 \sim N_1 k$. With this approximation, the coefficients $A^{(1)}$, $B^{(1)}$ and $C^{(1)}$ take the form

$$A^{(1)} \pm \sqrt{\frac{\epsilon_1}{\mu_1}} \cot k_1 \delta_1 \frac{\left[A^{(2)} - \sqrt{\frac{\epsilon_1}{\mu_1}} \tan k_1 \delta_1\right]\left[B^{(2)} + \sqrt{\frac{\mu_1}{\epsilon_1}} \cot k_1 \delta_1\right] + \left[\frac{in\cos\beta}{kb\lambda_0^2} + C^{(2)}\right]^2}{\left[A^{(2)} + \sqrt{\frac{\epsilon_1}{\mu_1}} \cot k_1 \delta_1\right]\left[B^{(2)} + \sqrt{\frac{\mu_1}{\epsilon_1}} \cot k_1 \delta_1\right] + \left[\frac{in\cos\beta}{kb\lambda_0^2} + C^{(2)}\right]^2}, \tag{41}$$

$$B^{(1)} = \left\{\text{same thing with } \epsilon_1 \longleftrightarrow \mu_1 \text{ and } A^{(2)} \longleftrightarrow B^{(2)}\right\}, \tag{42}$$

$$C^{(1)} = \frac{\left[\frac{in\cos\beta}{kb\lambda_0^2} + C^{(2)}\right](1 + \cot^2 k_1 \delta_1)}{\left[A^{(2)} + \sqrt{\frac{\epsilon_1}{\mu_1}} \cot k_1 \delta_1\right]\left[B^{(2)} + \sqrt{\frac{\mu_1}{\epsilon_1}} \cot k_1 \delta_1\right] + \left[\frac{in\cos\beta}{kb\lambda_0^2} + C^{(2)}\right]^2} \tag{43}$$

and the quantity D in (24) now has the form

$$D = -\left(A^{(0)} - A^{(1)}\right)\left(A^{(0)} - B^{(1)}\right) - \left[\frac{in\cos\beta}{ka\lambda_0^2} - C^{(1)}\right]^2 \tag{44}$$

18

In deriving the above equations, we have taken the index of refraction of the second layer to be that of free space $(N_2 = 1)$.

The next layer is the free-space layer $b > r > c$ with coefficients $A^{(2)}$, $B^{(2)}$, $C^{(2)}$ given by

$$A^{(2)} = \frac{1}{\lambda_0} \frac{\partial \ln Y^{(2)}}{\partial(k_0 b)} \cdot \frac{\left[A^{(3)} - \frac{1}{\lambda_0} \frac{\partial}{\partial(k_0 c)} \left(\ln \frac{\partial Y^{(2)}}{\partial(k_0 b)}\right)\right]\left[B^{(3)} - \frac{1}{\lambda_0} \frac{\partial \ln Y^{(2)}}{\partial(k_0 c)}\right] + \left[\frac{in \cos\beta}{kc\lambda_0^2} - C^{(3)}\right]^2}{\left[A^{(3)} - \frac{1}{\lambda_0} \frac{\partial \ln Y^{(2)}}{\partial(k_0 c)}\right]\left[B^{(3)} - \frac{1}{\lambda_0} \frac{\partial \ln Y^{(2)}}{\partial(k_0 c)}\right] + \left[\frac{in \cos\beta}{kc\lambda_0^2} - C^{(3)}\right]^2}$$

(45)

$$B^{(2)} = \left\{ \text{same thing with } A^{(3)} \longleftrightarrow B^{(3)} \right\},$$

(46)

$$C^{(2)} = \frac{\frac{16}{\pi^2(k_0 b)(k_0 c)}\left[\frac{in\cos\beta}{kc\lambda_0^2} - C^{(3)}\right]\left[Y^{(2)}\right]^{-2}}{\left[A^{(3)} - \frac{1}{\lambda_0} \frac{\partial \ln Y^{(2)}}{\partial(k_0 c)}\right]\left[B^{(3)} - \frac{1}{\lambda_0} \frac{\partial \ln Y^{(2)}}{\partial(k_0 c)}\right] + \left[\frac{in\cos\beta}{kc\lambda_0^2} - C^{(3)}\right]^2}.$$

(47)

The third layer is another absorbing layer with thickness $\delta_3 = c-d$ and index of refraction $N_3 = (\epsilon_3 \mu_3)^{1/2}$. The coefficients of this layer are

$$A^{(3)} = \sqrt{\frac{\epsilon_3}{\mu_3}} \cot k_3 \delta_3 \frac{\left[A^{(4)} - \sqrt{\frac{\epsilon_3}{\mu_3}} \tan k_3 \delta_3\right]\left[B^{(4)} + \sqrt{\frac{\mu_3}{\epsilon_3}} \cot k_3 \delta_3\right] + \left[\frac{in \cos\beta}{kd\lambda_o} \frac{}{2}\right]^2}{\left[A^{(4)} + \sqrt{\frac{\epsilon_3}{\mu_3}} \cot k_3 \delta_3\right]\left[B^{(4)} + \sqrt{\frac{\mu_3}{\epsilon_3}} \cot k_3 \delta_3\right] + \left[\frac{in \cos\beta}{kd\lambda_o} \frac{}{2}\right]^2} \quad , \quad (48)$$

$$B^{(3)} = \left\{\text{same thing with } \epsilon_3 \longleftrightarrow \mu_3 \text{ and } A^{(4)} \longleftrightarrow B^{(4)}\right\} \quad , \quad (49)$$

$$C^{(3)} = \frac{\left[\frac{in\cos\beta}{kd\lambda_o} \frac{}{2}\right] (1 + \cot^2 k_3 \delta_3)}{\left[A^{(4)} + \sqrt{\frac{\epsilon_3}{\mu_3}} \cot k_3 \delta_3\right]\left[B^{(4)} + \sqrt{\frac{\mu_3}{\epsilon_3}} \cot k_3 \delta_3\right] + \left[\frac{in\cos\beta}{kd\lambda_o} \frac{}{2}\right]^2} \quad (50)$$

Finally, the last layer is the free-space layer $d > r > e$, where e is the radius of the perfectly conducting core. The coefficients of this air space are

$$A^{(4)} = \frac{1}{\lambda_o} \frac{\partial \ln Y^{(4)}}{\partial (k_o d)} \quad ,$$

$$B^{(4)} = \frac{1}{\lambda_o} \frac{1}{\partial (k_o d)} \left[\ln \frac{\partial Y^{(4)}}{\partial (k_o e)}\right] \quad , \quad (51)$$

$$C^{(4)} = 0 \quad .$$

In the equations concerning the two air gaps, the functions $Y^{(2)}$ and $Y^{(4)}$ are given by

$$Y^{(2)} = H^{(2)}(k_o b) H^{(1)}(k_o c) - H^{(1)}(k_o b) H^{(2)}(k_o c) \quad,$$

(52)

$$Y^{(4)} = H^{(2)}(k_o d) H^{(1)}(k_o e) - H^{(1)}(k_o d) H^{(2)}(k_o e) \quad.$$

This completes the specification of the scattered field.

In view of the above results, we can immediately obtain the field scattered by a conducting cylinder surrounded by a single absorbing layer which encloses an air space. In this case, the coefficients of the outer absorbing layer are given by (41) to (43); however, the coefficients of the inner free-space layer are identical in form to those in (51), namely

$$A^{(2)} = \frac{1}{\lambda_o} \frac{\partial \ell n Y^{(2)}}{\partial (k_o b)} \quad,$$

$$B^{(2)} = \frac{1}{\lambda_o} \frac{\partial}{\partial (k_o b)} \left[\ell n \frac{\partial Y^{(2)}}{\partial (k_o c)} \right] \quad,$$

(53)

$$C^{(2)} = 0 \quad,$$

and these are the only coefficients that appear since the problem is now a two layer problem.

2.4 Simplification in the Case of Two Resistance Foils.

The equations pertaining to thin absorbing layers may be further specialized to the case of thin resistive foils as considered by Schmitt (1957). To

accomplish this, the absorbing layers are assumed to be non-magnetic and to be characterized by a very large imaginary electric permittivity. Thus, for the outer layer we take

$$\mu_1 = 1, \quad \epsilon_1 \sim \frac{i\kappa_1}{\omega\epsilon_0} \tag{54}$$

where κ_1 is the conductivity of this layer. In addition, the wall thickness δ_1 is allowed to vanish at the same time the conductivity κ_1 is increased so that the product

$$\kappa_1 \delta_1 = \frac{1}{R_{s_1}} \tag{55}$$

remains constant. We may then write

$$\sqrt{\frac{\epsilon_1}{\mu_1}} \tan k_1 \delta_1 \sim i \frac{Z_0}{R_{s_1}} , \quad \sqrt{\frac{\epsilon_1}{\mu_1}} \cot k_1 \delta_1 \sim \frac{R_{s_1}\kappa_1}{k} , \tag{56}$$

where Z_0 is the free-space impedance $Z_0 = \sqrt{\frac{\mu_0}{\epsilon_0}} = 377$ ohms, and take the limit $\kappa_1 \longrightarrow \infty$ in the expressions (41) thru (43) for $A^{(1)}$, $B^{(1)}$, $C^{(1)}$. The quantity R_{s_1} represents the surface resistance of the outer foil. The following results are obtained

$$A^{(1)} = \left[A^{(2)} - i \frac{Z_o}{R_{s_1}} \right] + \frac{\left[\frac{in \cos\beta}{2} + C^{(2)} \right]^2}{B^{(2)} - i \frac{R_{s_1}}{Z_o}} \quad , \qquad (57)$$

$$B^{(1)} = \frac{1}{\frac{1}{B^{(2)}} + i \frac{Z_o}{R_{s_1}}} \quad , \qquad (58)$$

$$C^{(1)} = - i \frac{R_{s_1}}{Z_o} \frac{\frac{in \cos\beta}{2} + C^{(2)}}{B^{(2)} - i \frac{R_{s_1}}{Z_o}} \qquad (59)$$

The expressions for $A^{(2)}$, $B^{(2)}$, $C^{(2)}$ remain unchanged. The coefficients $A^{(3)}$, $B^{(3)}$, $C^{(3)}$ are similarly given by

$$A^{(3)} = \left[A^{(4)} - i \frac{Z_o}{R_{s_3}} \right] + \frac{\left[\frac{in \cos\beta}{2} \right]^2}{B^{(4)} - i \frac{R_{s_3}}{Z_o}} \quad , \qquad (60)$$

$$B^{(3)} = \frac{1}{\frac{1}{B^{(4)}} + i \frac{Z_o}{R_{s_3}}} \quad , \qquad (61)$$

$$C^{(3)} = - i \frac{R_{s_3}}{Z_o} \frac{\frac{in \cos\beta}{2}}{B^{(4)} - i \frac{R_{s_3}}{Z_o}} \qquad (62)$$

while the expressions for $A^{(4)}$, $B^{(4)}$, $C^{(4)}$ remain unchanged. We note that duality has now been sacrificed, since the layers have been taken to be non-magnetic. The specialization to a single-foil structure is accomplished, as previously indicated, by employing (53) in place of (45) thru (47). The scattering of a plane wave normally incident on such a single-foil structure was derived by Schmitt (1957). Our results, when reduced to normal incidence $(\beta = \frac{\pi}{2})$, agree with his.

III

CURRENT MEASUREMENTS ON FINITE HOLLOW CYLINDERS

A series of measurements have been carried out to determine the currents induced on finite, hollow, conducting, circular cylinders by an incident plane electromagnetic wave. The measurements were restricted to obtaining the magnitude and phase of particular current components in the vicinity of the leading end of the cylinders, both inside and outside, where the term leading end is used to refer to the end of the cylinder directed toward the transmitter. Two orientations of the cylinders and two different cylinders were involved in the measurements which were performed at 3.03 GHz. The orientations correspond to end-on incidence (incident propagation vector along the axis) and 30° from end-on (where the propagation vector makes an angle of 30° with the cylinder axis). The two cylinders, both the same diameter, were distinguished from each other in that one had both ends open, whereas the other had its rear end capped or closed. The inner diameter, outer diameter and length of the open cylinder were 4.375", 4.5" and 33.125", respectively. The length of the closed-end cylinder was 33.375".

The measurements were carried out in an anechoic chamber, with the current measured by a small loop probe, which was suspended vertically from the ceiling. The incident field was horizontally polarized, thus minimizing a any interference effects of the probe lead.

Slots were cut into the cylinders to permit insertion of the probe into the cylinder, so that the internal currents may be probed. As shown in Fig. 1a, the probe was inserted only far enough so that the measurements essentially

were of the inside currents. Two kinds of slots were required: very short circumferential slots and a long axial slot. These were oriented along the expected direction of current flow in order to minimize radiation from the slots. The internal circumferential and axial currents are measured only at the appropriate slots; i.e., the axial currents are not probed through the short slots. The external surface fields were measured with all slots concealed by conducting tape.

For oblique incidence, the cylinders were tipped sideways, so that the probe lead still remains perpendicular to the direction of incident polarization. The axis of the cylinder thus lies in the plane of incident polarization. This is shown in Fig. 1, where the axis of the cylinder is taken to be the z-axis of a rectangular Cartesian coordinate system. The leading end of the cylinder lies on the xy plane, with the xz plane being the plane of polarization. For Fig. 1, the angle α is the angle of incidence, thus, for the end-on case, α is zero, and for the other series of measurements α is 30°. The longitudinal current component (directed parallel to the z-axis) will be denoted by j_z, and the circumferential component by j_θ. In referring to a position on the cylinder, the parameter z and θ will be used, with z referring to distance along a generator measured from the leading end, and θ referring to angular position measured from the x-axis. The following series of measurements were performed:

Measurement Order	Surface Measured	Angular Position θ	Current Component	Incident Angle α
1	Outside	0	j_z	0
2	Inside	0	j_z	0
3	Outside	$\pi/2$	j_θ	0
4	Inside	$\pi/2$	j_θ	0
5	Outside	0	j_z	30°
6	Inside	0	j_z	30°
7	Inside	π	j_z	30°
8	Outside	$\pi/2$	j_z	30°
9	Inside	$\pi/2$	j_z	30°
10	Outside	$\pi/2$	j_θ	30°
11	Inside	$\pi/2$	j_θ	30°

Each measurement order consisted of measuring the indicated current component, at discrete intervals along a generator of the cylinder starting at the leading edge. This measurement was performed for both the open and closed rear end cylinders. The angular position given by θ indicates that the measurements were either along the top of the cylinders $(\theta = \frac{\pi}{2})$ or the sides $(\theta = 0$ or $\pi)$, see Fig. 1.

Each measurement was calibrated by measurements upon a sphere of known size. Different probes were required for measurements along the sides and tops of the cylinders, see Fig. 1a. In order to have a meaningful calibration, the same probe used for the cylinder measurement was used for the sphere calibration. Since the probe must be held normal to the surface of the sphere, and the orientation of the plane of the probe with respect to the probe lead cannot be changed once it is set, only certain points of the sphere can be used for calibration. Using computed values for the currents on a sphere (Ducmanis and Liepa, 1965), the current component j_z along the sides of the cylinder were calibrated with the measured current component in front of the sphere. The current components on top of the cylinders were calibrated against the measured current component on the top of the sphere.

The resulting current measurements, both phase and amplitude, are presented in Figs. 2 to 45. The magnitude of the current has been normalized with respect to the incident field, which as calibrated as indicated above, for each series of measurements described by the pair of figures giving phase and amplitude of the current along a specific generator of a particular cylinder. An exception to this is the measurement of current magnitude given in Fig. 10. Here it was normalized with respect to the calibrated incident field associated with the measurement series given by Fig 12. In addition, it should be recalled that the phases of the current components are relative.

A block diagram of the basic receiving system is shown in Fig 46. In this arrangement, the probe signal is compared to a controllable reference signal in a hybrid tee, after the reference signal has passed through a coaxial switch. When the switch is closed, both signals are present and the operator commences tuning both the attenuator and the phase shifter in the reference arm, seeking a null indication (no signal) on the receiver. When he has obtained a

null, signifying that reference and probe signals have the same amplitude but opposite phase, he records the phase shifter setting. The switch is then thrown open, permitting only the probe signal to enter the receiver circuits; the signal level is then displayed at the receiver output and the operator records the amplitude. Thus, the phase measurement is performed with the switch closed and the amplitude is measured with the switch open. During the measurement, of course, the probe is held at the desired point on the surface to be probed; it is moved to the next position of interest only when the above sequence is completed.

This scheme is the one adapted in lieu of a more conventional system in which both phase and attenuation values are read from the dial settings of the respective devices. Here, the receiver linearity over a 40 db range is utilized in the place of the attenuator. All the phase angles determined this way are relative.

The phase shifter settings are directly proportional to the relative phase angle measured. The relative phase is obtained by multiplying the phase shifter settings by the frequency used (in GHz). A phase shifter setting of 32.0 at 3.00 GHz, therefore, implies a phase angle of 96.0 degrees.

As the measured phase progressively advances, the required phase shifter setting for the nulling process approaches the limit of its capability. Then a new setting must be sought which is electrically 360° from this limit and the raw data shows a sudden shift in the dial settings. When this occurs, the operator records both values so that the remainder of the readings may be related to those previously obtained. These two values, when multiplied by the frequency in GHz, are usually very nearly 360° apart.

During the course of a measurement run, the range operator plots the
amplitude values as they are recorded, showing the trend of the measurements.
This technique helps him spot any anomalous behavior due to recording or
positioning errors at or near the time they occur, permitting him to go back
and re-examine the datum point in question.
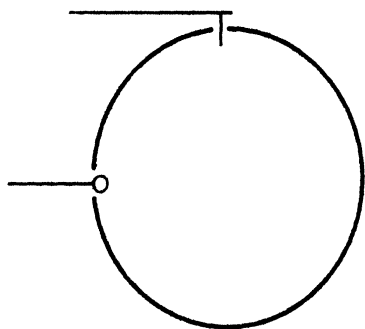
FIG. 1a: PROBE POSITIONS THROUGH THE SLOTS.

Direction of Incident Propagation
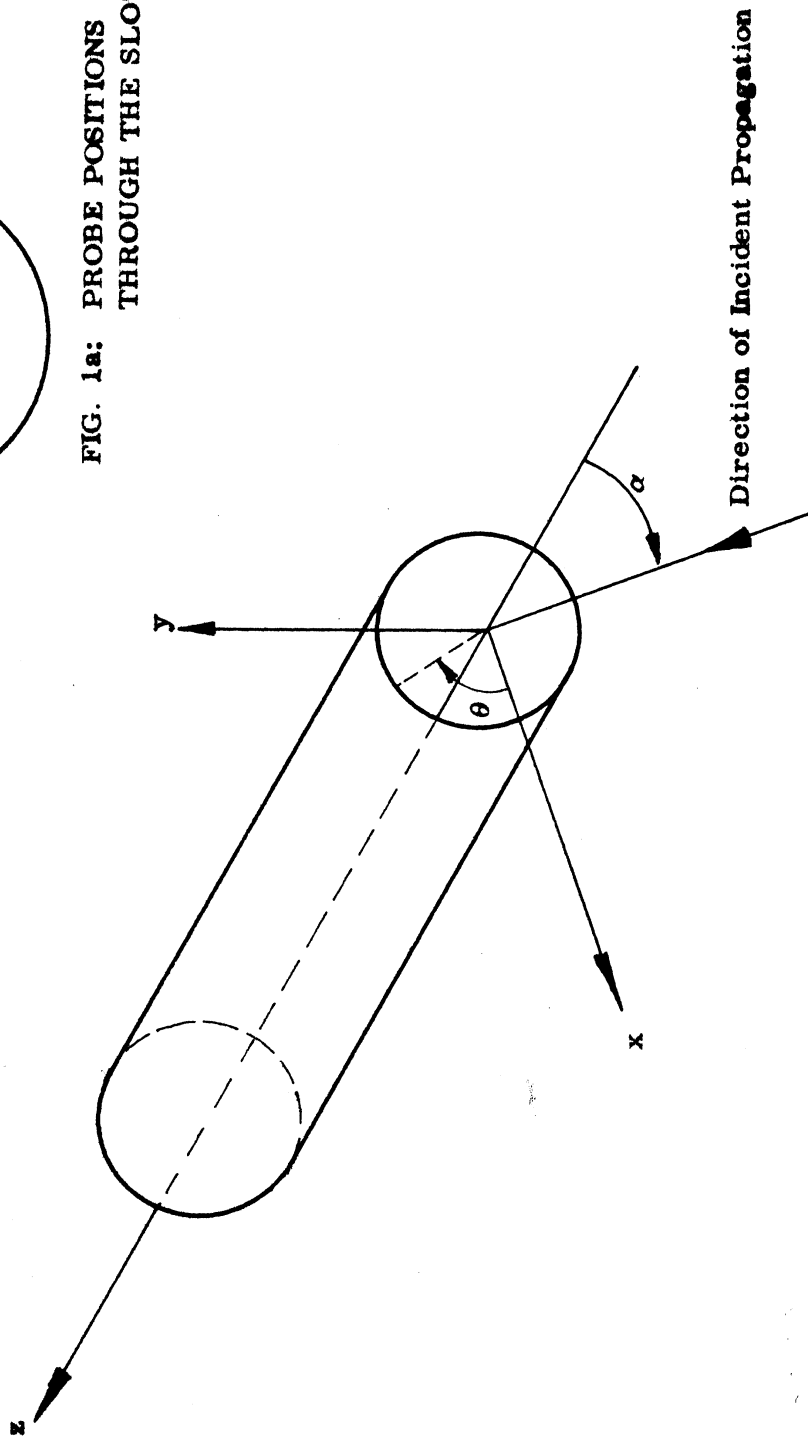
FIG. 1: COORDINATE SYSTEM FOR THE CYLINDER.
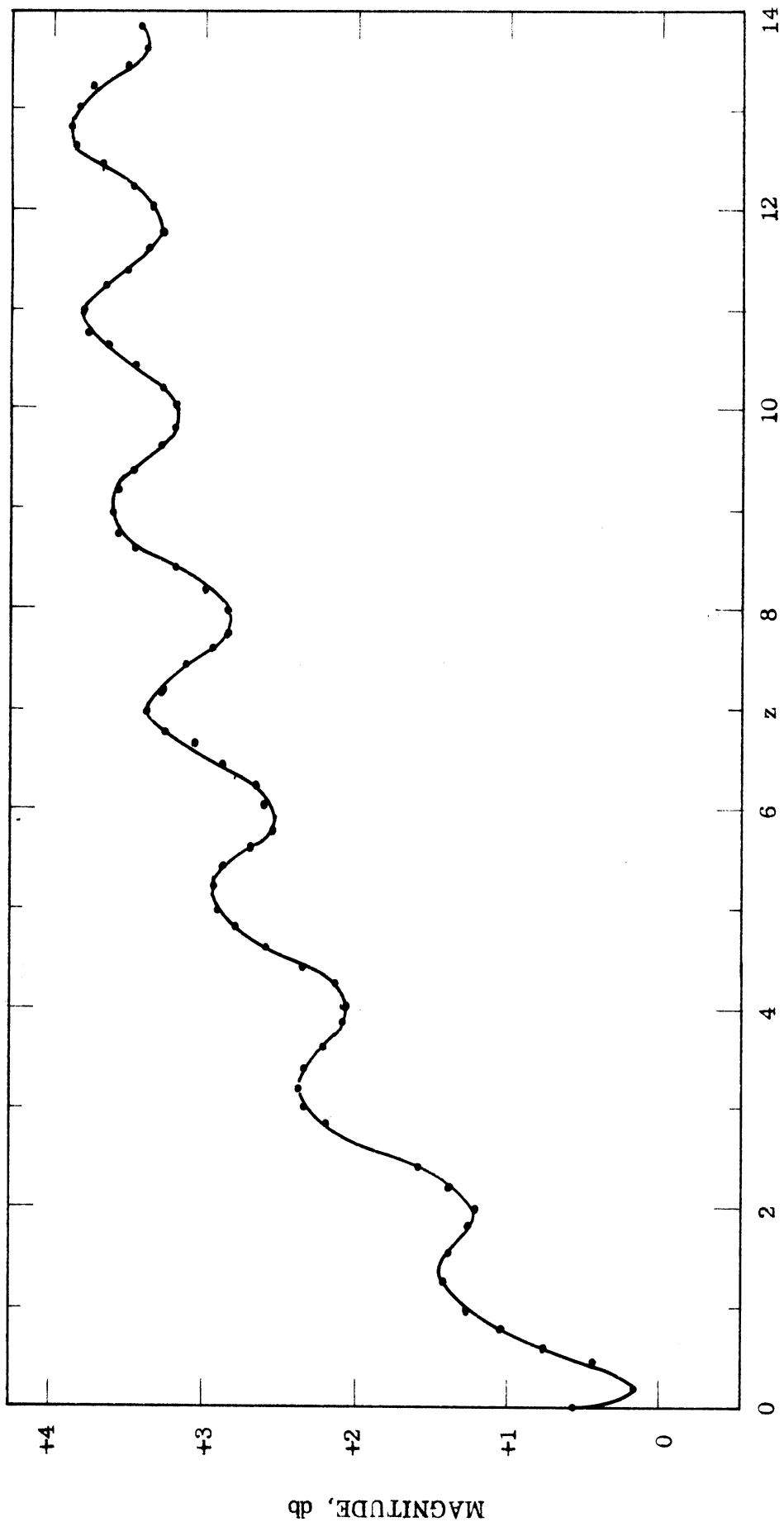
FIG. 2: MAGNITUDE OF CURRENT COMPONENT j_z OUTSIDE OF OPEN CYLINDER. ($\theta = 0$, $\alpha = 0$)
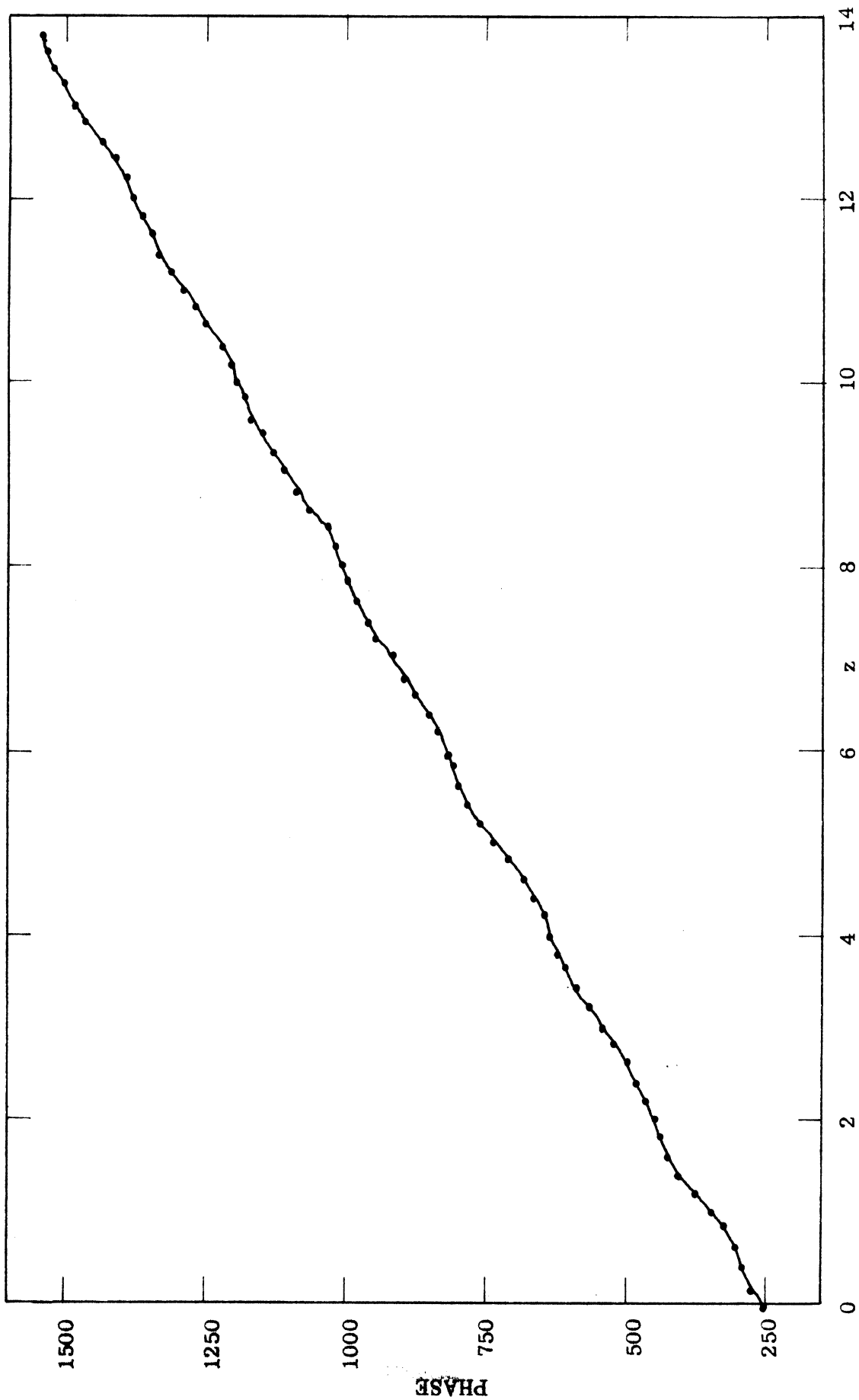
FIG. 3: PHASE OF CURRENT COMPONENT j_z OUTSIDE OF OPEN CYLINDER. $(\theta = 0, \ \alpha = 0)$
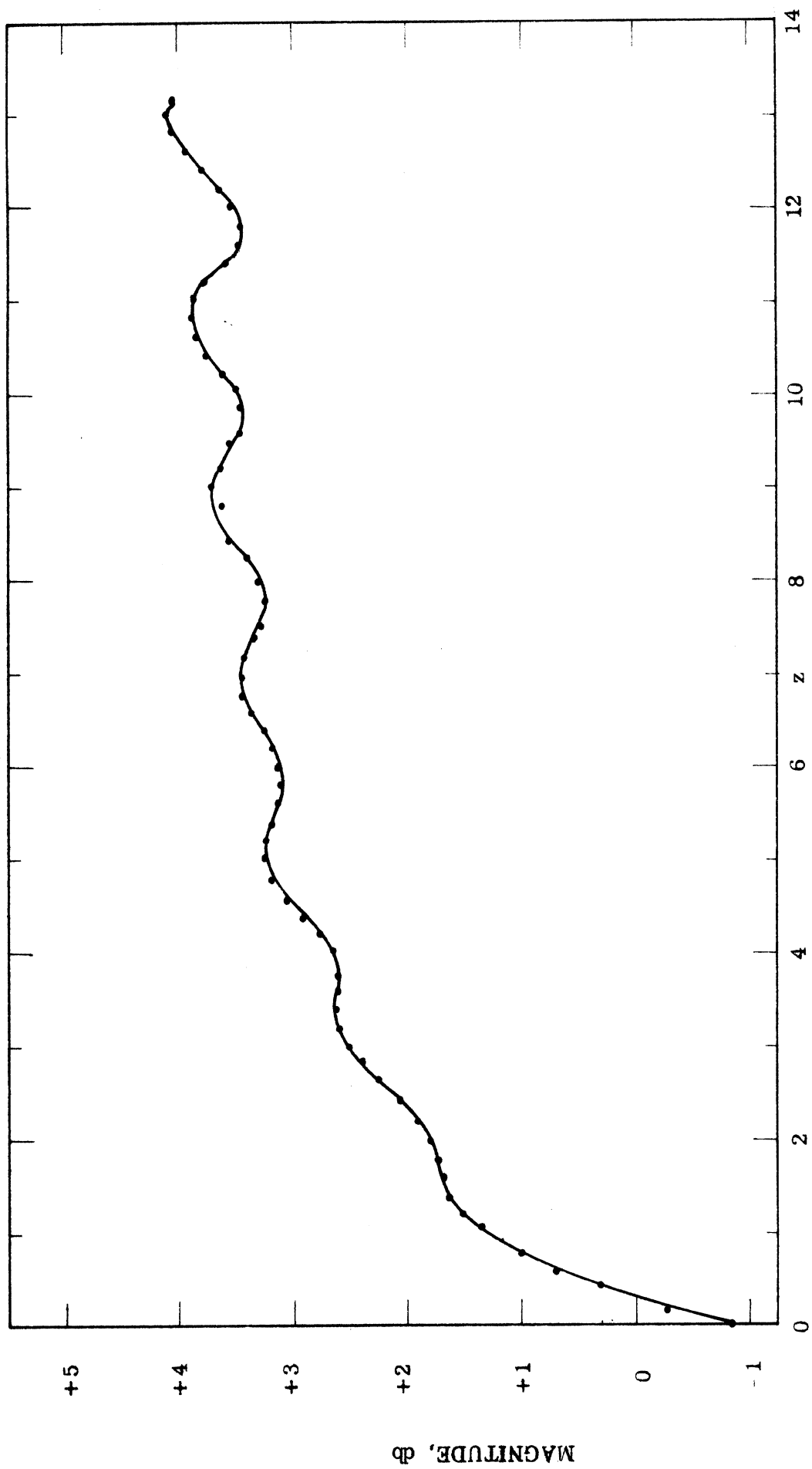
FIG. 4: MAGNITUDE OF CURRENT COMPONENT j_z OUTSIDE OF CLOSED CYLINDER. ($\theta = 0$, $\alpha = 0$)
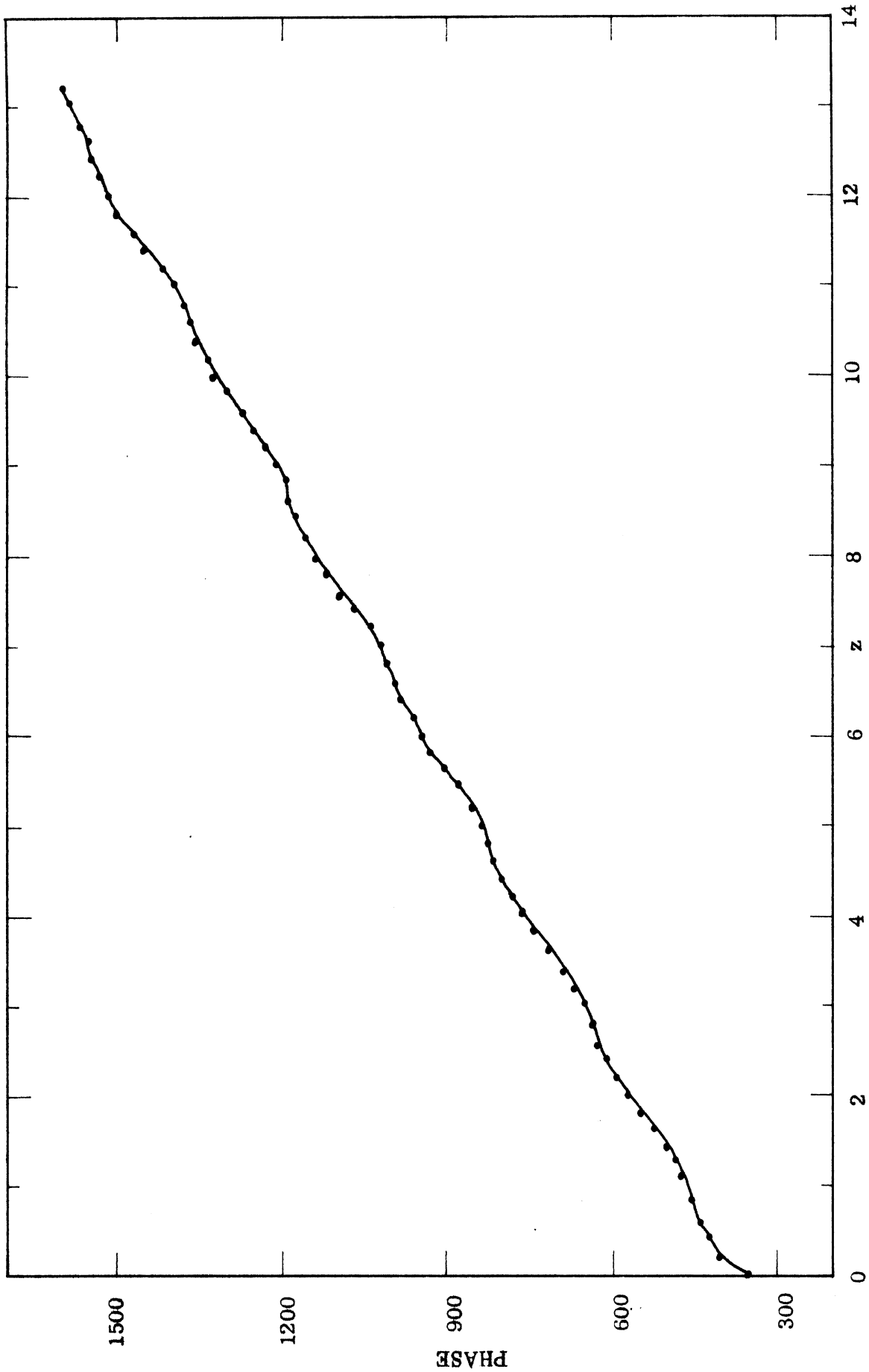
FIG. 5: PHASE OF CURRENT COMPONENT j_z OUTSIDE OF CLOSED CYLINDER. ($\theta = 0$, $\alpha = 0$)
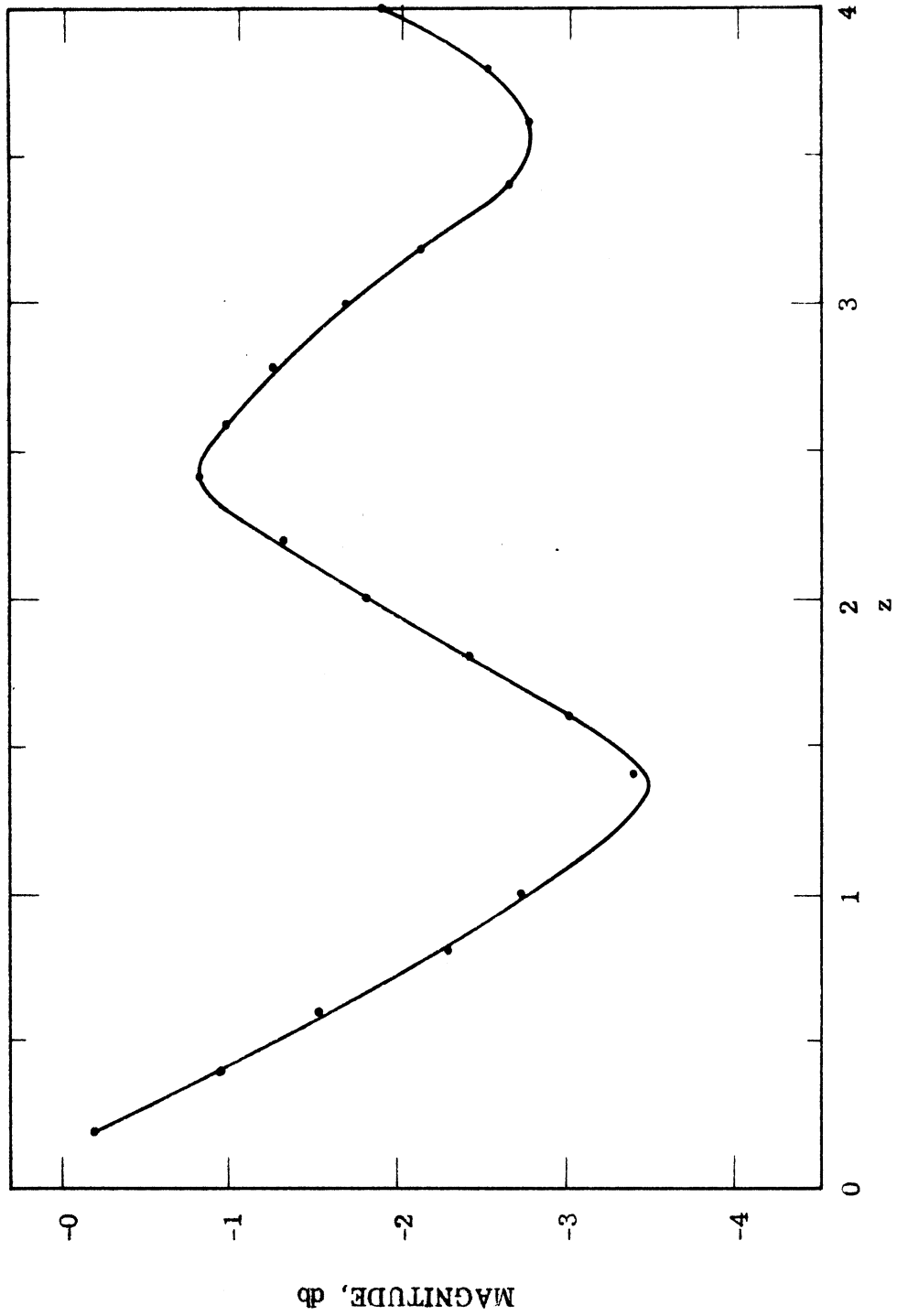
FIG. 6: MAGNITUDE OF CURRENT COMPONENT j_z INSIDE OPEN CYLINDER. $(\theta = 0, \alpha = 0)$
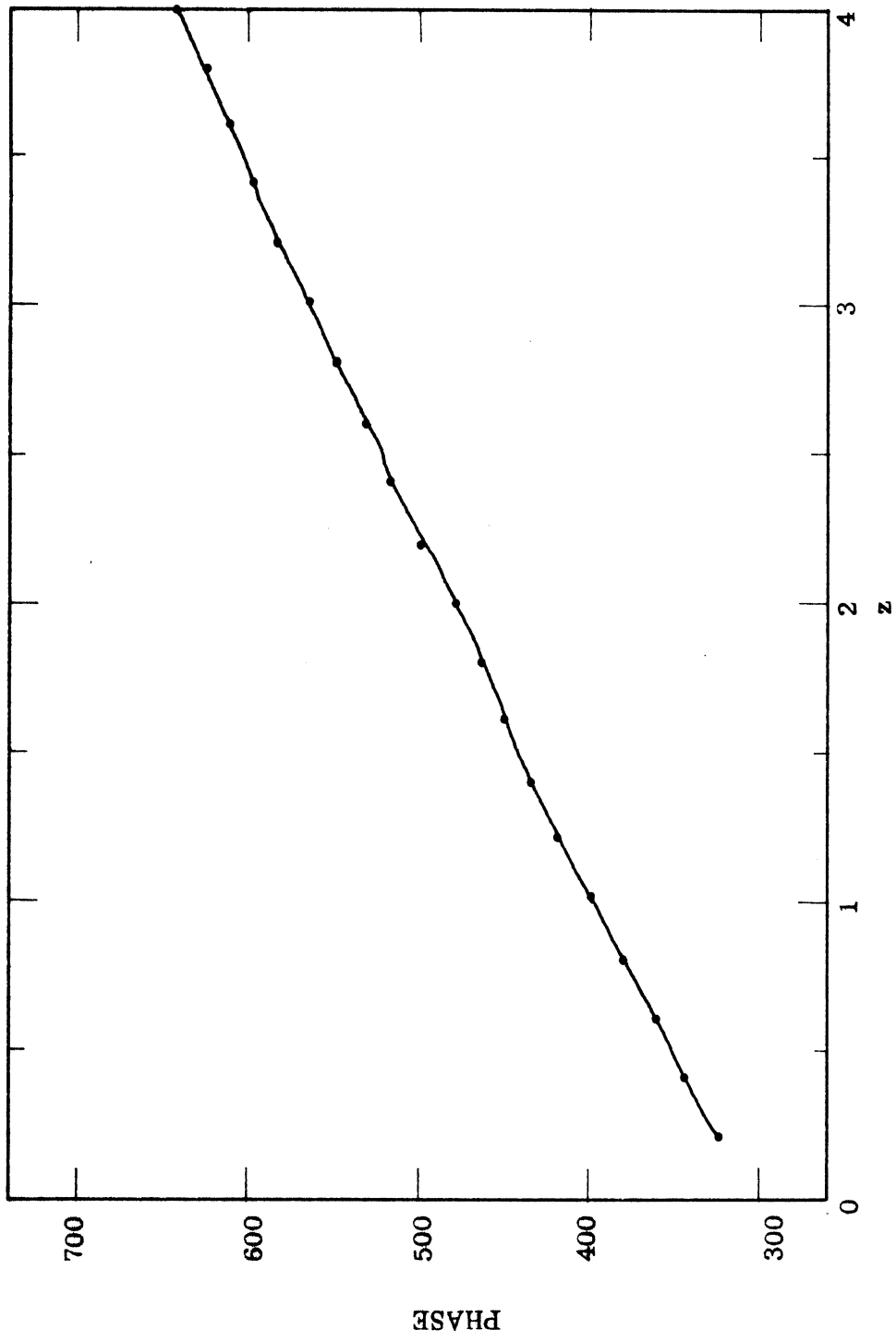
FIG. 7: PHASE OF CURRENT COMPONENT j_z INSIDE OPEN CYLINDER. $(\theta=0, \alpha=0)$
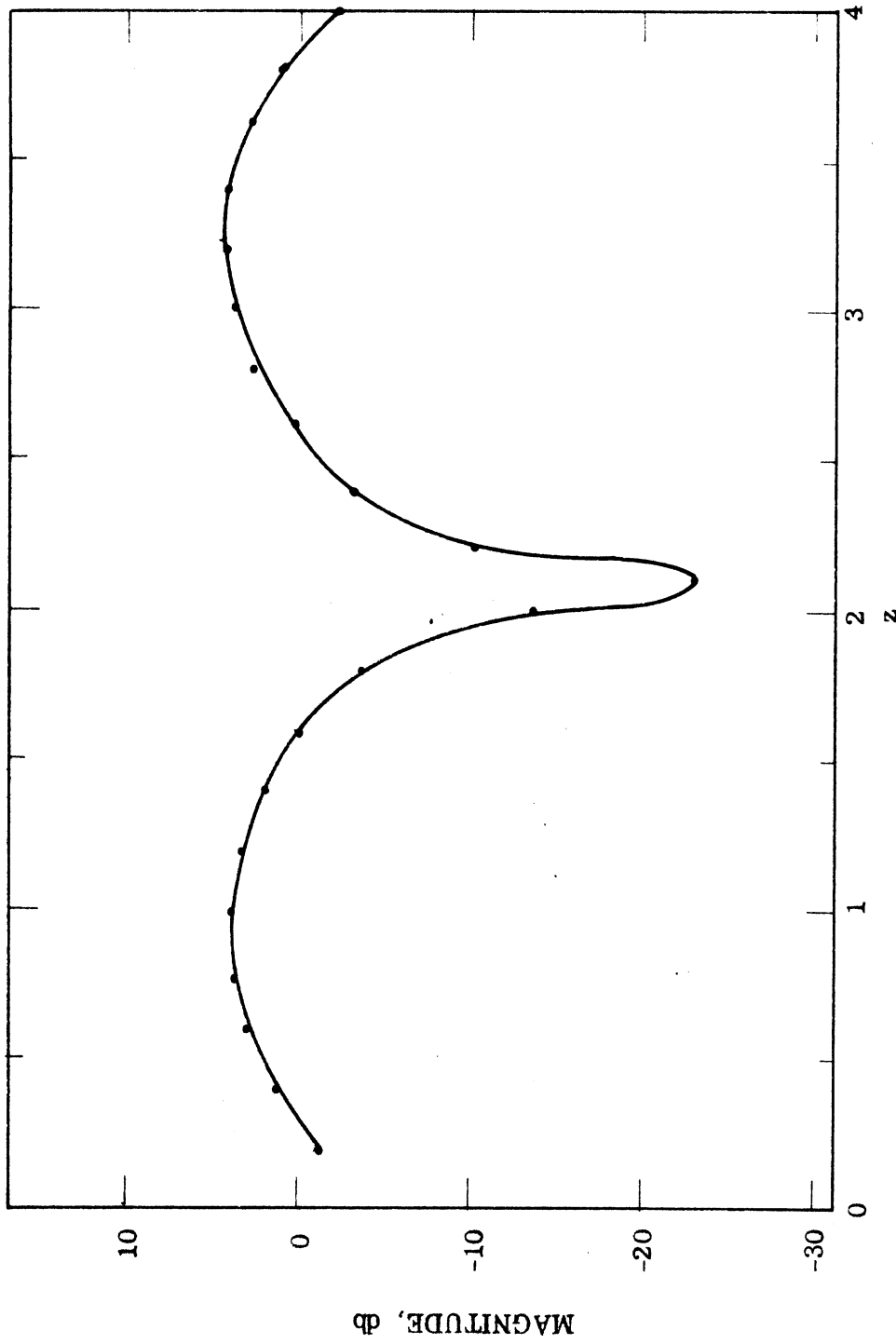
FIG. 8: MAGNITUDE OF CURRENT COMPONENT j_z INSIDE CLOSED CYLINDER. $(\theta = 0, \alpha = 0)$
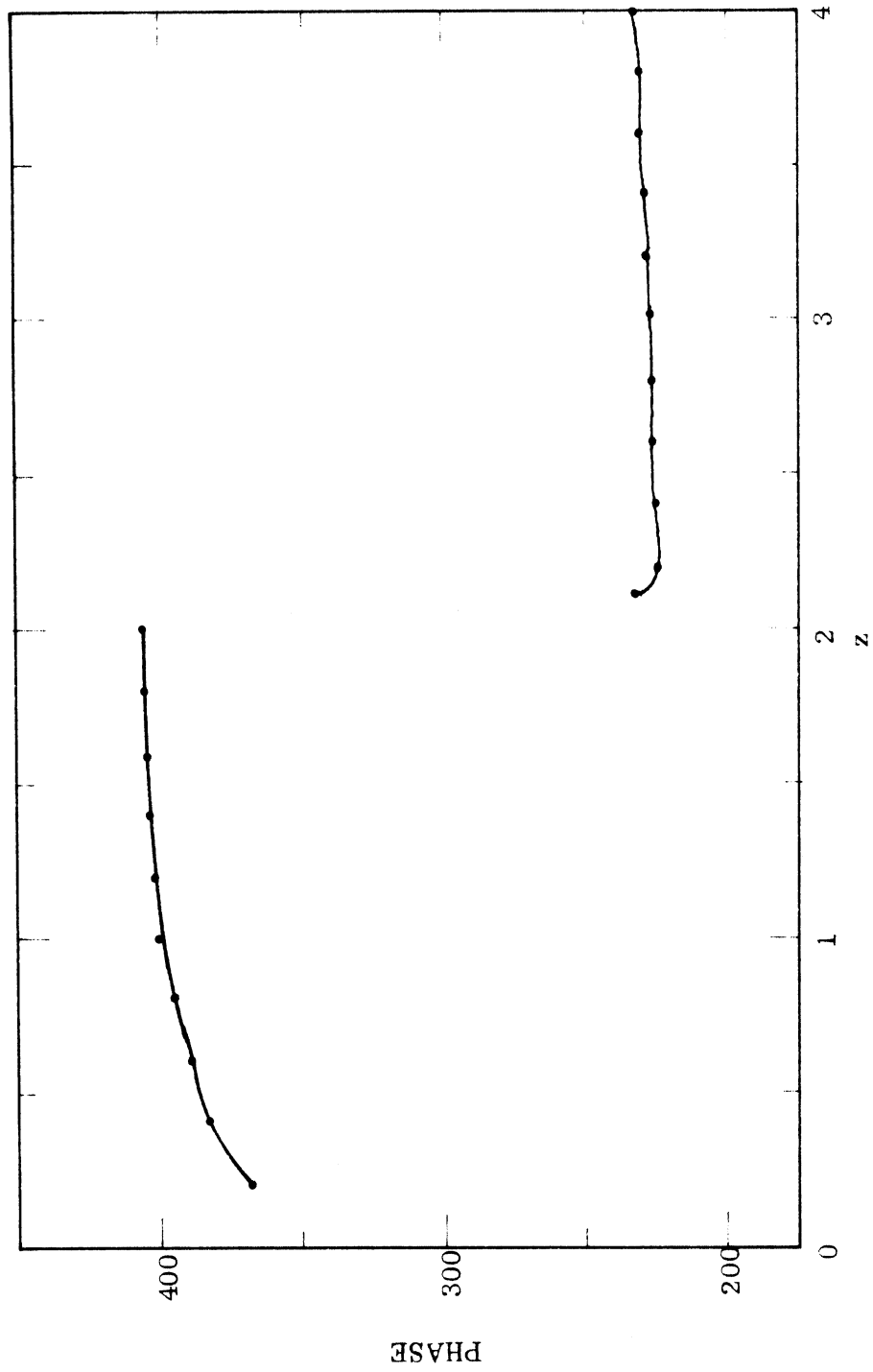
FIG. 9: PHASE OF CURRENT COMPONENT j_z INSIDE CLOSED CYLINDER. $(\theta = 0, \ \alpha = 0)$
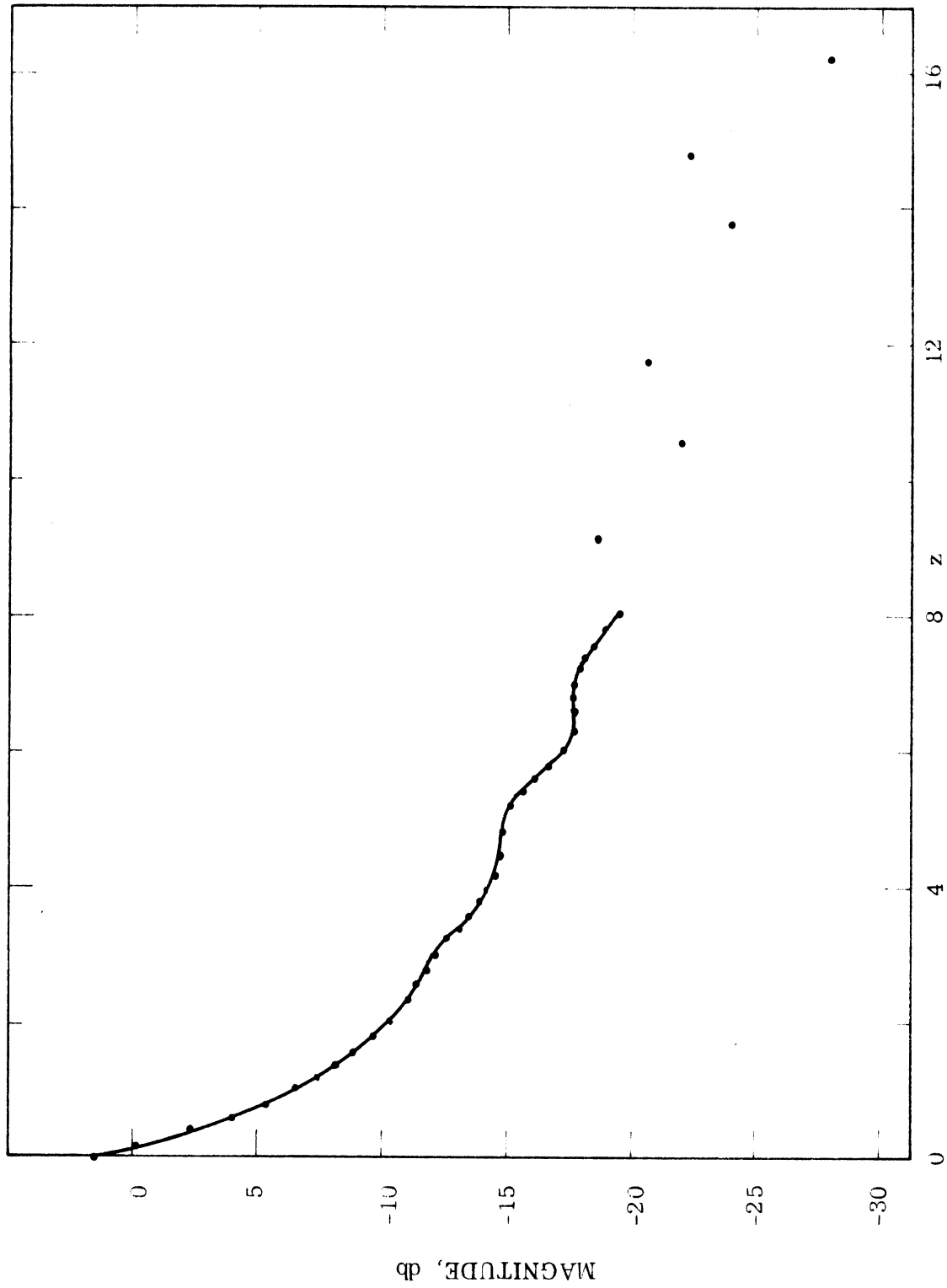
FIG. 10: MAGNITUDE OF CURRENT COMPONENT j_θ OUTSIDE OPEN CYLINDER. $(\theta = \frac{\pi}{2}, \alpha = 0)$
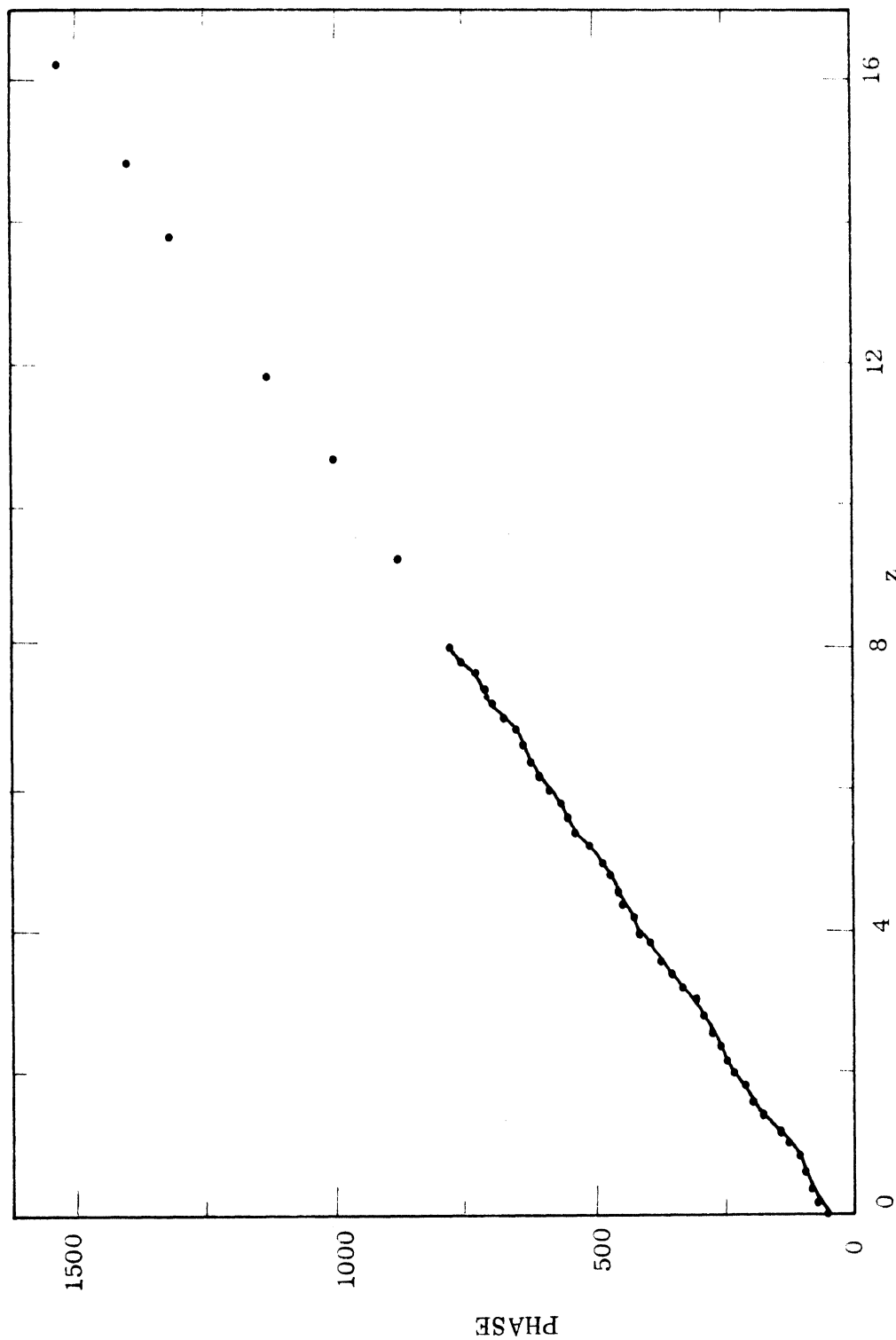
FIG. 11: PHASE OF CURRENT COMPONENT j_θ OUTSIDE OPEN CYLINDER. $(\theta = \frac{\pi}{2}, \quad \alpha = 0)$
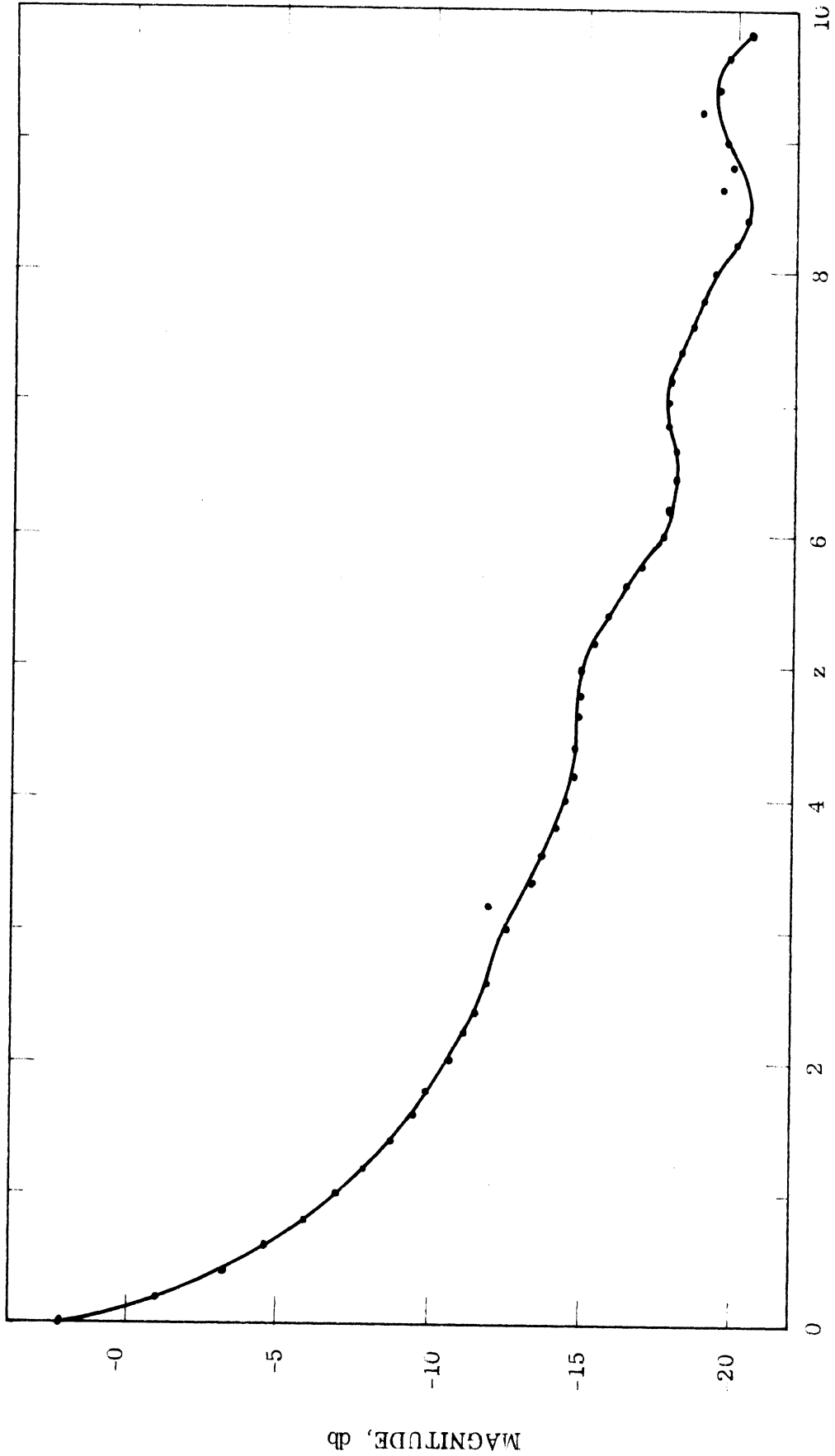
FIG 12: MAGNITUDE OF CURRENT COMPONENT j_θ OUTSIDE OF CLOSED CYLINDER. $(\theta = \frac{\pi}{2}, \ \alpha = 0)$
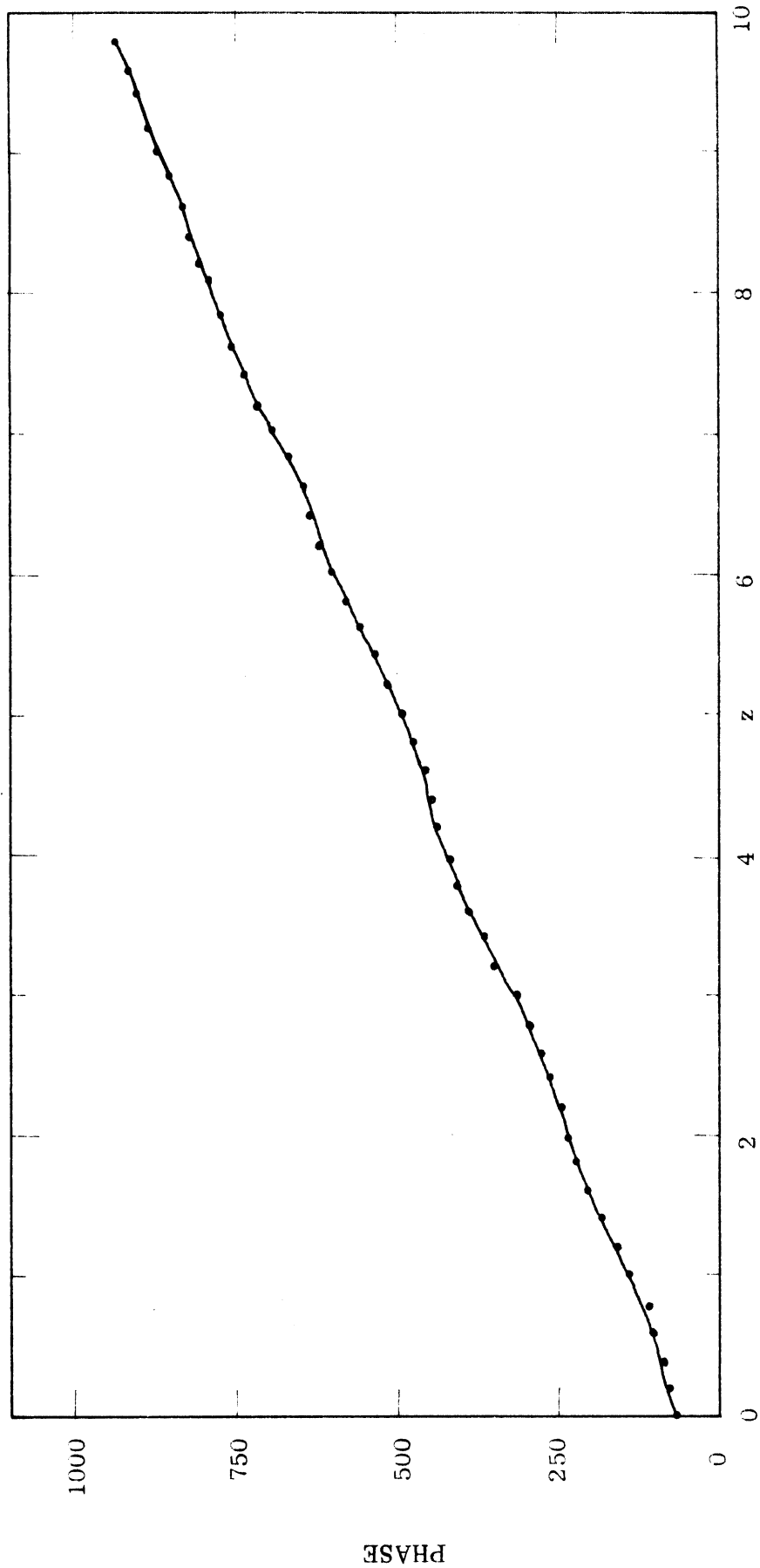
FIG 13: PHASE OF CURRENT COMPONENT j_θ OUTSIDE OF CLOSED CYLINDER. $(\theta = \frac{\pi}{2}, \alpha = 0)$
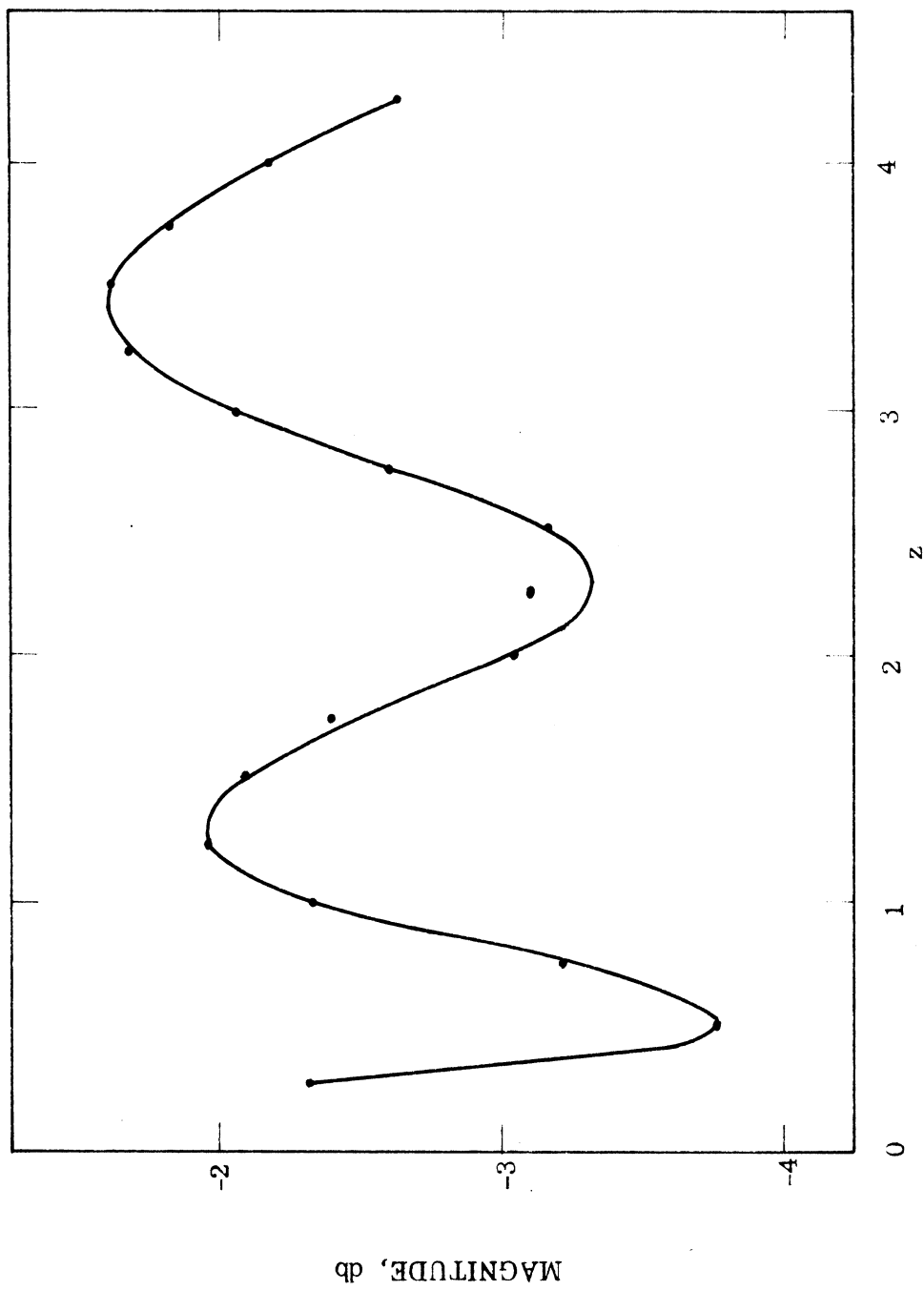
FIG. 14: MAGNITUDE OF CURRENT COMPONENT j_θ INSIDE OPEN CYLINDER. $(\theta = \frac{\pi}{2}, \alpha = 0)$
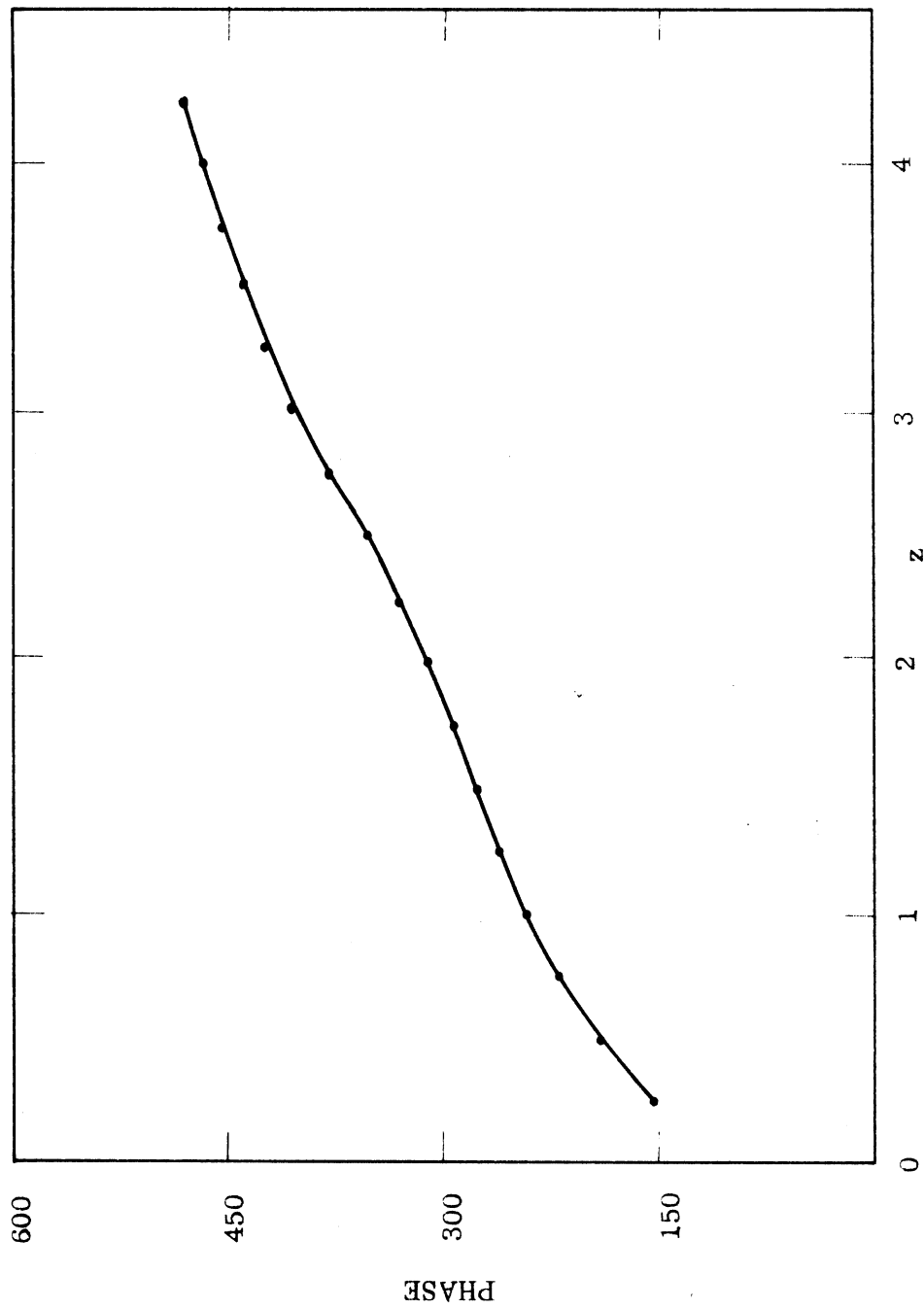
FIG. 15: PHASE OF CURRENT COMPONENT j_θ INSIDE OPEN CYLINDER. $(\theta = \frac{\pi}{2}, \alpha = 0)$
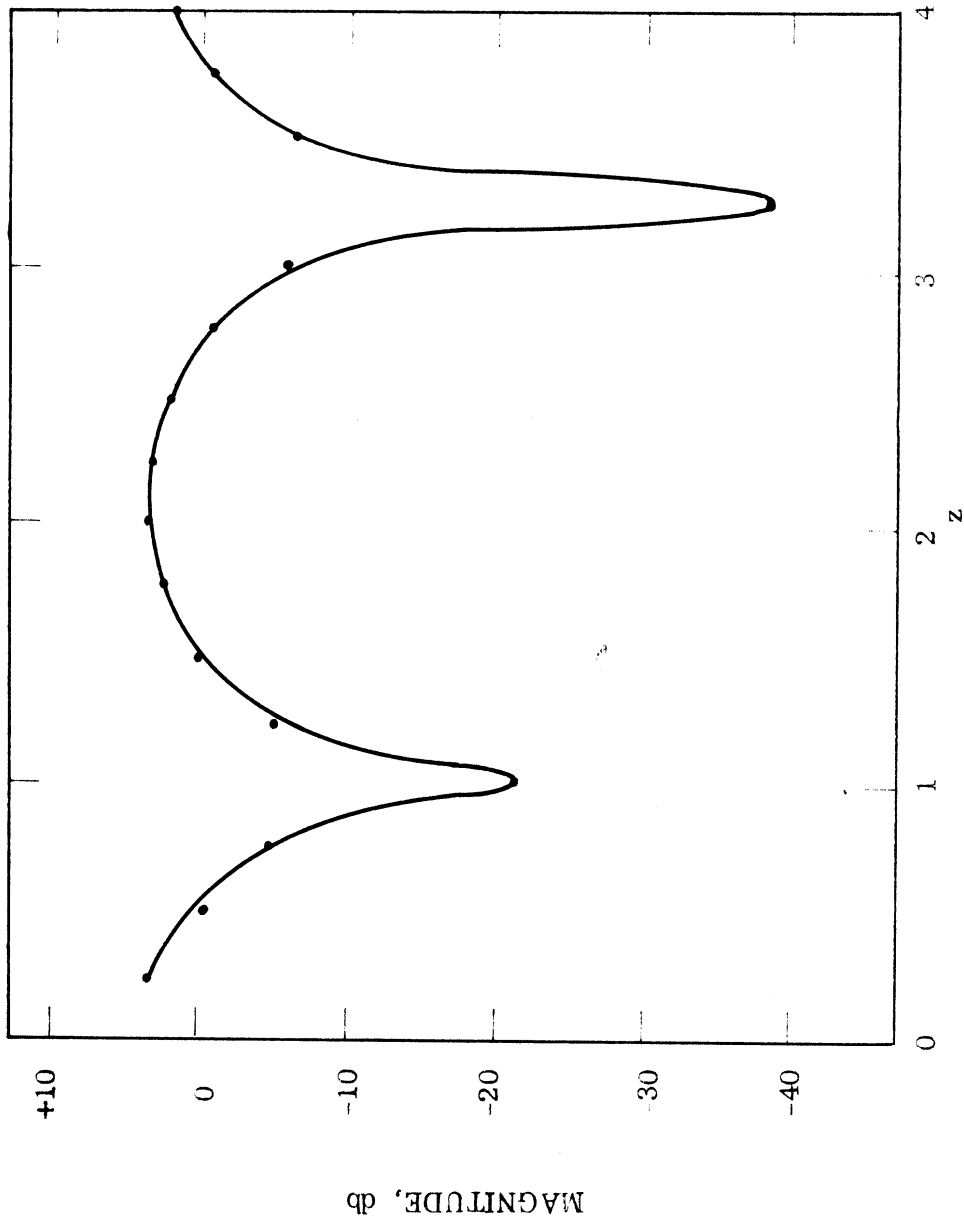
FIG 16: MAGNITUDE OF CURRENT COMPONENT j_θ INSIDE CLOSED CYLINDER. $(\theta = \frac{\pi}{2}, \sigma = 0)$
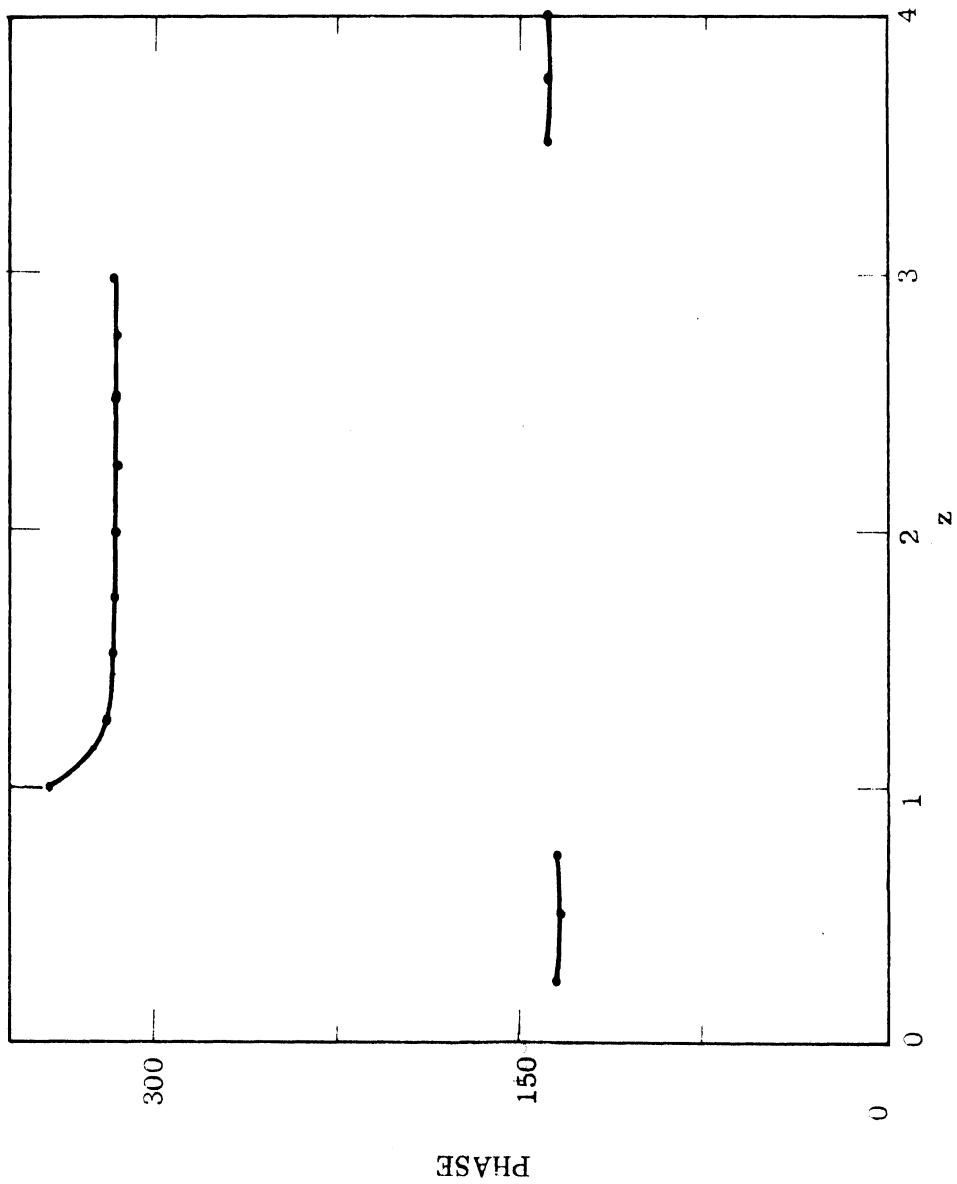
FIG. 17: PHASE OF CURRENT COMPONENT j_θ INSIDE CLOSED CYLINDER. $(\theta = \frac{\pi}{2}, \; \alpha = 0)$
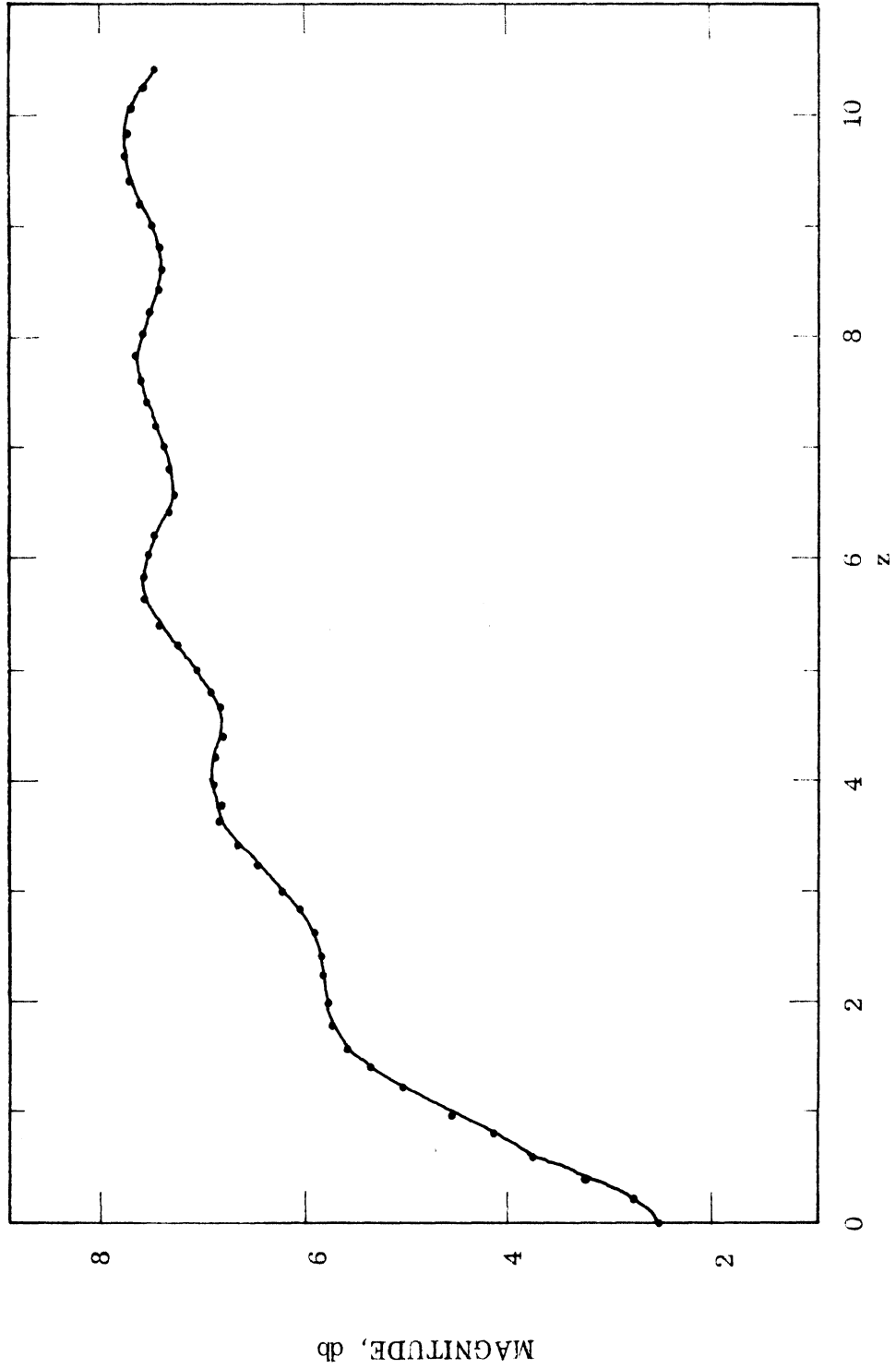
FIG. 18: MAGNITUDE OF CURRENT COMPONENT j_z ON OUTSIDE OF ILLUMINATED SIDE OF OPEN CYLINDER. $(\theta = 0, \ \alpha = 30^{\circ})$
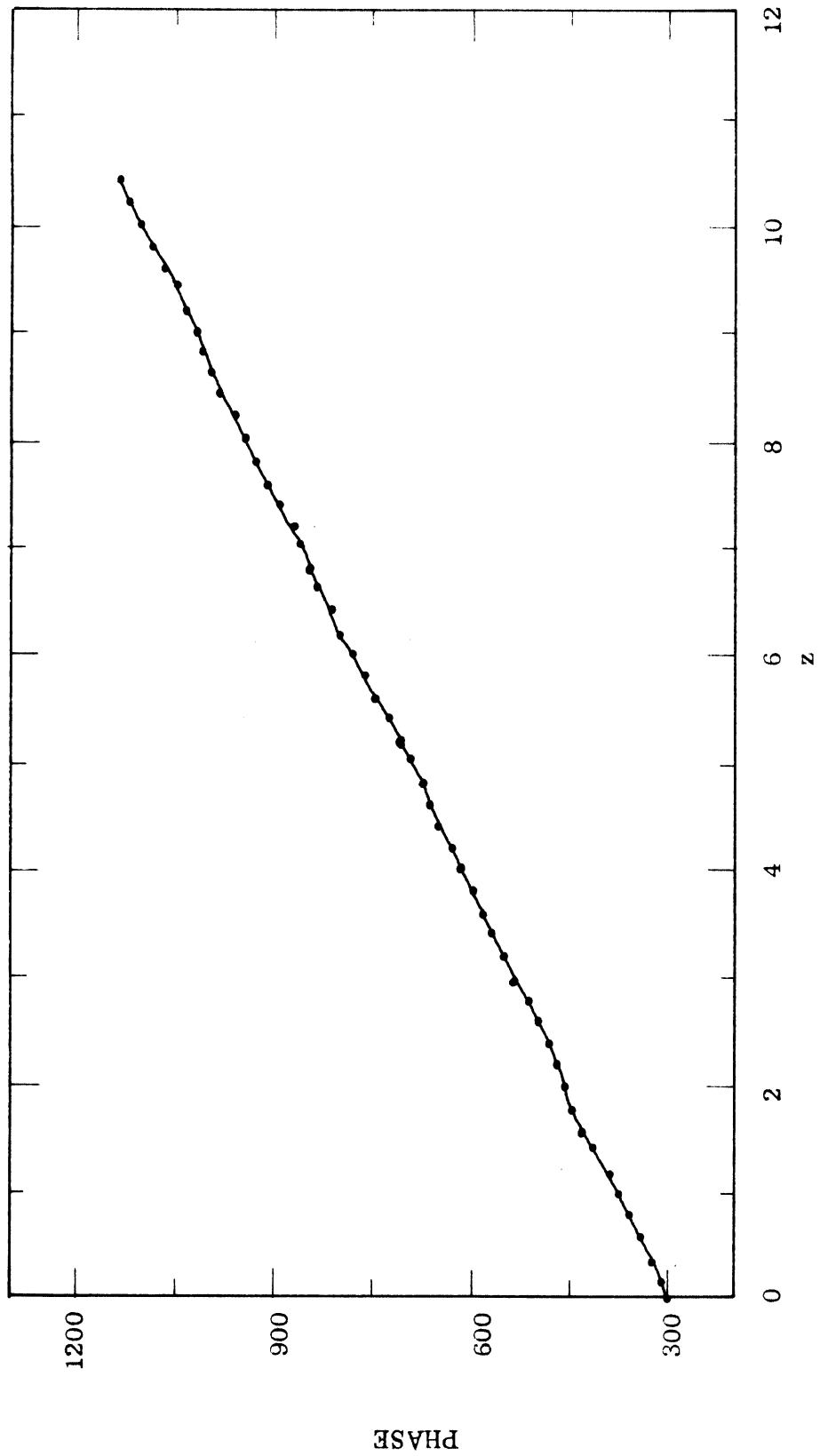
FIG. 19: PHASE OF CURRENT COMPONENT j_z ON OUTSIDE OF ILLUMINATED SIDE OF OPEN CYLINDER. $(\theta = 0, \ \alpha = 30^{\circ})$
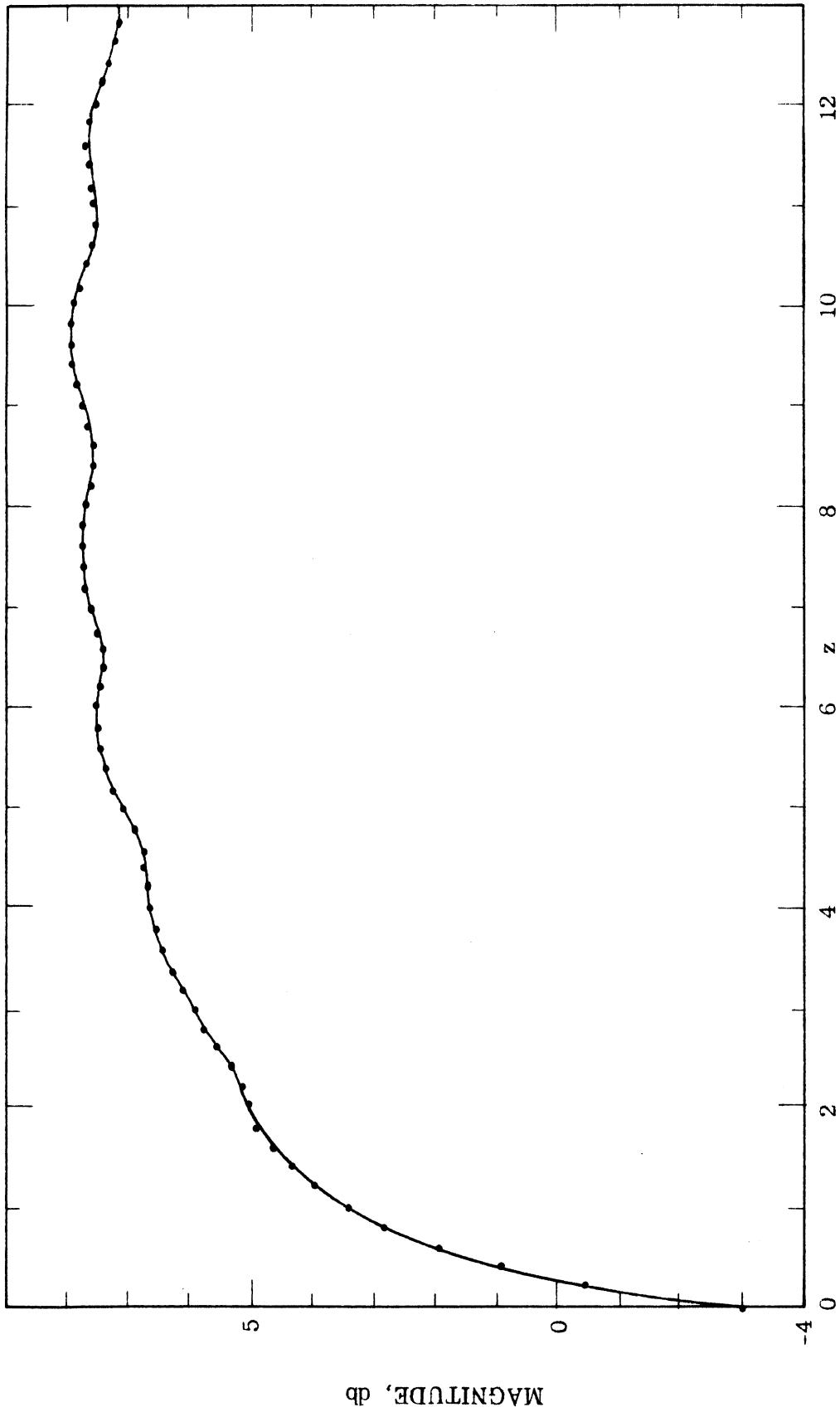
FIG. 20: MAGNITUDE OF CURRENT COMPONENT j_z ON OUTSIDE OF ILLUMINATED SIDE OF CLOSED CYLINDER. $(\theta = 0, \ \alpha = 30^{\circ})$
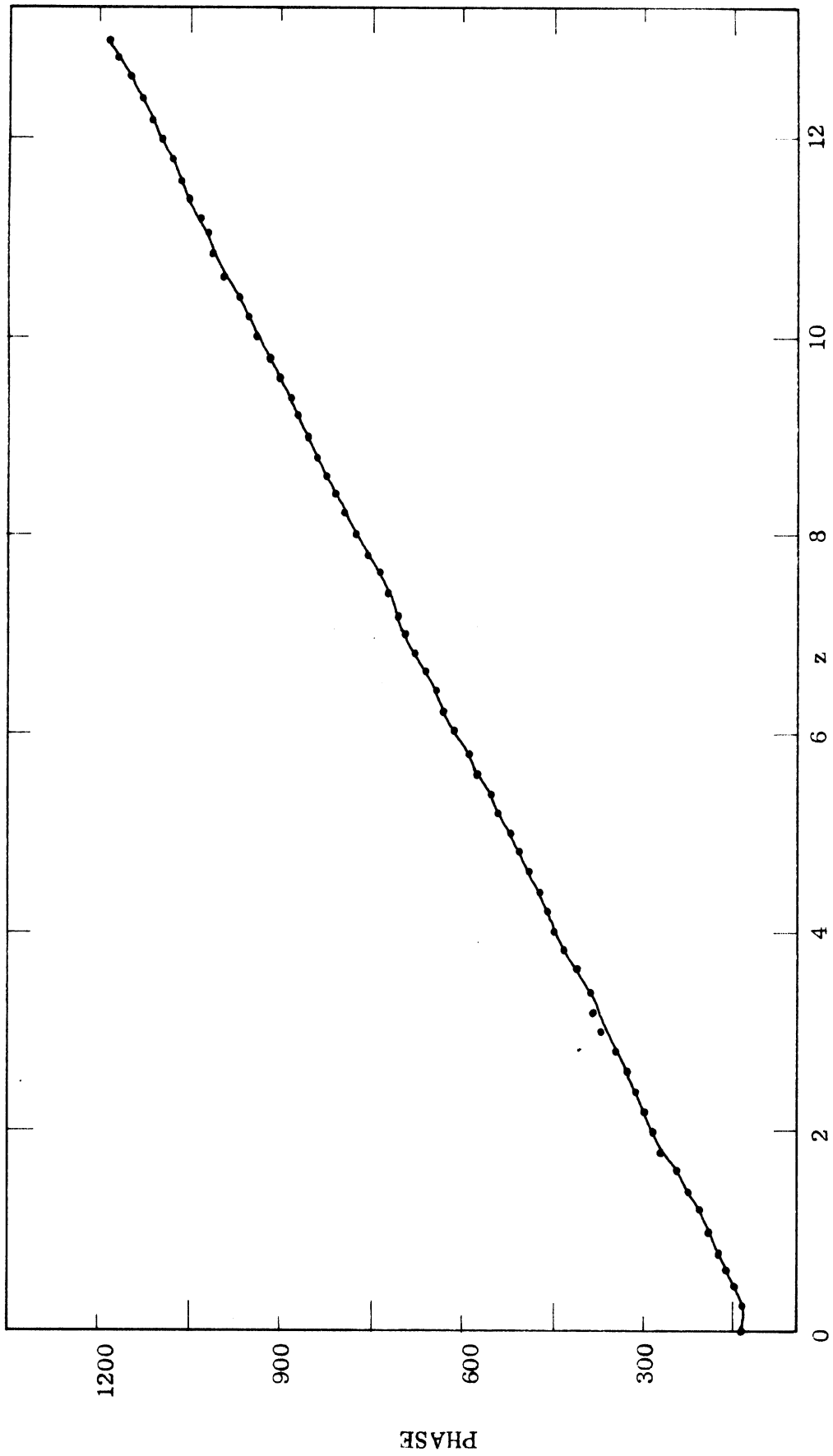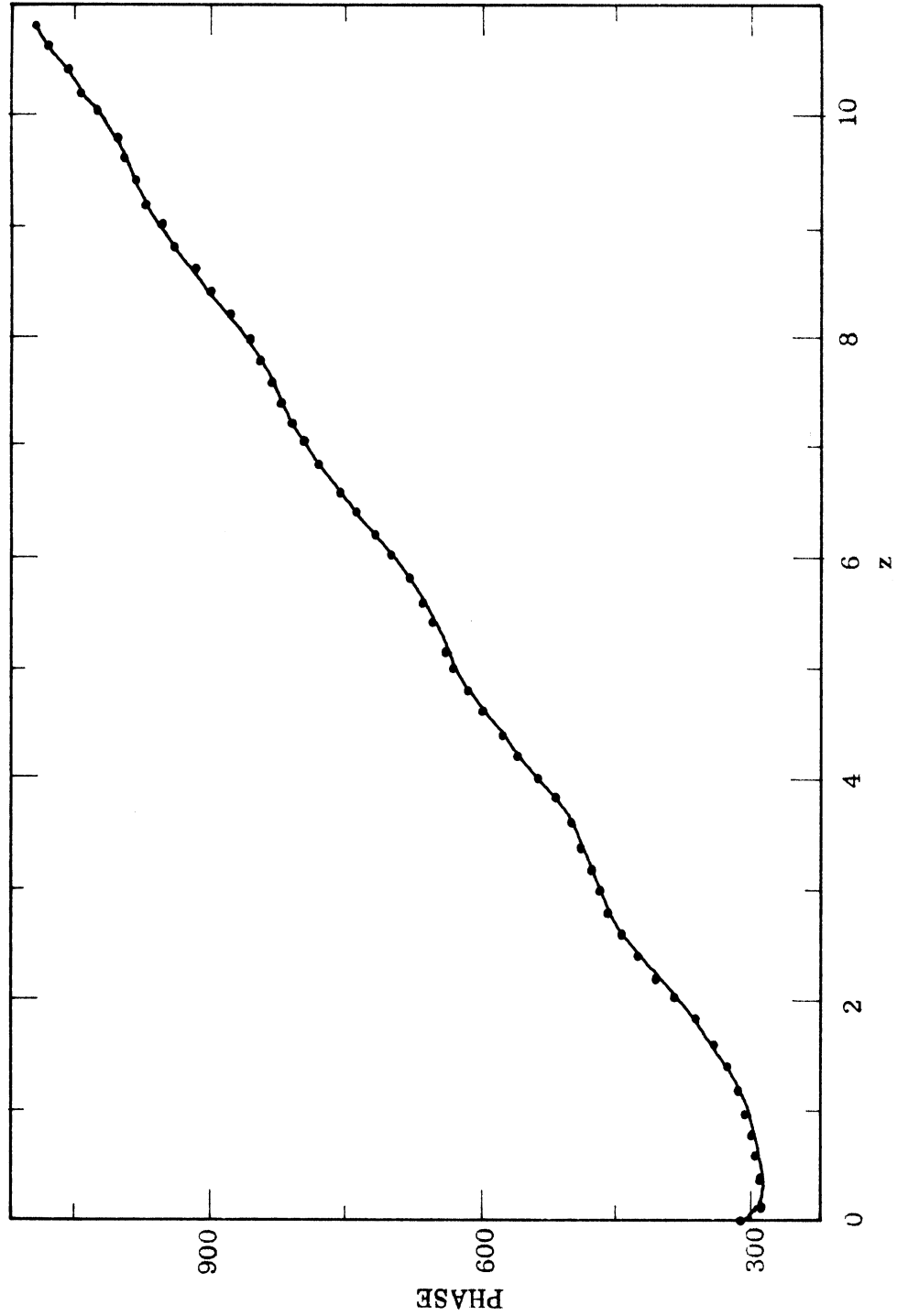
FIG. 21: PHASE OF CURRENT COMPONENT j_z ON OUTSIDE OF ILLUMINATED SIDE OF CLOSED CYLINDER. ($\theta = 0$, $\alpha = 30^\circ$)
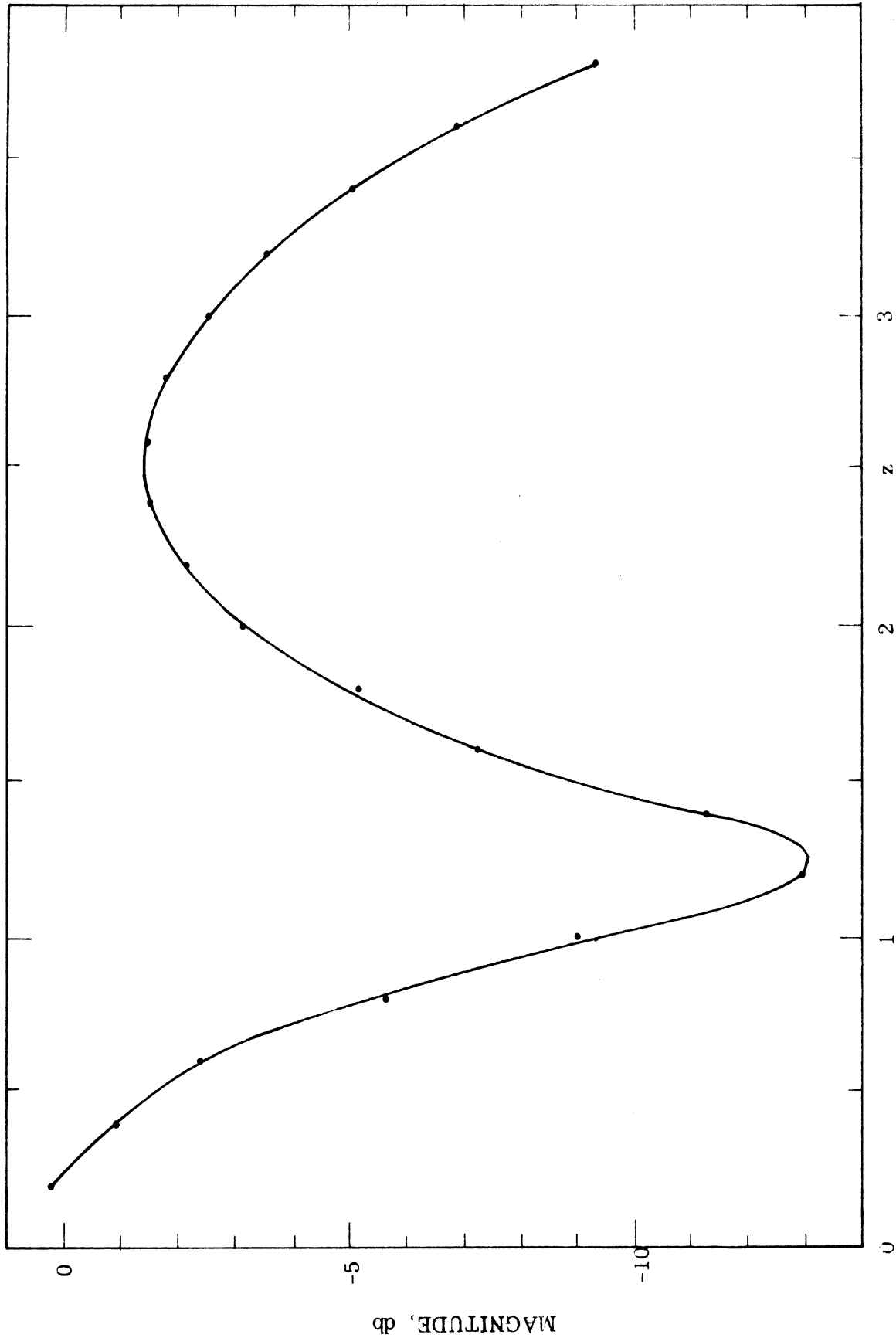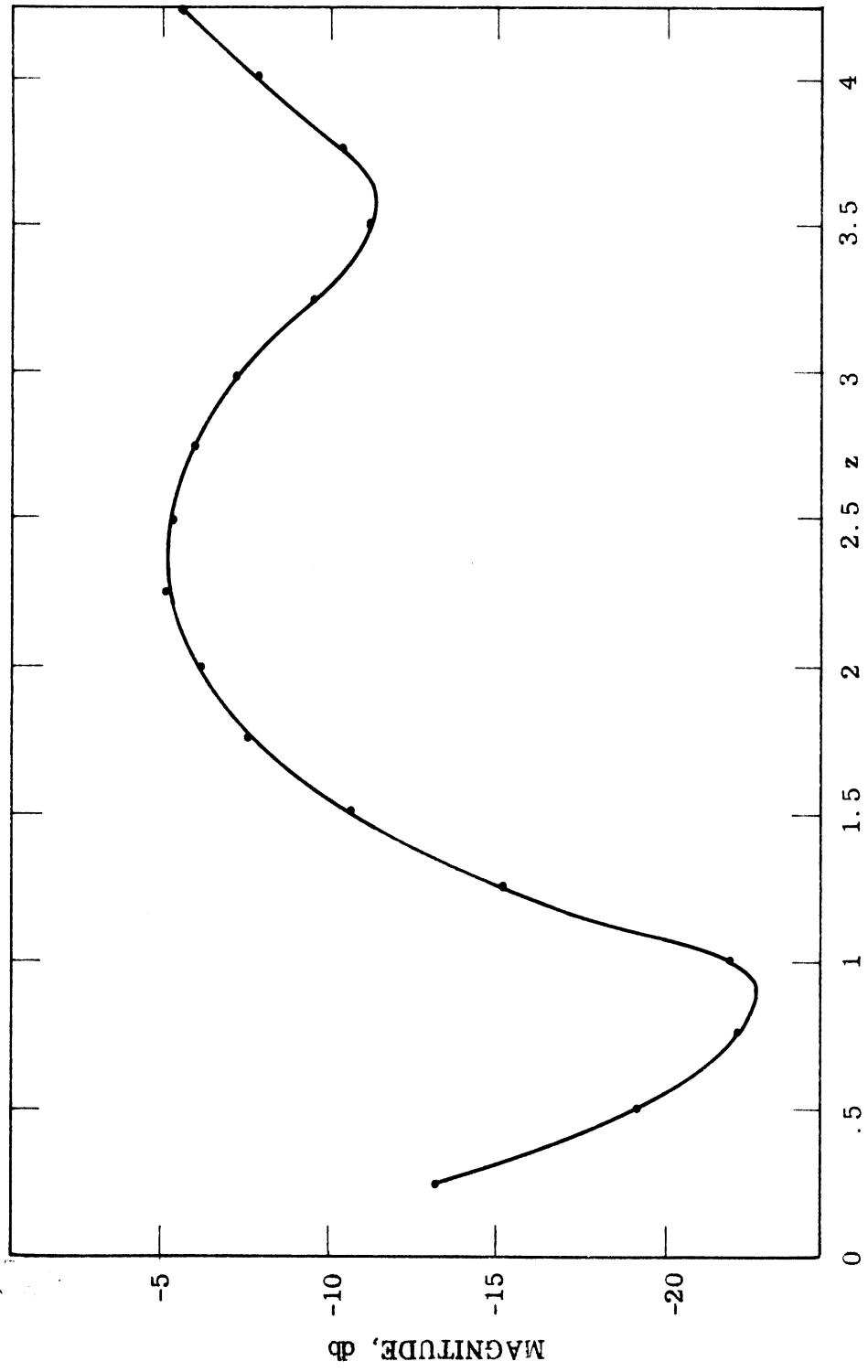
FIG. 22: MAGNITUDE OF CURRENT COMPONENT j_z ON INSIDE SHADOW PORTION
OF OPEN CYLINDER ($\theta = 0$, $\alpha = 30^{\circ}$)
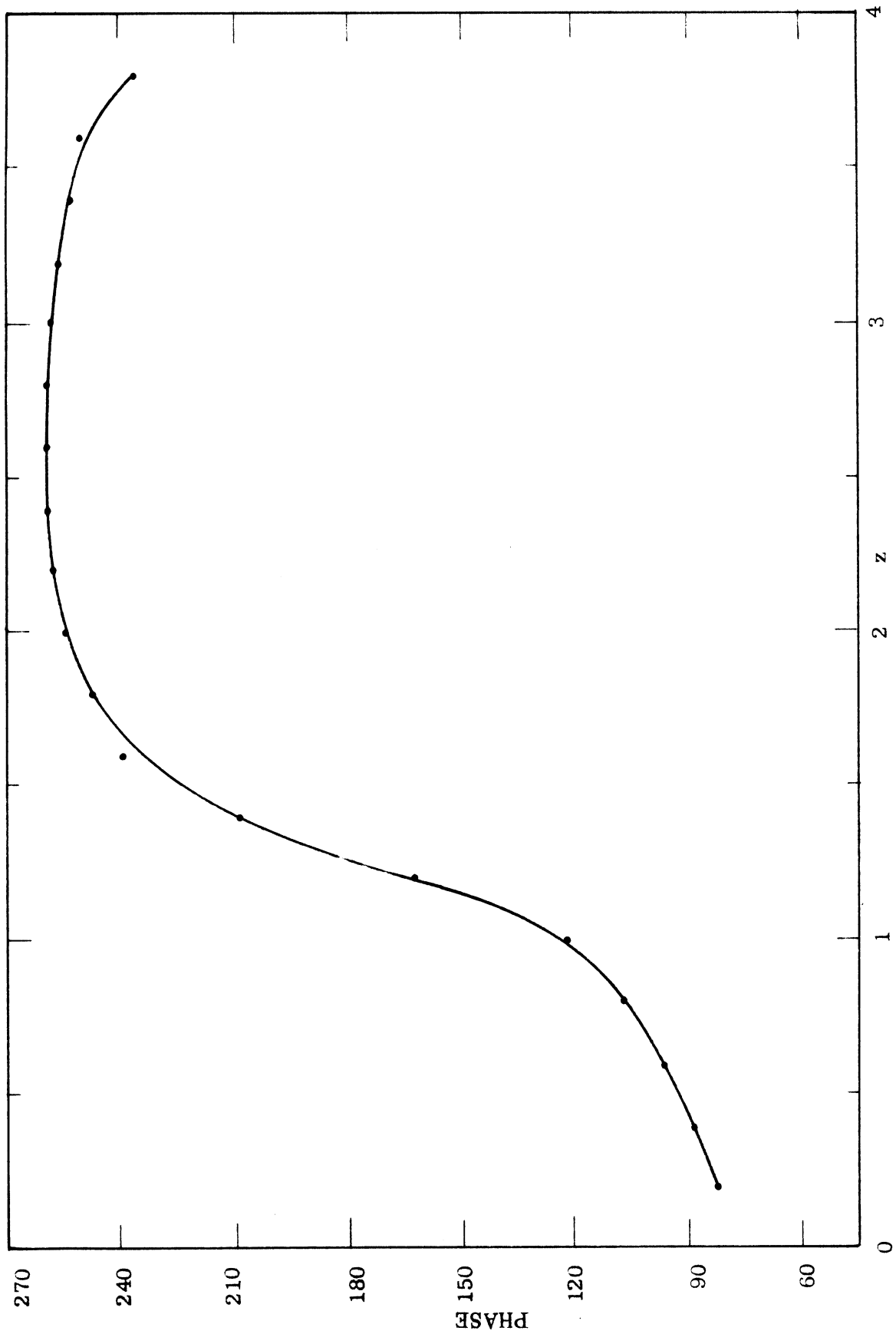
FIG. 23:   PHASE OF CURRENT COMPONENT j_z ON INSIDE SHADOW PORTION OF OPEN CYLINDER.   ($\theta = 0$, $\alpha = 30^\circ$)
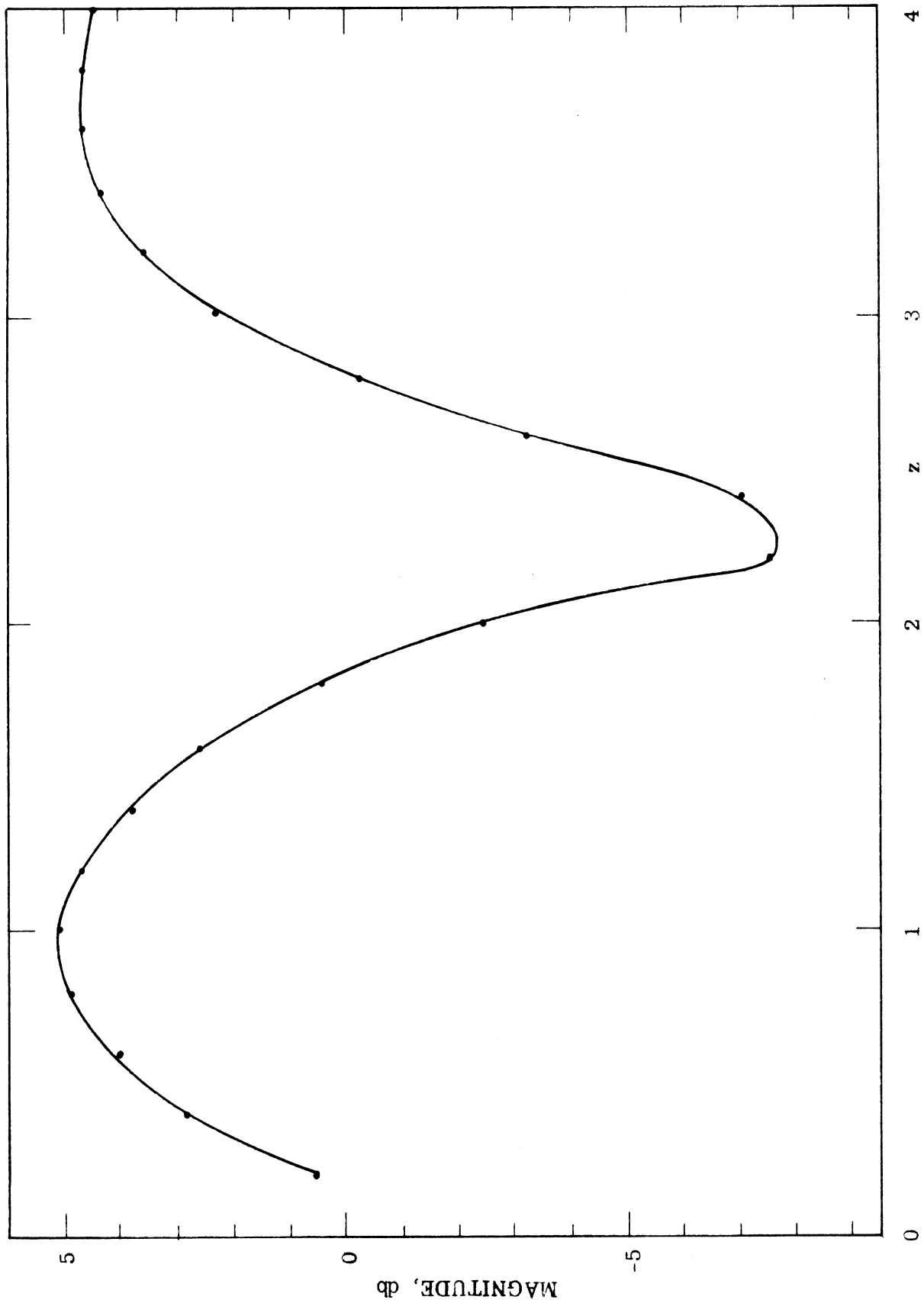
FIG. 24:   MAGNITUDE OF CURRENT COMPONENT j_z ON INSIDE SHADOW PORTION
OF CLOSED CYLINDER $(\theta = 0, \ \alpha = 30^\circ)$
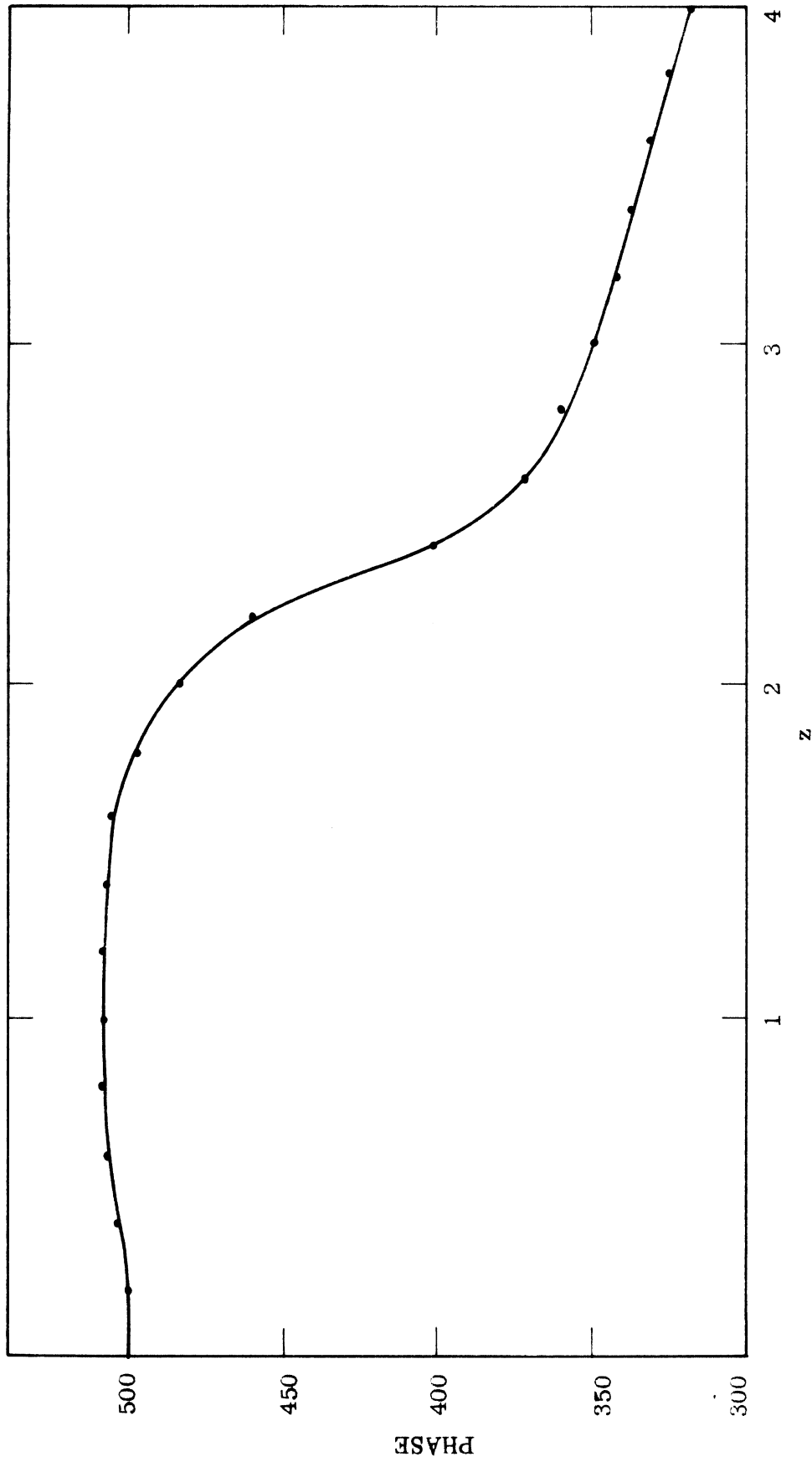
FIG. 25: PHASE OF CURRENT COMPONENT j_z ON INSIDE SHADOW PORTION OF CLOSED CYLINDER.
($\theta = 0$, $\alpha = 30°$)
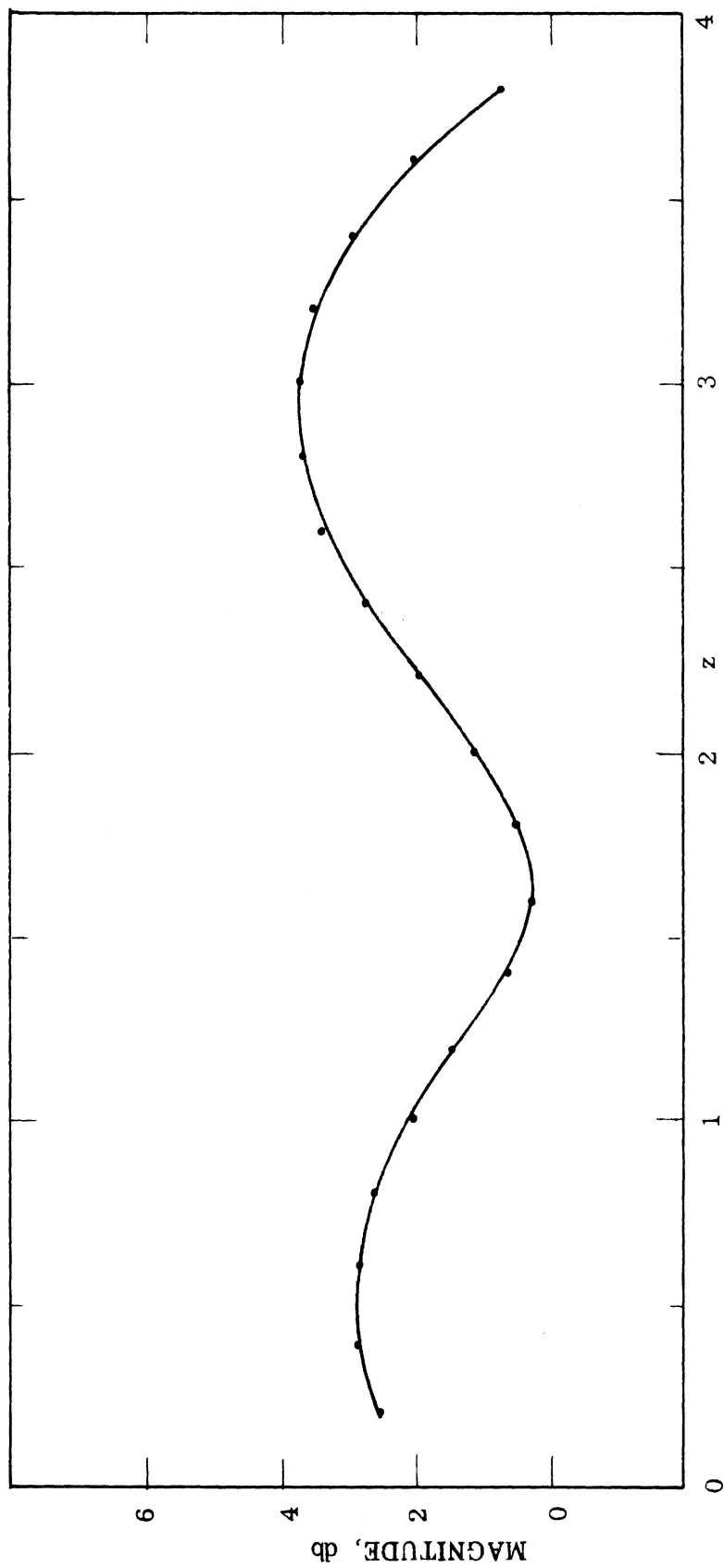
FIG. 26: MAGNITUDE OF CURRENT COMPONENT j_z ON INSIDE ILLUMINATED FACE OF OPEN CYLINDER. ($\theta = \pi$, $\alpha = 30°$)
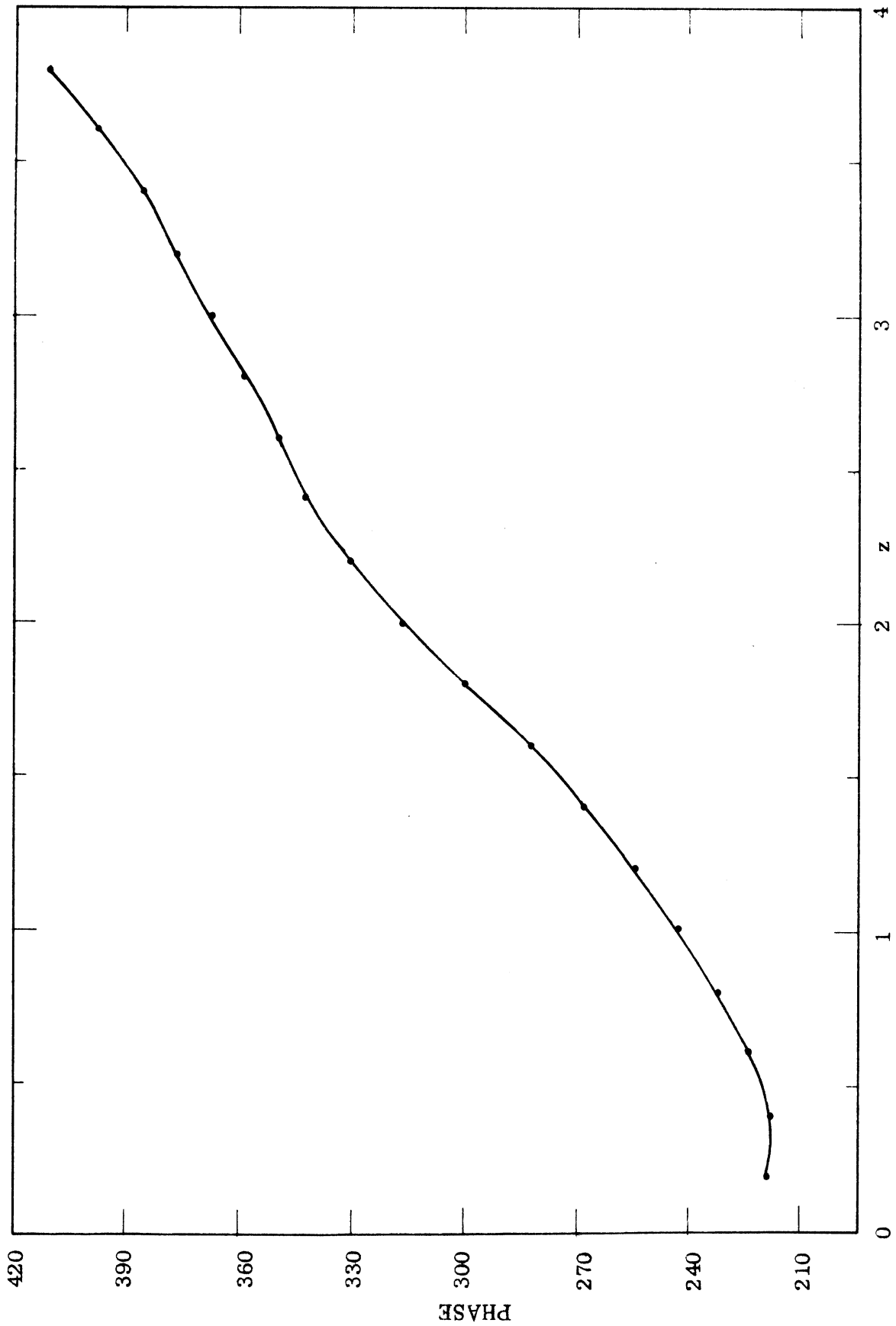
FIG. 27: PHASE OF CURRENT COMPONENT j_z ON INSIDE ILLUMINATED FACE OF OPEN CYLINDER. $(\theta = \pi, \ \alpha = 30^{\circ})$
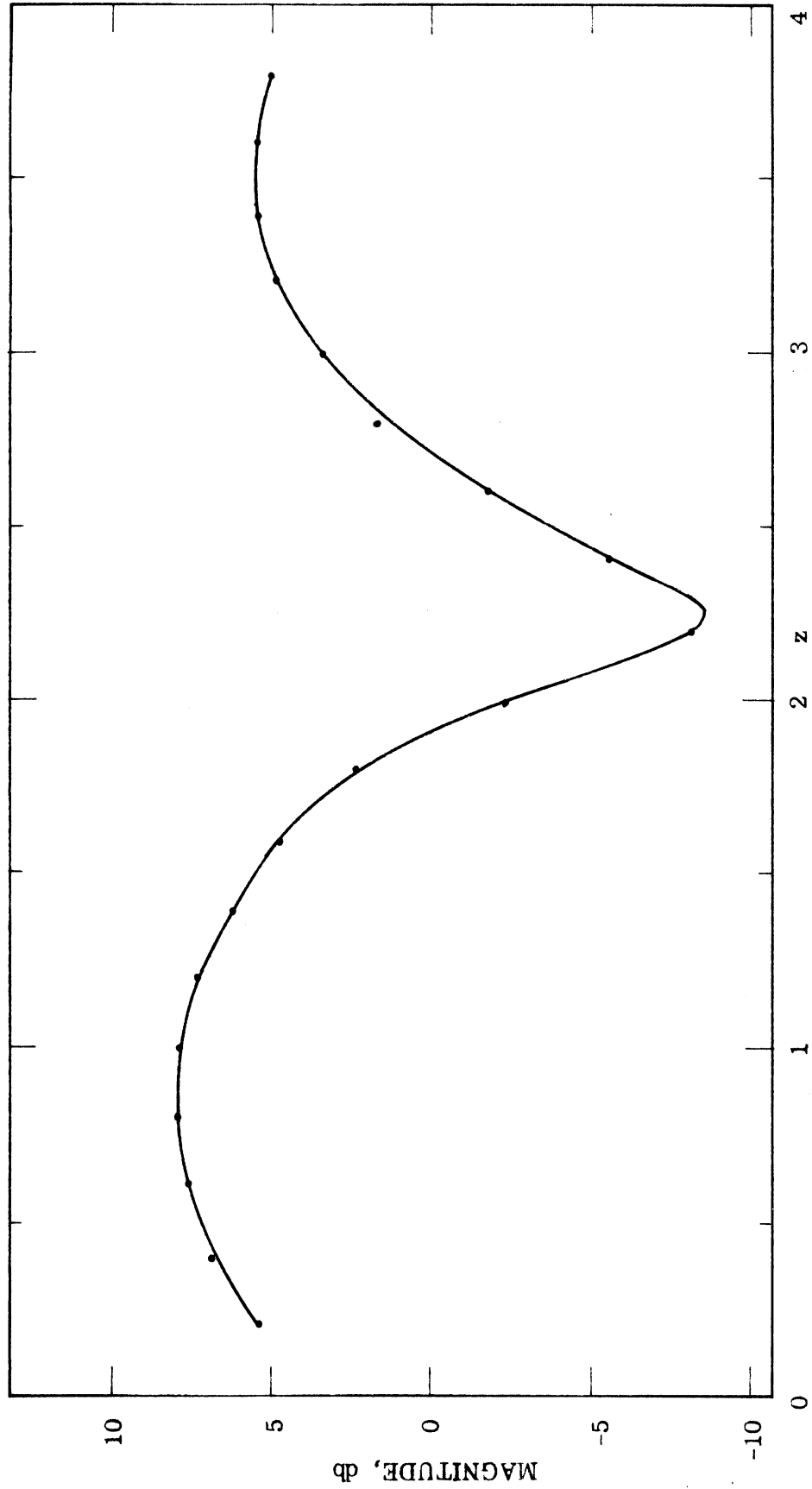
FIG. 28: MAGNITUDE OF CURRENT COMPONENT j_z ON INSIDE ILLUMINATED FACE OF CLOSED CYLINDER. $(\theta = \pi, \alpha = 30^\circ)$
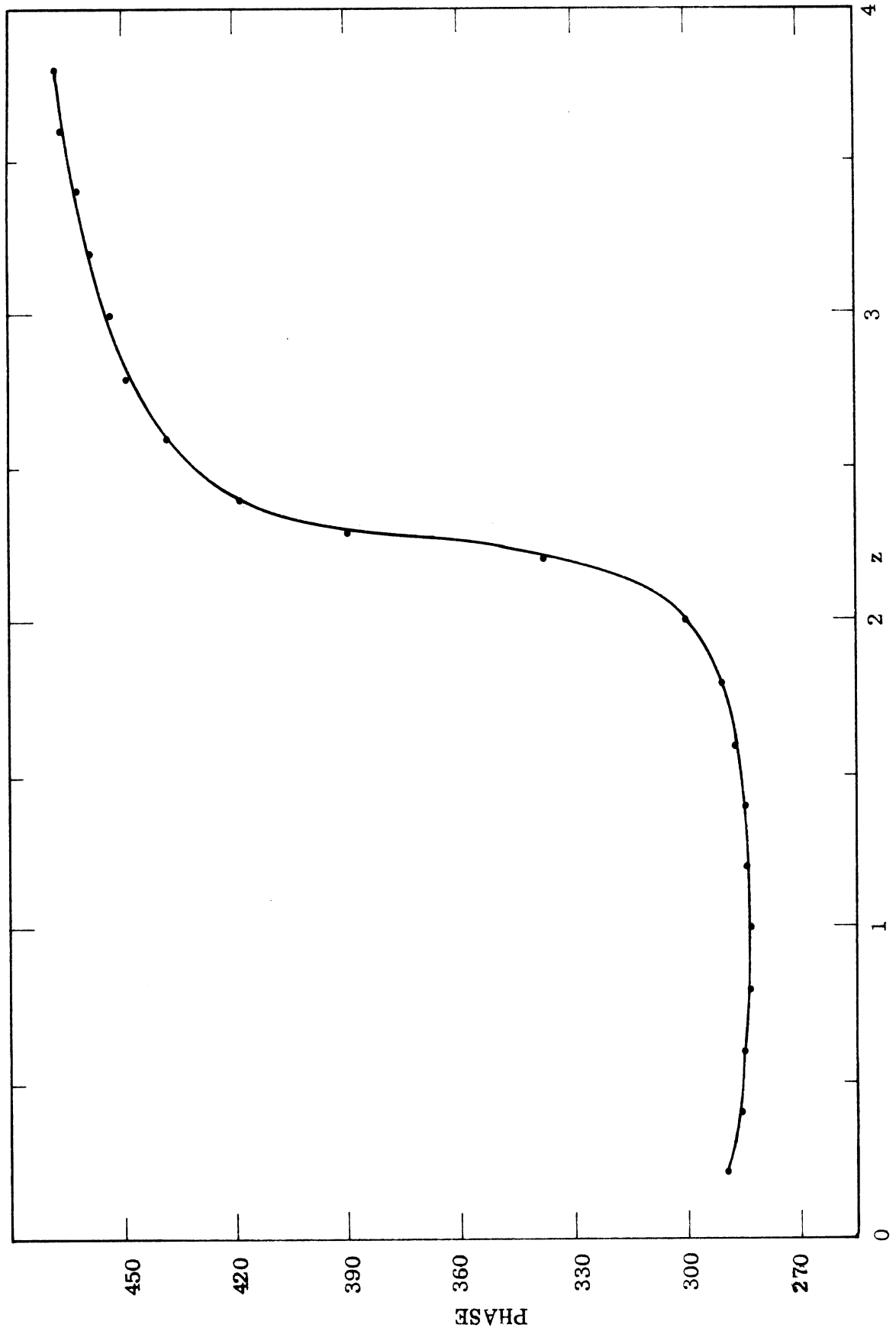
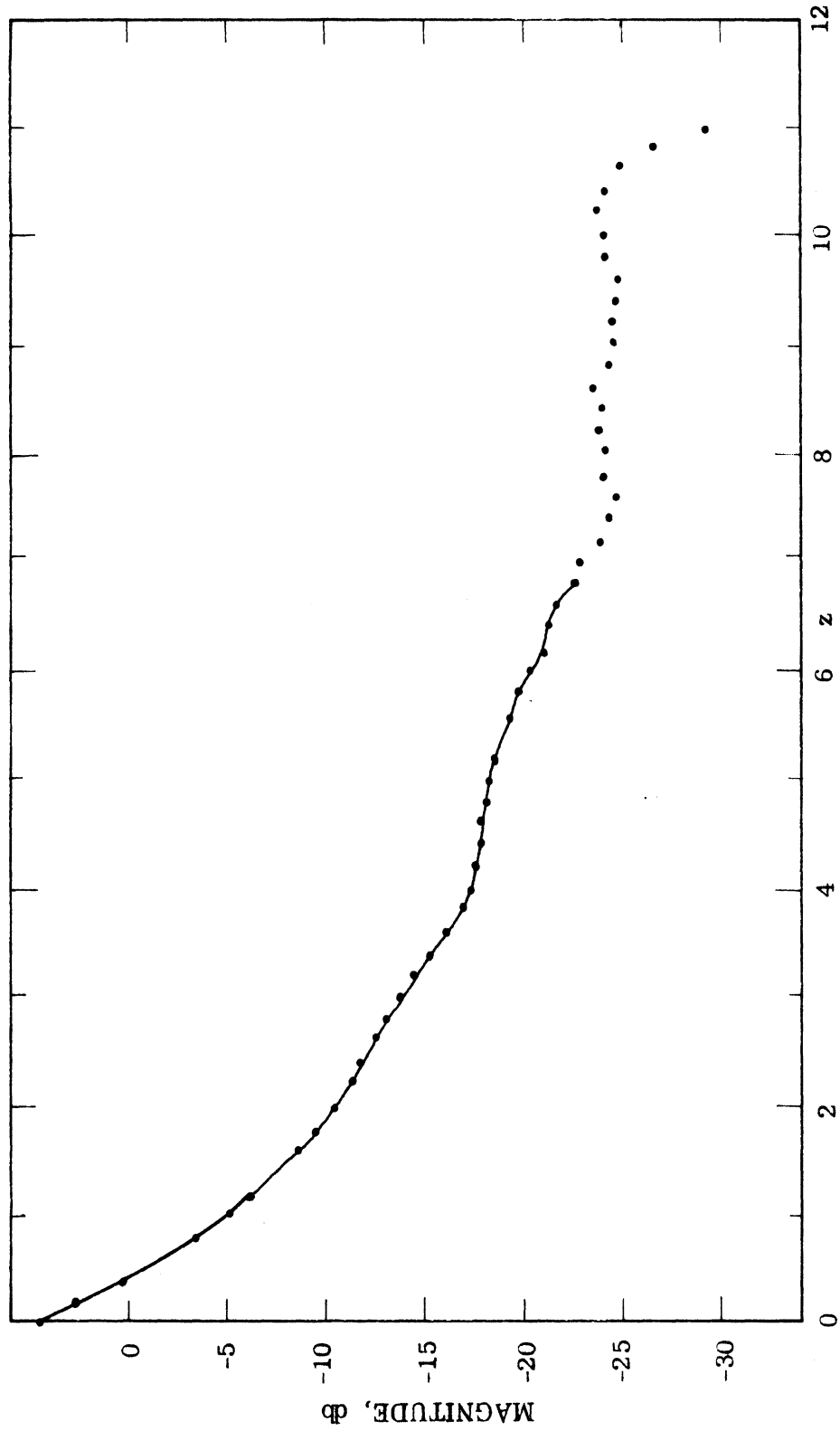FIG. 29: PHASE OF CURRENT COMPONENT j_z ON INSIDE ILLUMINATED FACE OF CLOSED CYLINDER. ($\theta = \pi$, $\alpha = 30°$)
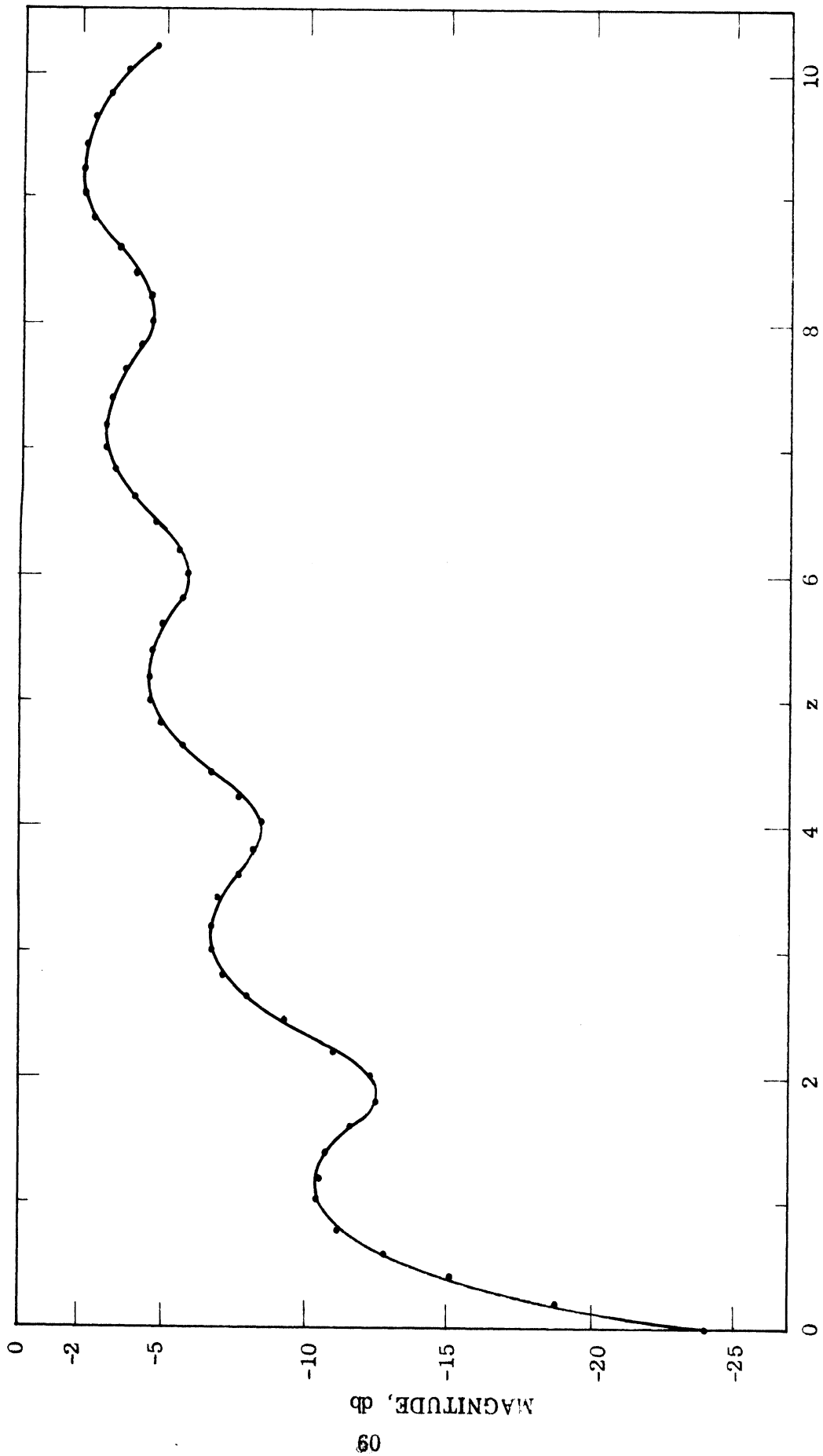
FIG. 30: MAGNITUDE OF CURRENT COMPONENT j_z ON TOP OF OUTSIDE OF OPEN CYLINDER. $(\theta = \frac{\pi}{2}, \alpha = 30^{\circ})$
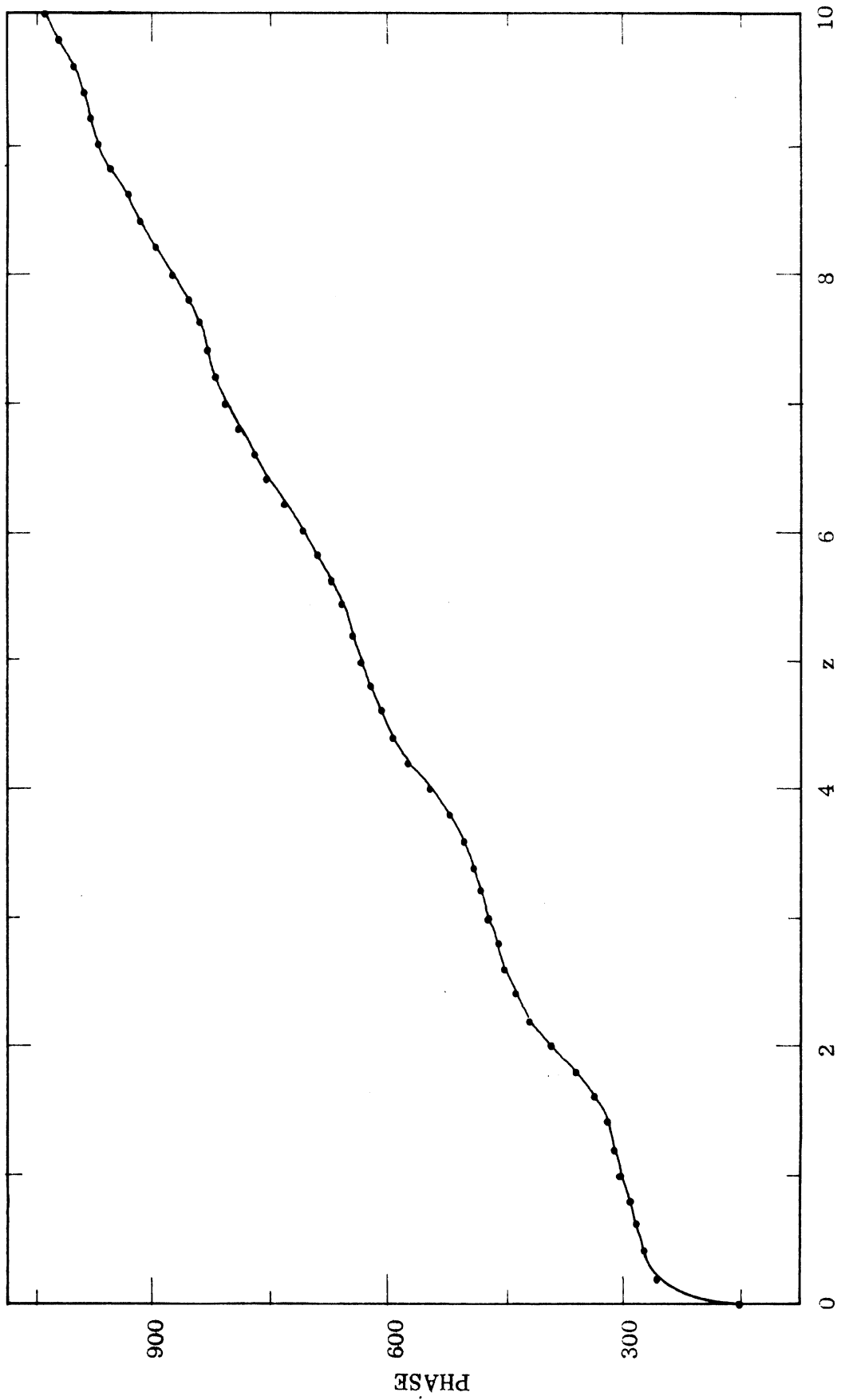
FIG. 31: PHASE OF CURRENT COMPONENT j_z ON TOP OF OUTSIDE OF OPEN CYLINDER. $(\theta = \frac{\pi}{2}, \alpha = 30^{\circ})$
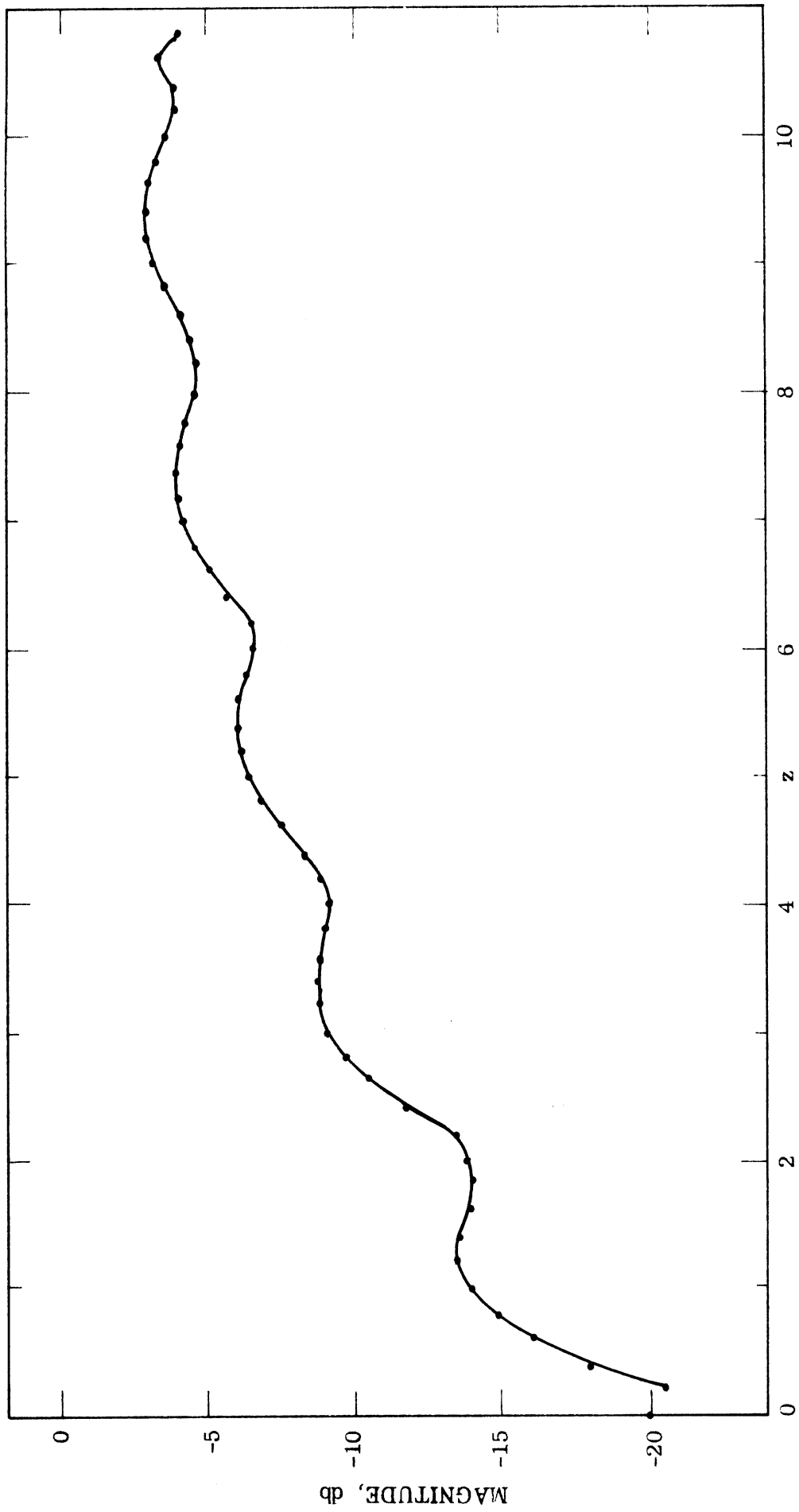
FIG. 32:   MAGNITUDE OF CURRENT COMPONENT j_z ON TOP OF OUTSIDE OF CLOSED CYLINDER.
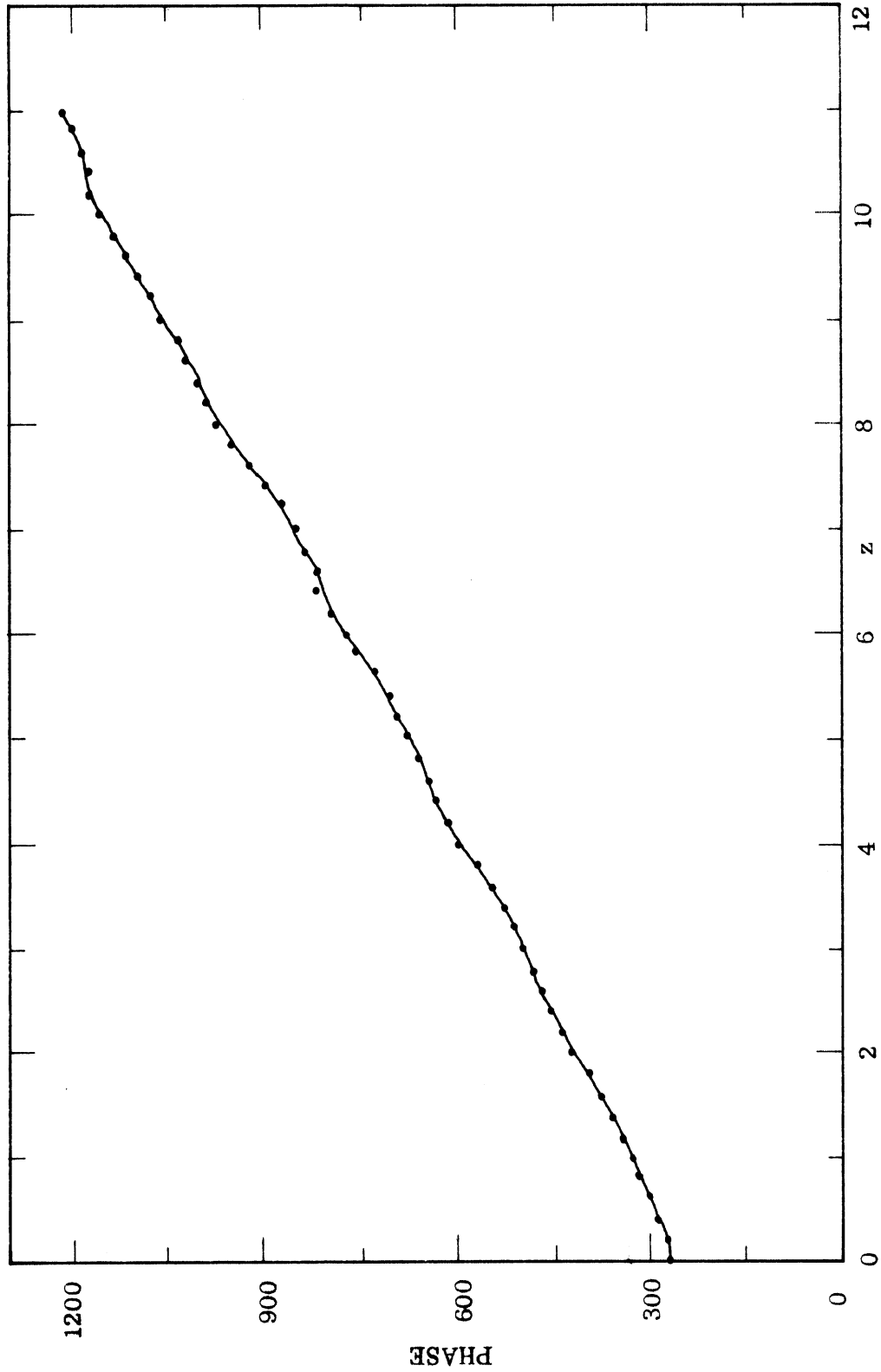($\theta = \frac{\pi}{2}$, $\alpha = 30^\circ$)

FIG. 33: PHASE OF CURRENT COMPONENT j_z ON TOP OF OUTSIDE OF CLOSED CYLINDER. $(\theta = \frac{\pi}{2}, \ \alpha = 30^\circ)$
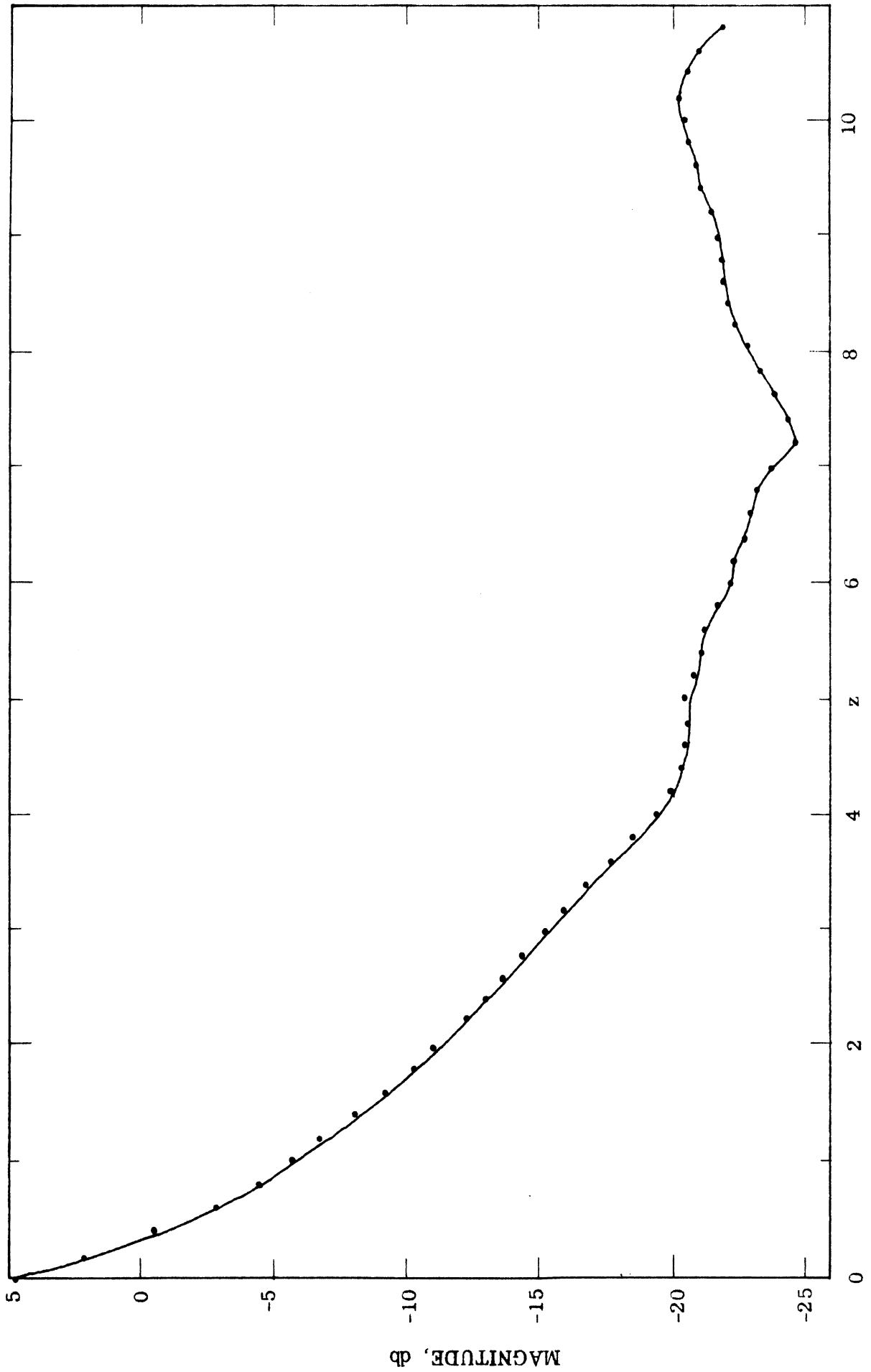
FIG. 34: MAGNITUDE OF CURRENT COMPONENT j_z ON INSIDE TOP OF OPEN CYLINDER.
$(\theta = \frac{\pi}{2}, \ \alpha = 30^\circ)$
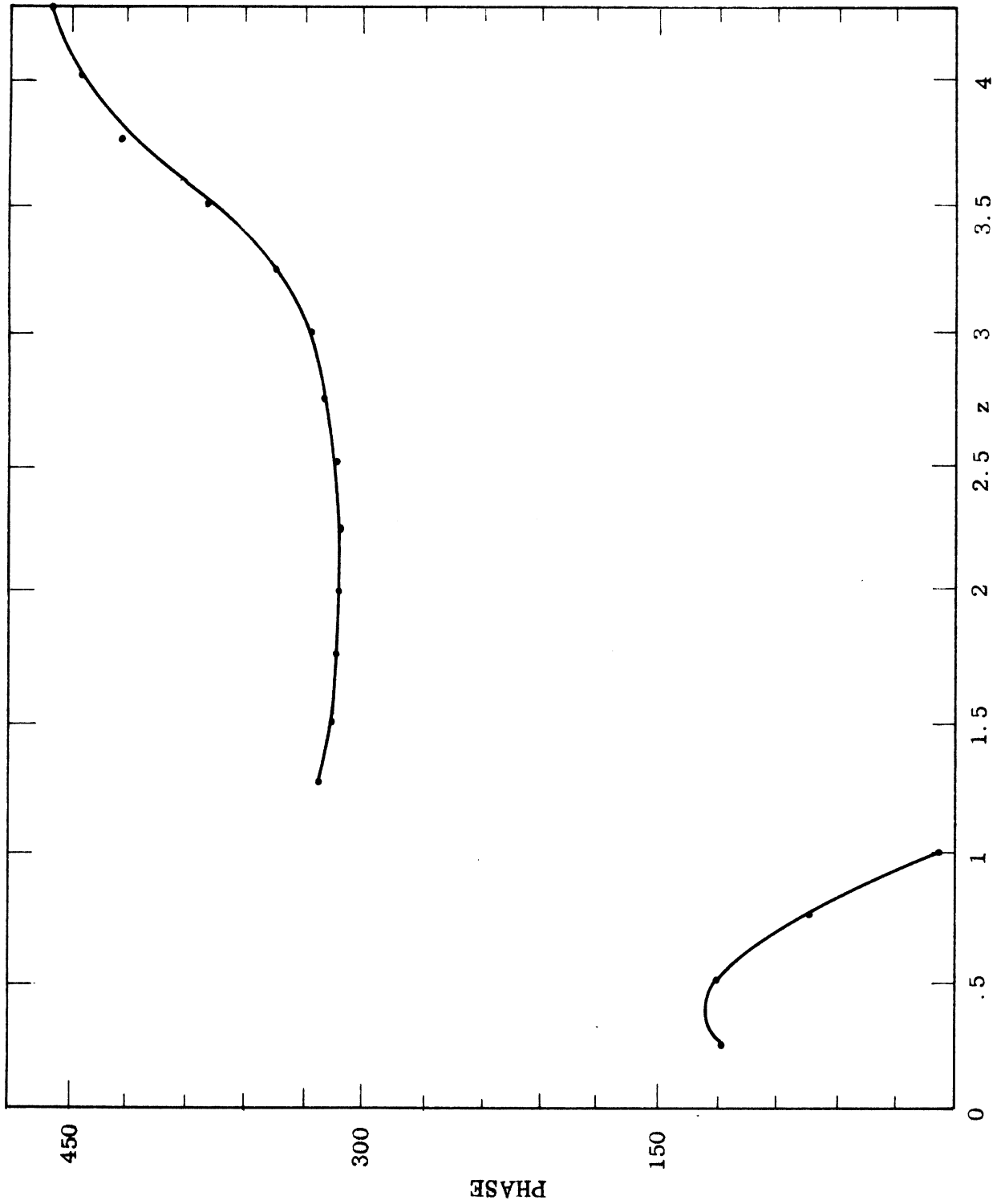
FIG. 35: PHASE OF CURRENT COMPONENT j_z ON INSIDE TOP OF OPEN CYLINDER.
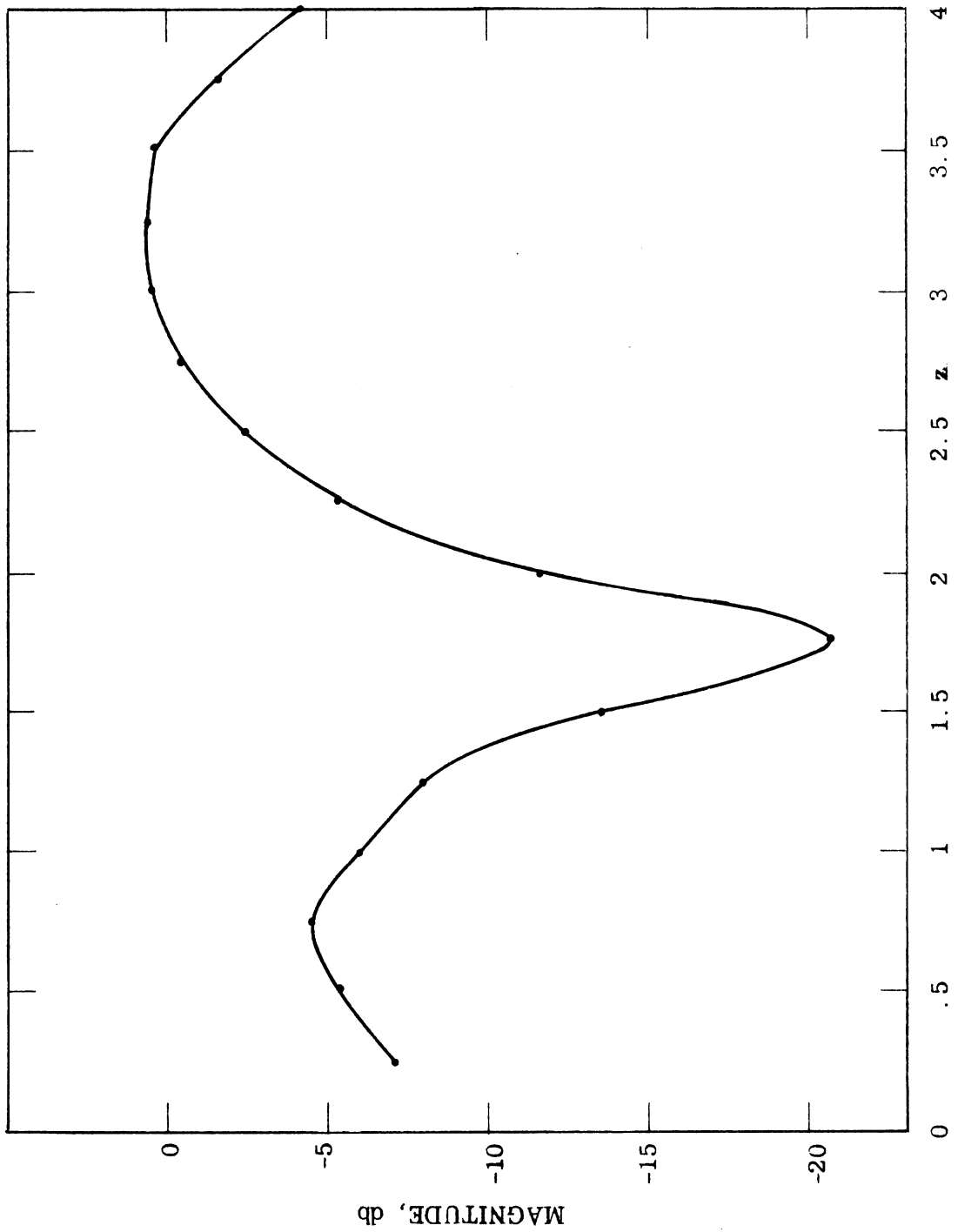
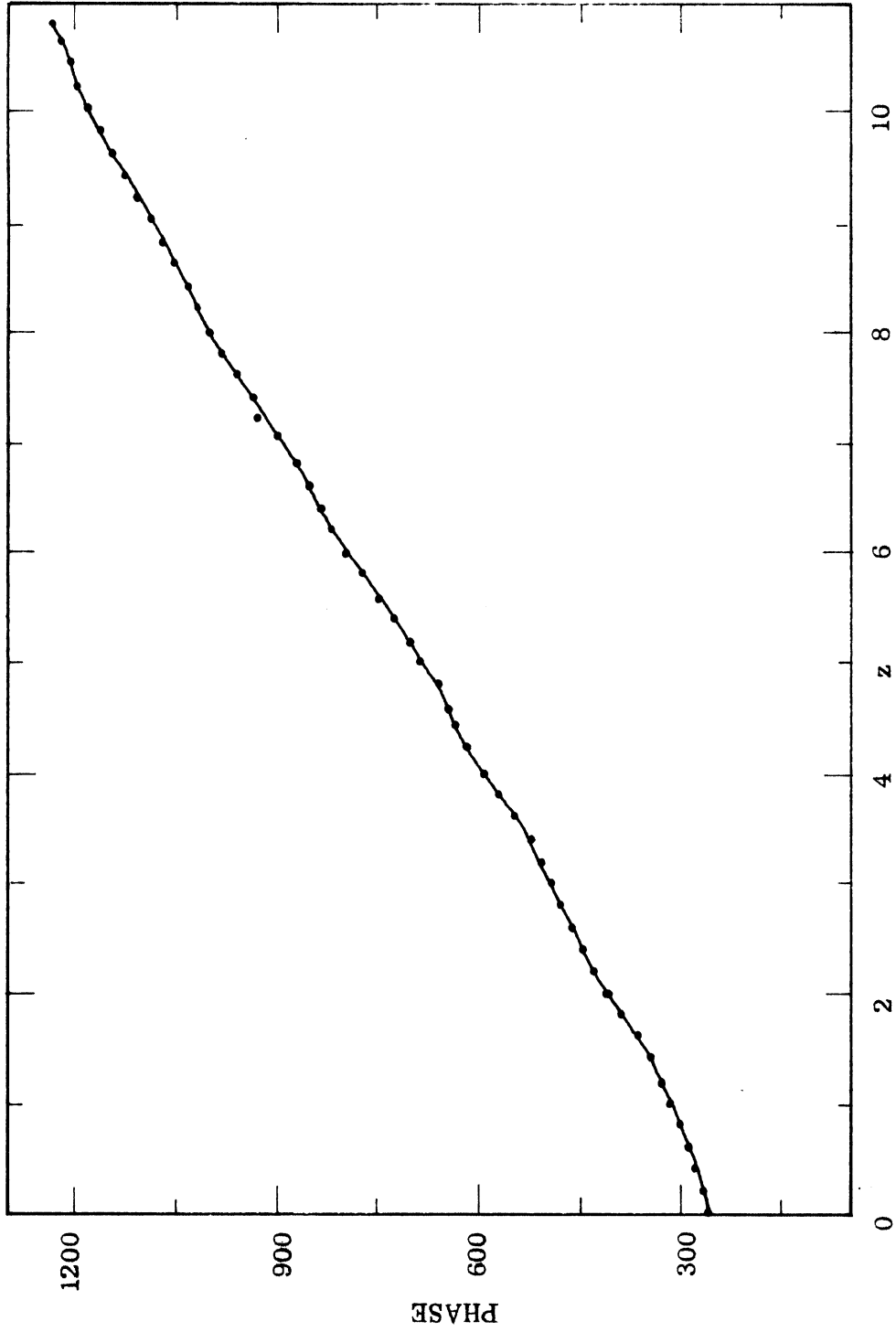FIG. 36: MAGNITUDE OF CURRENT COMPONENT j_z ON INSIDE TOP OF CLOSED CYLINDER. $(\theta = \frac{\pi}{2}, \ \alpha = 30^{\circ})$
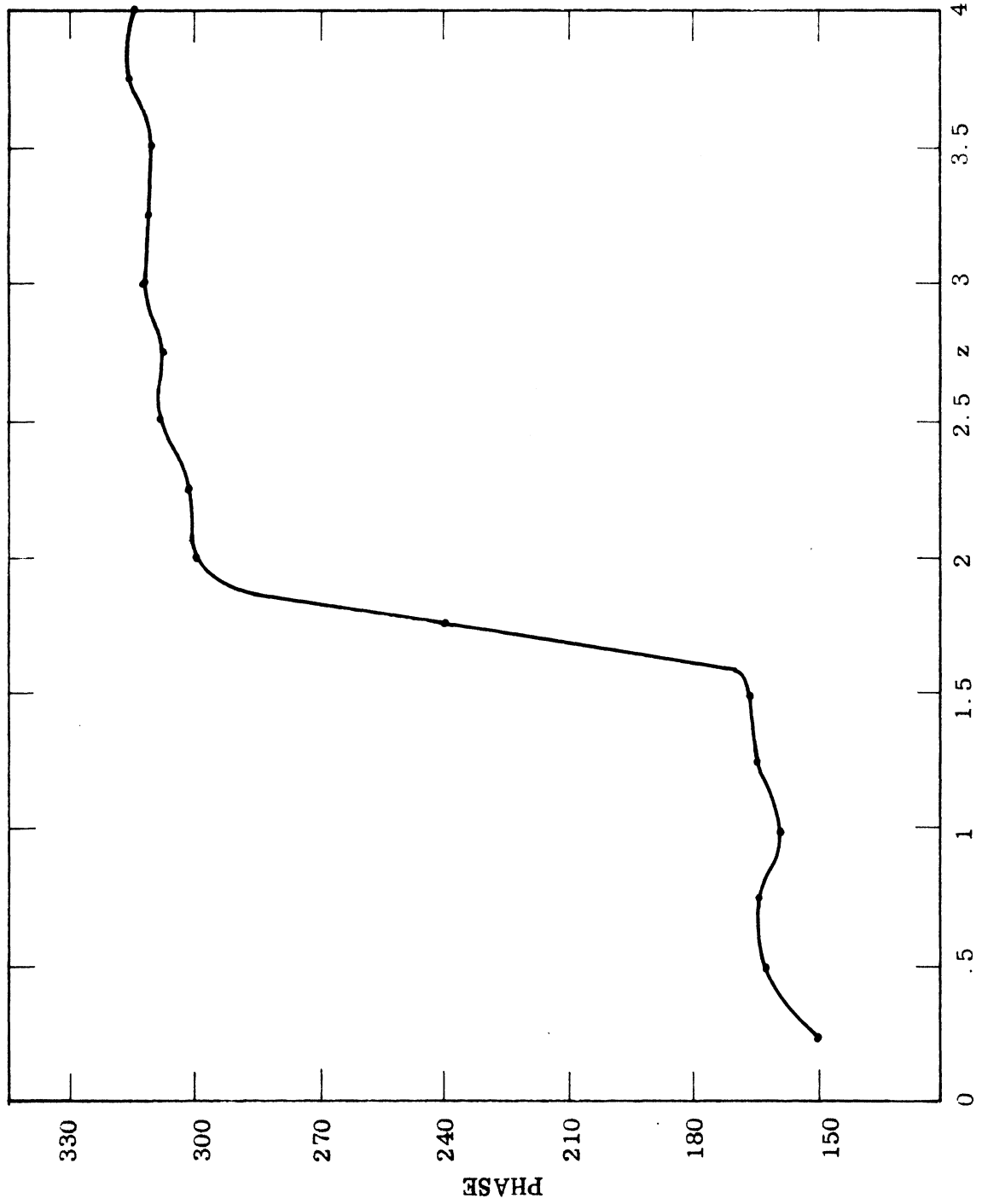
FIG. 37: PHASE OF CURRENT COMPONENT j_z ON INSIDE TOP OF CLOSED CYLINDER.
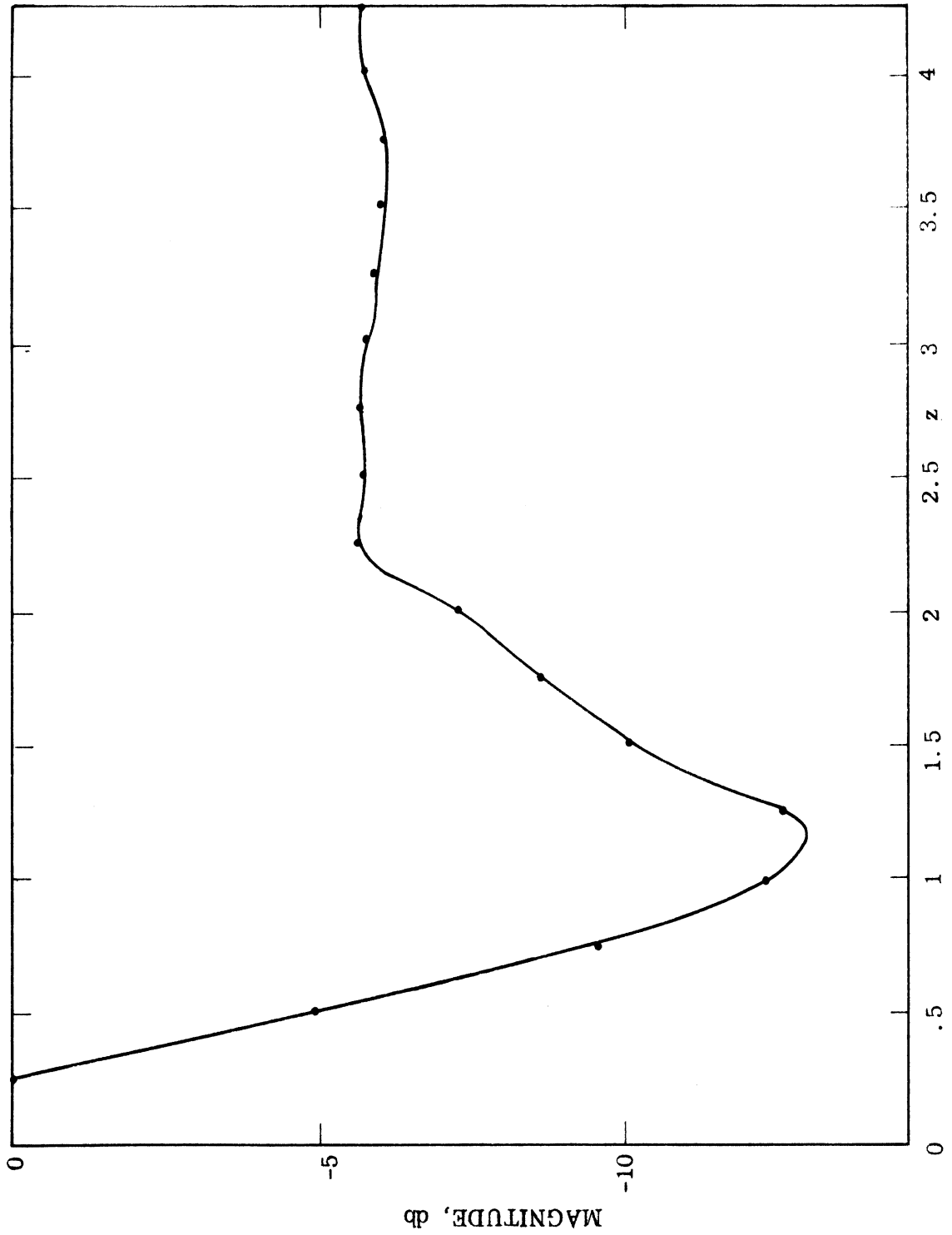$(\theta = \frac{\pi}{2}, \ \alpha = 30^\circ)$

FIG. 38: MAGNITUDE OF CURRENT COMPONENT j_θ ON TOP OUTSIDE OF OPEN CYLINDER. $(\theta = \frac{\pi}{2}, \ \alpha = 30^\circ)$

FIG. 39: PHASE OF CURRENT COMPONENT j_θ ON TOP OUTSIDE OF OPEN CYLINDER. $(\theta = \frac{\pi}{2},\ \alpha = 30^\circ)$

FIG. 40: MAGNITUDE OF CURRENT COMPONENT j_θ ON OUTSIDE TOP OF CLOSED CYLINDER.

$(\theta = \frac{\pi}{2}, \ \alpha = 30^\circ)$

FIG. 41: PHASE OF CURRENT COMPONENT j_θ ON OUTSIDE TOP OF CLOSED CYLINDER.
$(\theta = \frac{\pi}{2}, \; \alpha = 30^\circ)$

FIG. 42: MAGNITUDE OF CURRENT COMPONENT j_θ ON INSIDE TOP OF OPEN CYLINDER. $(\theta = \frac{\pi}{2}, \ \alpha = 30^\circ)$
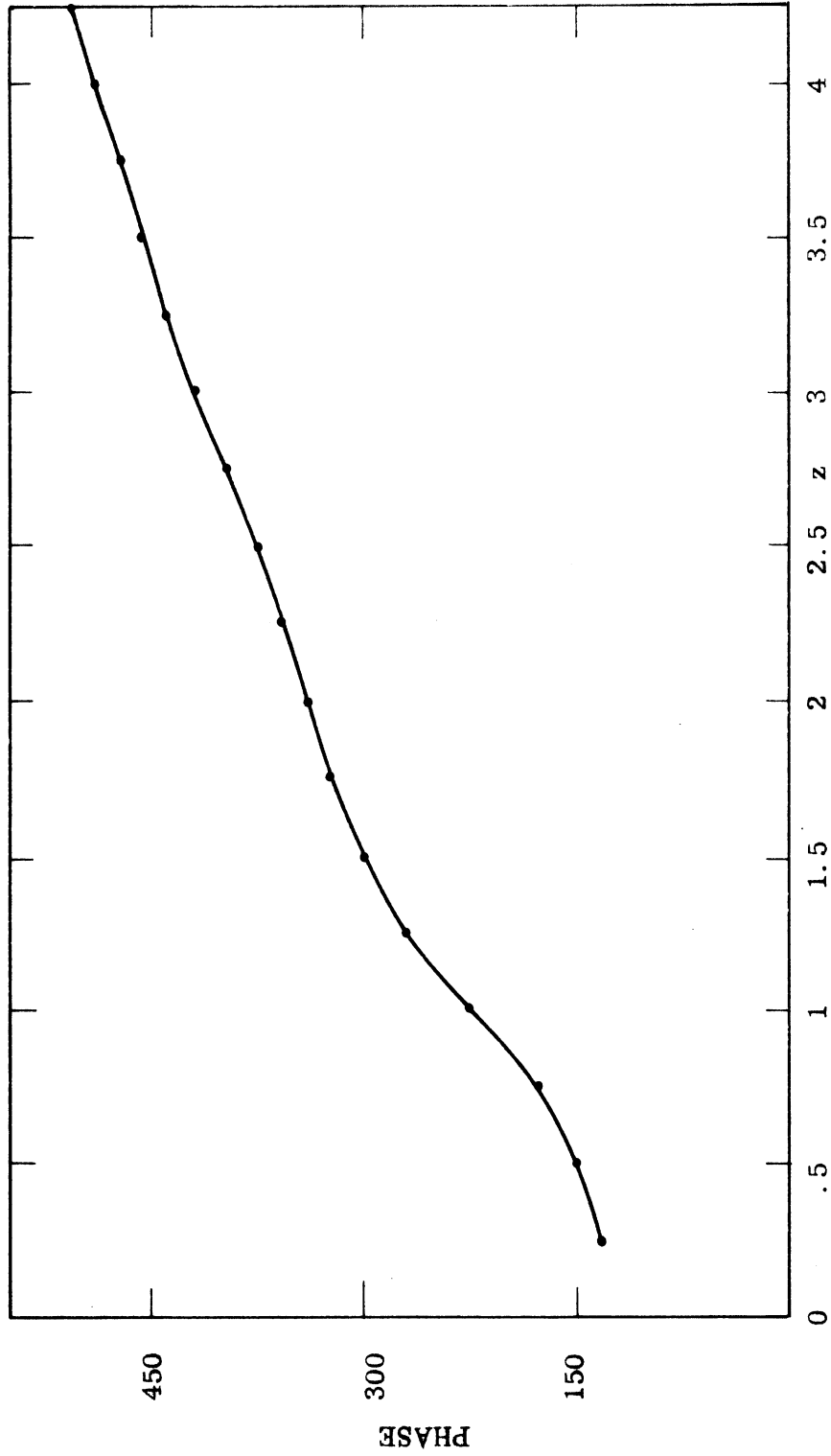
FIG. 43: PHASE OF CURRENT COMPONENT j_θ ON INSIDE TOP OF OPEN CYLINDER.
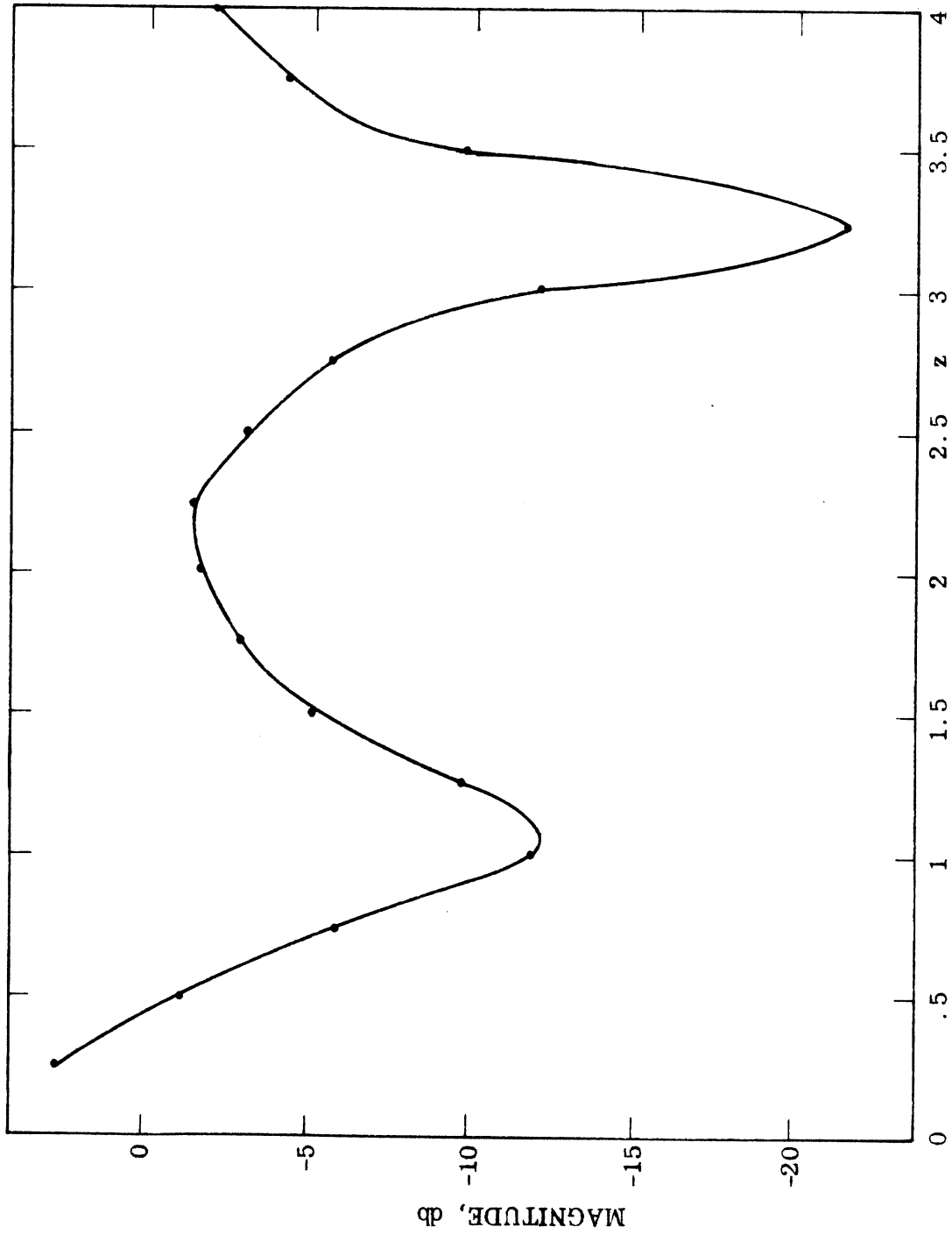$(\theta = \frac{\pi}{2},\ \alpha = 30^\circ)$

FIG. 44: MAGNITUDE OF CURRENT COMPONENT j_θ ON INSIDE TOP OF CLOSED CYLINDER. $(\theta = \frac{\pi}{2},\ \alpha = 30^o)$
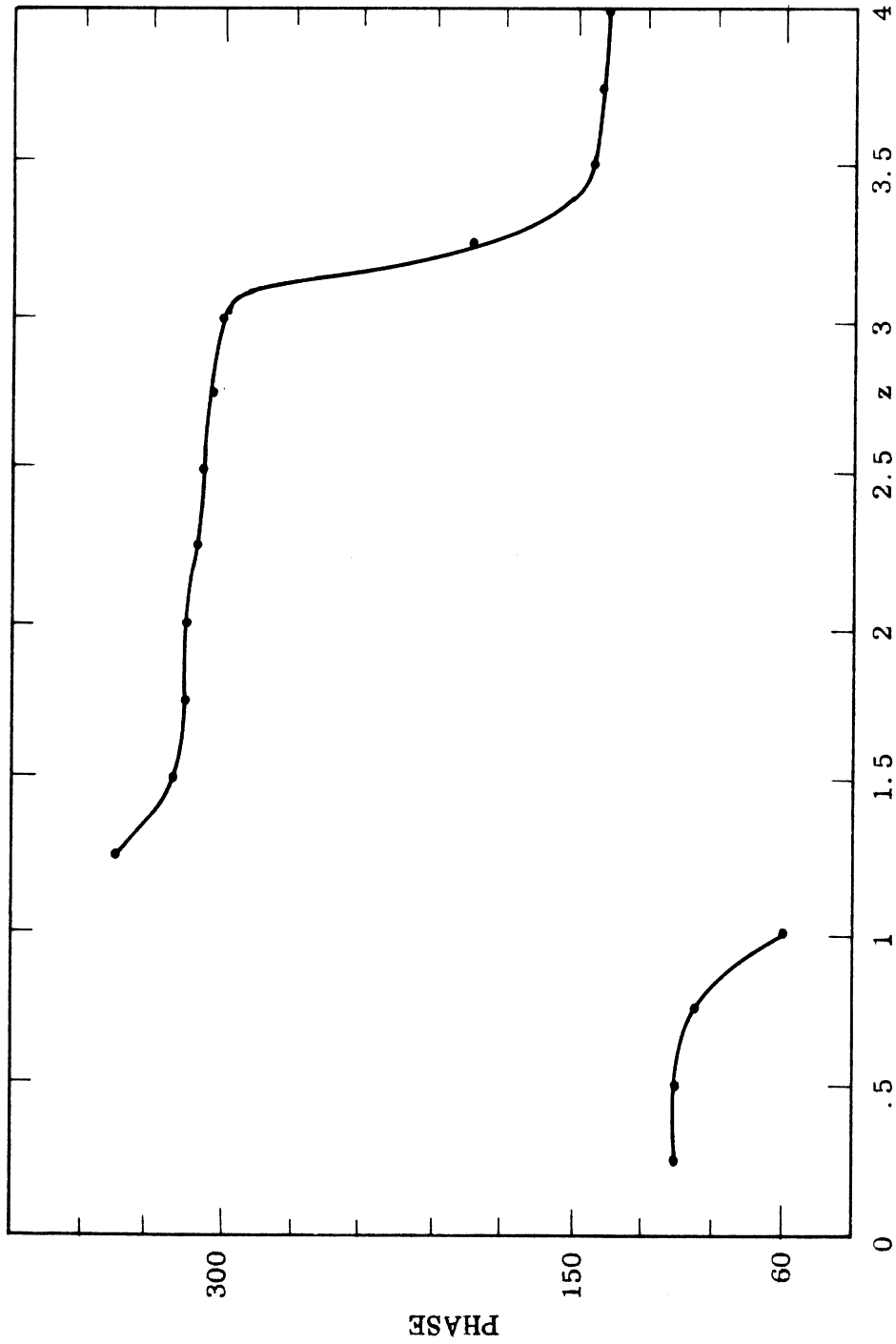
FIG. 45: PHASE OF CURRENT COMPONENT j_θ ON INSIDE TOP OF CLOSED CYLINDER. $(\theta = \frac{\pi}{2},\ \alpha = 30^\circ)$

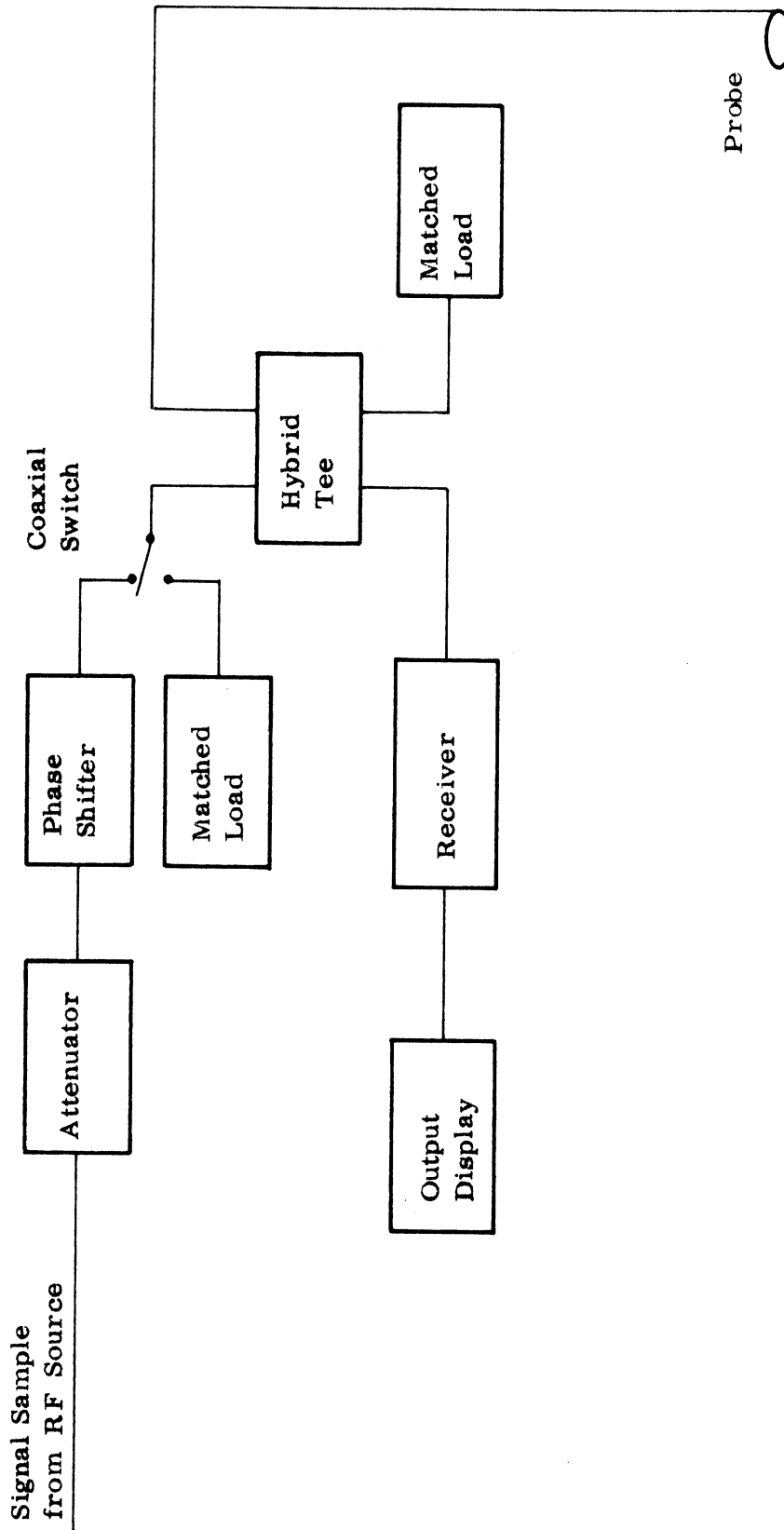FIG. 46: ELEMENTS OF THE RECEIVING SYSTEM.

REFERENCES

Bowman, J. J. and V. H. Weston (1965), "The Effect of Curvature on the Reflection Coefficient of Layered Absorber," (Submitted for publication).

Ducmanis, J. A. and V. V. Liepa (1965), "Surface Field Components for a Perfectly Conducting Sphere," The University of Michigan Radiation Laboratory Report No. 5548-3-T.

Kerker, M. and E. Matijevic (1961), "Scattering of Electromagnetic Waves from Concentric Infinite Cylinders," J. Opt. Soc. Amer., 51, 506-508.

Schmitt, H. J. (1957), "Back-Scattering Cross Section of Circular Metallic Cylinders Surrounded by a Resistance Foil," Cruft Laboratory Scientific Report No. 11, Harvard University, Cambridge, Mass., (ASTIA Document No. AD-133636).

Wait, J. R. (1955), "Scattering of a Plane Wave from a Circular Dielectric Cylinder at Oblique Incidence," Can. J. Phys., 33, 189-195.

Weston, V. H. and R. Hemenger (1962), "High-Frequency Scattering from a Coated Sphere," J. Res. NBS, 66D, 613-619 (Sept. -Oct.).